


For Reference

NOT TO BE TAKEN FROM THIS ROOM

Ex LIBRIS
UNIVERSITATIS
ALBERTAENSIS





Digitized by the Internet Archive
in 2024 with funding from
University of Alberta Library

<https://archive.org/details/Marks1976>

THE UNIVERSITY OF ALBERTA

RELEASE FORM

NAME OF AUTHOR Larry W. Marks
TITLE OF THESIS Dynamic Properties of Head Waves
..... Near the Critical Point
.....
DEGREE FOR WHICH THESIS WAS PRESENTED Master of Science
YEAR THIS DEGREE GRANTED 1976

Permission is hereby granted to THE UNIVERSITY OF ALBERTA LIBRARY to reproduce single copies of this thesis and to lend or sell such copies for private, scholarly or scientific research purposes only.

The author reserves other publication rights, and neither the thesis nor extensive extracts from it may be printed or otherwise reproduced without the author's written permission.

THE UNIVERSITY OF ALBERTA

DYNAMIC PROPERTIES OF HEAD WAVES
NEAR THE CRITICAL POINT

by



LARRY W. MARKS

A THESIS

PRESENTED TO THE FACULTY OF GRADUATE STUDIES AND RESEARCH
IN PARTIAL FULFILMENT OF THE REQUIREMENTS FOR THE DEGREE
OF MASTER OF SCIENCE

IN
GEOPHYSICS

DEPARTMENT OF PHYSICS

EDMONTON, ALBERTA

FALL, 1976

THE UNIVERSITY OF ALBERTA

FACULTY OF GRADUATE STUDIES AND RESEARCH

The undersigned certify that they have read, and recommend to the Faculty of Graduate Studies and Research, for acceptance, a thesis entitled "DYNAMIC PROPERTIES OF HEAD WAVES NEAR THE CRITICAL POINT" submitted by Larry W. Marks in partial fulfilment of the requirements for the degree of Master of Science.

ABSTRACT

Asymptotic ray theory, as presented by Cerveny and Ravindra (10) or Hron and Kanasevich (16), provides a conceptually clear and simple theory to solve a variety of problems dealing with the propagation of head waves in common media. The use of the theory is limited, however, due to singular points in the spatial domain. With this limitation in mind, it is desirable to calculate a more exact solution which lends itself to easy numerical calculation. The integrand in these expressions can be obtained by satisfying boundary conditions. By a suitable deformation of the original integration contours, and use of the method of steepest descent, results are obtained. The formulae give a continuous amplitude at the critical point of the ray and tend to the results obtained from asymptotic ray theory for epicentral distances beyond the end of the zone where pure reflected and head waves interfere.

Amplitude-distance curves for various interference waves will be presented. The separation of head waves and reflected waves in a synthetic seismogram near the critical point will also be given.

ACKNOWLEDGEMENTS

I would like to express my appreciation to my supervisor Dr. F. Hron for his kind advice and stimulating course.

Dr. Clement Leibovitz was a treasure house of help with certain aspects of the numerical analysis.

The writer received financial support through a National Research Council grant, a University of Alberta Graduate Teaching Assistantship, and a scholarship from the Society of Exploration Geophysicists, Tulsa, Oklahoma.

TABLE OF CONTENTS

CHAPTER		Page
1	INTRODUCTION TO HEAD WAVES.....	1
2	A WAVE METHOD SOLUTION FOR RAY AMPLITUDE...	16
	2.1 Introduction to the Exact Wave Method.....	16
	2.2 The PP Reflected Wave.....	19
	2.3 Receiver Near the First Critical Point.....	41
	2.4 Receiver Near the Second Critical Point.....	43
	2.5 The PPP Head Wave.....	46
	2.6 The PSP Head Wave.....	61
	2.7 The Interference Wave.....	67
	2.8 Generalized Amplitude Formulae.....	74
3	NUMERICAL RESULTS.....	80
	3.1 The Weber Function.....	80
	3.2 Computed Dynamic Properties.....	85
	3.3 Dynamic Properties and Frequency.....	86
	3.4 Dynamic Properties and Multi- Layered Media.....	92
	3.5 Dynamic Properties and Head Wave Multiplicity.....	104
	3.6 Reflected Pulses Near the Critical Point.....	112
4	CONCLUSION.....	117
	BIBLIOGRAPHY.....	120
	APPENDIX.....	122

LIST OF TABLES

CHAPTER 1		Page
1.1	Velocity Distributions and Head Wave Existence.....	10

LIST OF ILLUSTRATIONS

CHAPTER 1		Page
1.1	Schematic picture of incident, reflected, transmitted and head waves.....	8
1.2	The interference zone.....	13
CHAPTER 2		
2.1	The medium description.....	18
2.2	Contours of integration.....	28
2.3	Head wave multiplicity.....	50
2.4	Total surface incident amplitude.....	76
CHAPTER 3		
3.1	The function $G(y)$	84
3.2	Dynamic properties and frequency.....	87
3.3	Dynamic properties in a multi-layered medium.....	94
3.4	Dynamic properties for multiply-reflected head waves.....	105
3.5	Source pulse for synthetic seismograms.....	113
3.6	Pulse separation.....	115

CHAPTER 1

INTRODUCTION TO HEAD WAVES

In the time domain, asymptotic ray theory provides a solution to the wave equation and boundary conditions in the form of an asymptotic series in inverse powers of frequency. Details of this method can be found in Hron and Kanasewich (16) and Cervený and Ravindra (10). The ray theory is useful in finding expressions for the reflected and head waves in many problems which prove difficult to solve by integral methods (such as curved and dipping interfaces or inhomogeneous media). It will be shown in this thesis that for a situation in which both the integral solution and asymptotic ray solution are known, they turn out to be the same for high frequencies.

The general equation of motion for waves in a homogeneous, perfectly elastic and isotropic medium is

$$\rho \frac{\partial^2 \bar{W}}{\partial t^2} = (\lambda + \mu) \nabla(\nabla \cdot \bar{W}) + \mu \nabla^2 \bar{W} \quad 1.1$$

where \bar{W} is the particle displacement vector and t is the time. The time-harmonic solution to this equation is assumed expressible in inverse powers of frequency according to asymptotic ray theory

$$\bar{W} = \exp(i \omega(t-\tau)) \sum_{k=0}^{\infty} (i \omega)^{-k} \bar{W}_k \quad 1.2$$

where τ and \bar{W}_k are independent of t and ω .

This expansion is called a ray series, τ a phase function, and \bar{W}_k the amplitude coefficients of the series. Moving surfaces of constant phase, $t = \tau(x,y,z)$ will be called wavefronts and the orthogonal projections of these surfaces will be termed rays.

If the solution for equation 1.1 is known for harmonic waves, the results can easily be generalized for impulsive waves using Fourier Transforms. The impulsive solution, denoted by \bar{W}_I can be expressed as

$$\bar{W}_I = \frac{1}{\pi} \operatorname{Re} \int_0^{\infty} S(\omega) \bar{W} d \omega$$

where \bar{W} is the steady state solution of 1.1 and $S(\omega)$ is the spectrum of the impulse. From 1.2 and the definition of \bar{W}_I we find that

$$\bar{W}_I = \frac{1}{\pi} \operatorname{Re} \sum_{k=0}^{\infty} \bar{W}_k f_k(t - \tau)$$

where

$$f_k(t - \tau) = \int_0^{\infty} (i \omega)^{-k} S(\omega) \exp[i \omega(t - \tau)] d \omega$$

It can be seen from this definition of f_k that

$$\frac{d f_k(t - \tau)}{d(t - \tau)} = f_{k-1}(t - \tau).$$

Cerveny and Ravindra (10) state that this ray series is invalid at points where the function $\tau(x,y,z)$ is non-analytic. Therefore the ray series is invalid where the time-distance curve of the wave has discontinuous derivatives, at a triplication point, for example. The invalid point to be considered in this study is the critical point. At this point on the surface the travel-time curves of reflected and head waves are still continuous, although they are tangential to each other. This tangency implies that the critical point is a multiple valued point. Beyond the critical point the head wave retains its linear travel-time relation while the reflected wave still maintains a hyperbolic relation. It will be shown that the region of invalidity (called an interference zone or critical region) of the ray series depends on the source frequency.

Cerveny and Ravindra (10) have used asymptotic ray theory to derive the following amplitude formulae for head and reflected waves:

$$H_{\text{waves}} = \frac{v_1}{2 \pi i f \cos \theta_1} \frac{\prod_{m=1}^{k-1} B_m}{r^{1/2} (r - r^*)^{1/2}}$$

$$R_{\text{waves}} = \frac{v_1}{\cos \theta_1} \frac{\prod_{m=1}^{k-1} B_m}{\left(\prod_{m=1}^k \frac{h_m v_m}{\cos \theta_m} \cdot \prod_{m=1}^k \frac{h_m v_m}{\cos^3 \theta_m} \right)^{1/2}}$$

where v_m = velocity of propagation of the m-th ray segment

θ_m = angle of incidence of the m-th ray segment on the interface upon which it impinges

h_m = thickness of the layer housing the m-th ray segment

k = total number of ray segments

f = source frequency

r = epicentral distance

r^* = critical distance for the ray. This is the minimum distance at which the head wave can physically exist. It corresponds to the ray which is critically reflected.

The product term in the numerator represents the product of all reflection, transmission, and head wave coefficients encountered by the ray during its propagation from source to receiver. It is obvious that the head wave amplitude tends to infinity as $r \rightarrow r^*$.

A theoretical analysis of the region near the critical point is of great practical seismological importance (Musgrave (21)). First, the local maxima of the amplitude of the reflected waves lies in the region of the critical points and therefore are at the most favorable position to detect these strong waves. Second, if the critical point can be determined by experimental data, then the mean

velocity of the overburden can be calculated by examining the travel time curves of the head waves. Finally, on the basis of kinematic data alone, a seismic interpreter can select a series of equally true earth models, but will not be able to choose the correct one. If the maximum of the amplitude distance curves can be found experimentally and the position of the critical point calculated for several earth models, then the correlation between the actual value and the calculated one can be used as proof of the validity of the earth model chosen.

It is the aim of this thesis to conduct a theoretical and numerical investigation of the reflected waves which emerge near critical points. Expressions for the dynamic properties of interfering reflected and head waves will be derived.

Head waves have been given several different names in the literature. These include conical, lateral, refracted, and Mintrop waves. The study of head waves from a plane interface between two homogeneous media has been well done in the field of seismic theory, for example Muskat (22). Head waves were later studied using the Sommerfeld integral method. The most concise of these studies is Heelan (14). Studies of the interference reflected wave-head wave system in the critical region have been considerably rarer. This was first investigated by Brekhovskikh (4) for liquid media. Cervený (6) studied this interference phenomena for solid media for a single-

layered model with an arbitrary velocity distribution at the refracting interface. The arbitrary velocity distribution allowed one to consider media in which either P or S type head waves could exist. Later, Cerveny (9) solved the problem for a multi-layered medium, but with only one critical point in existence. Thus, the problem of solving interference wave amplitudes for multi-layered media and arbitrary ray paths remains unsolved. (The problem of multiply-reflected head waves is also in need of investigation.) This thesis aims to present a solution to these. This solution is for horizontally-stratified media with all layers homogeneous. The formal solution is in the form of a single integral with a simple integrand for the one interface problem and an extremely cumbersome one for multi-layered media. These integrals have been evaluated exactly by several authors for the one interface problem (see Cagniard (5), Dix (11), Bortfeld (2), (3), Muller (20)). An excellent bibliography and a simple picture of head waves are given in Cerveny and Ravindra (10).

A head wave is basically formed by the concave parabolic wave front impinging upon a plane interface whose refractive index is less than one. The ray must strike the interface at the critical angle θ^* defined by

$$\sin \theta^* = n = \text{refractive index.}$$

Two criteria necessary for head wave formation are:

- (1) the radius of curvature of the incident wave front must be finite (plane waves cannot generate head waves)
- (2) the refracted segment of the ray must propagate with the greatest velocity of the entire ray.

Every head wave is closely associated with a reflected and transmitted wave. The head wave is a plane wave whose end points are the point where the transmitted wave touches the interface and the point of tangency of head wave and reflected wave. This is shown diagrammatically in Fig. 1.1. This thesis concerns itself only with the head waves classified as of the first kind (Cerveny and Ravindra (10), pp. 123-127), in which the head wave is generated in a manner shown in Fig. 1.1. The velocity distribution of this interface is taken to be $\alpha_2 > \beta_2 > \alpha_1 > \beta_1$. This is the most general distribution resulting in all eight types of head waves being formed. The first diagram in Fig. 1.1 is for a P wave whose wave front is labelled 1 incident upon the interface. Wave fronts which propagate as P waves are shown as solid lines while those propagating as S waves are depicted as dashed lines. The reflected PP and PS (11, 12), as well as transmitted PP and PS (13, 14) are shown. The four possible head waves which can occur are labelled using the numbering system described in Appendix A.2. The second diagram shows a similar schematic for an S wave (2) incident upon the interface.

The head wave is a conical wave and in three dimensions

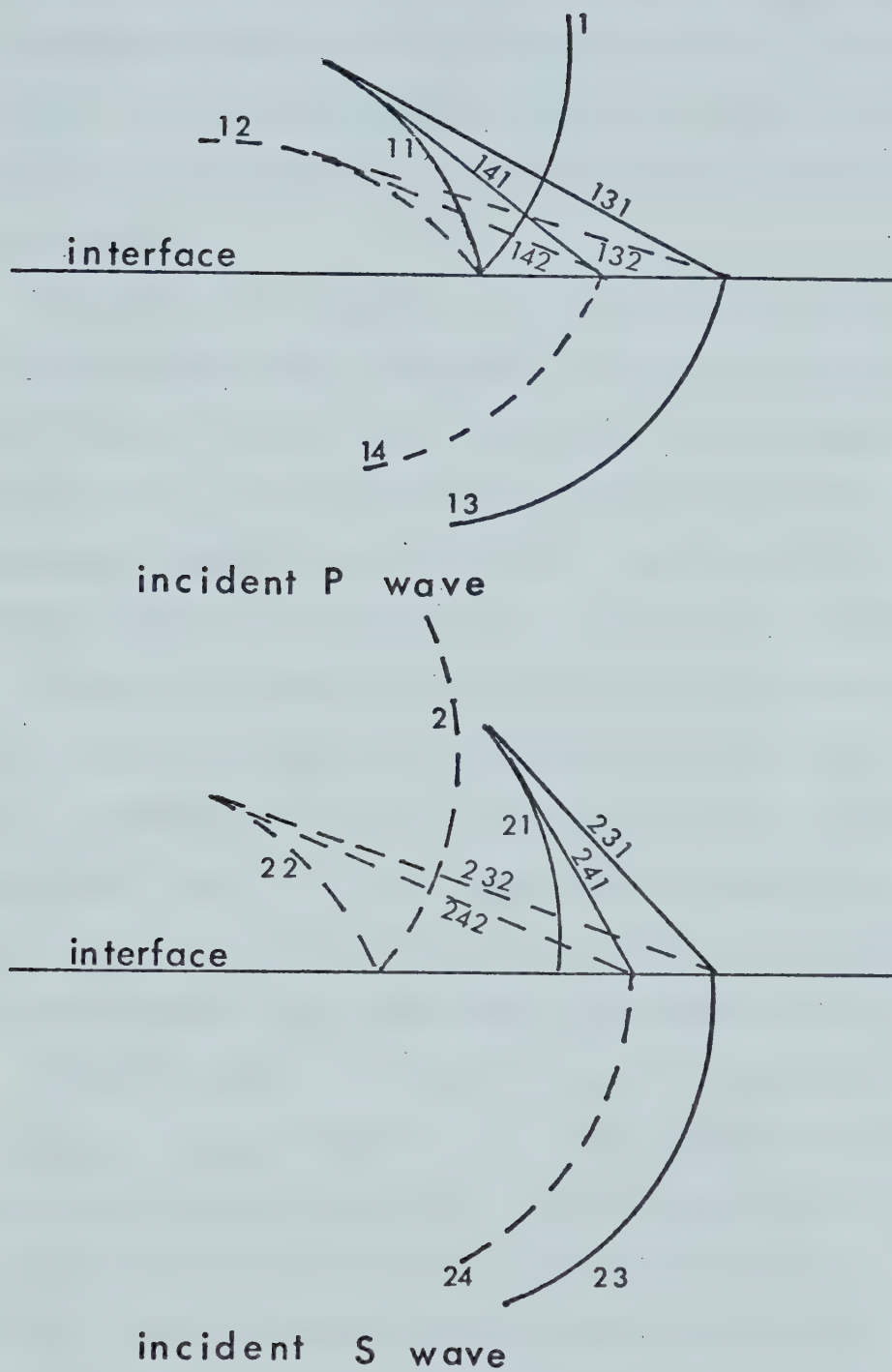


Figure 1.1. Schematic picture of incident, reflected, transmitted and head waves.

can be depicted as the frustum of a cone. Therefore, only one head wave segment can be produced per ray since the spherical wave has been transformed to a conical wave front with an infinite radius of curvature in the plane of incidence.

Velocity distributions at the refracting interface are vital to head wave formation. Table 1.1 shows the possibility of forming any of the eight basic types of head waves as a function of velocity distribution. α and β represent compressional and shear wave velocities. The subscripts refer to the upper (1) or lower (2) medium.

There is a region in which the impulsive head wave always interferes with its corresponding reflected wave. This is commonly referred to as the critical region or interference zone. It lies immediately beyond the critical point $r = r^*$. At the critical point the travel times of the head wave and its associated reflected wave are identical. The difference in travel times of these waves, $t_{\text{reflected}} - t_{\text{head}}$, beyond $r = r^*$ is a positive monotonically-increasing function of r . If the duration $\Delta t = 1/f$ (f = predominant frequency) of the source pulse is larger than this time difference the two waves interfere. If it is smaller, both waves exist independently. Hence, the end of the interference zone is determined by the expression

$$t_{\text{reflected}} - t_{\text{head}} = \Delta t \quad 1.3$$



Table 1.1. Velocity distributions and head wave existence. This table displays the possibility of formation of any of the eight basic types of head waves resulting from an R-wave interacting with any of the six types of interfaces.

Interface Type

R-wave	H-wave	$\sin \theta^*$	A	B	C	D	E	F
PP	PPP	α_1/α_2	N	N	N	Y	Y	Y
	PSP	α_1/β_2	N	N	N	N	N	Y
PS	PPS	α_1/α_2	N	N	N	Y	Y	Y
	PSS	α_1/β_2	N	N	N	N	N	Y
SP	SPP	β_1/α_2	N	N	N	Y	Y	Y
	SSP	β_1/β_2	N	N	N	N	N	Y
SS	SPS	β_1/α_2	N	Y	Y	Y	Y	Y
	SSS	β_1/β_2	N	N	Y	N	Y	Y

Interface: A: $\alpha_1 > \beta_1 > \alpha_2 > \beta_2$ D: $\alpha_2 > \alpha_1 > \beta_1 > \beta_2$ θ^* = critical angle

B: $\alpha_1 > \alpha_2 > \beta_1 > \beta_2$ E: $\alpha_2 > \alpha_1 > \beta_2 > \beta_1$ Y - head wave can exist

C: $\alpha_1 > \alpha_2 > \beta_2 > \beta_1$ F: $\alpha_2 > \beta_2 > \alpha_1 > \beta_1$ N - head wave cannot exist

In general it is not possible to find an explicit formula for the length of the interference zone and equation 1.3 must be solved numerically. Appendix A.4 gives more details on this.

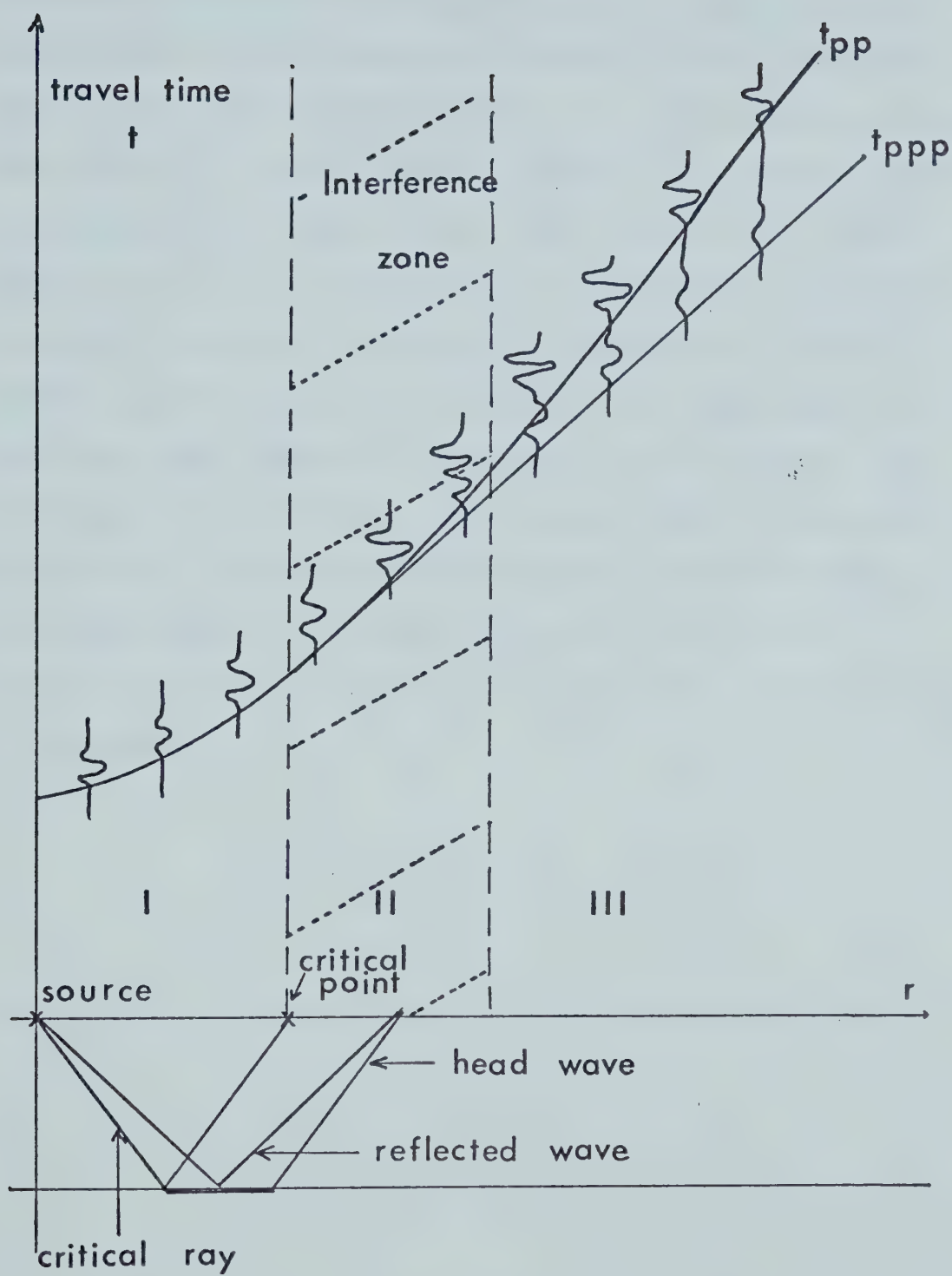
A schematic picture of the interference phenomenon is shown in Fig 1.2 (from Cervený and Ravindra (10), p. 168). In region I only the reflected PP wave exists. In region II the reflected PP and head PPP interfere with each other. In region III both waves exist independently of each other. Amplitudes of head waves calculated using asymptotic ray theory cannot be used in region II due to proximity to the singularity $r = r^*$. It is with the total interference wave amplitude in this region that this study concerns itself.

The possibility exists that the receiver may lie within the interference zones of the reflected wave and P type and S type head wave. This would occur only if the distance between first and second critical points was less than the length of the P-type head wave's interference zone. In this case, all three waves would interfere. However, this is a rather artificial situation since it requires a large velocity contrast at the refracting interface (or small difference in P and S velocities in the refractor) as well as a very low source frequency. This phenomena will not be considered in this study, however the formulae for it could be easily obtained from the mathematics contained herein.

It was necessary to calculate the expressions for



Figure 1.2. The interference zone. Interference zone is denoted by II. The head wave exists only beyond the critical point.



wave amplitude for all eight head waves listed in Table 1.1. To maintain brevity in this publication, only two cases, PPP and PSP, will be analyzed in detail as the other six cases follow the same formulation. The PPP case has only been solved for a multi-layered medium with exactly two P ray segments per layer and with only one critical point (Cerveny (9)). It is the object of the author to present theoretical formulae and numerical evaluations for the general problem consisting of any of the eight types of head waves with arbitrary velocity distributions at any interface. Multiple head waves as described in Chapter 2 will also be considered. The formulae for interference wave amplitudes of all eight cases are presented in Appendix A.5. These represent the main new contributions by the author.

CHAPTER 2

A WAVE METHOD SOLUTION FOR RAY AMPLITUDE

2.1 Introduction to the Exact Wave Method

The medium under consideration, must consist of m elastic, isotropic, homogeneous layers over an elastic half-space. The interfaces separating these layers must be plane and parallel. At the free surface let there be a source of harmonic waves. Also let there be a receiver at a given distance, r , from the source and also at the free surface. The coordinates in use shall be cylindrical, (r, z, ψ) with the origin on the first interface vertically below the source. This implies that the source is at $(0, h_1, 0)$ where h_1 is the thickness of the first layer. It will be assumed that the source is symmetrical so that the solution is ψ -independent. The velocities of propagation of compressional and shear waves, and density in the j^{th} layer will be denoted by $\alpha_j, \beta_j, \rho_j, j=1,2,\dots,m+1$, respectively. The velocity distribution at the bottom interface will be vital in determining what type of head waves will arise from the bottoming interface. By consulting Table 1.1 we find that the velocity distribution $\alpha_{m+1} > \beta_{m+1} > \alpha_m > \beta_m$ will produce all eight types of head waves. In the ensuing discussion, this is the velocity distribution which will be taken.

The kinematic properties (i.e., travel-time curves) of any ray can be totally expressed by the P and S wave velocities and the number of P-type and S-type ray segments in each layer. The latter quantities are denoted by N_{Pj} and N_{Sj} , $j=1,2,\dots,m$. Figure 2.1 summarizes all the quantities discussed above.

It is desirable to derive expressions for horizontal, u , and vertical, w , components of displacement due to the arrival of an arbitrary ray at the receiver. If the potentials of compressional waves and shear waves are represented by Φ and Ψ respectively, then the following equations are valid in all m layers and the half-space (Cerveny (9))

$$u = \frac{\partial \Phi}{\partial r} + \frac{\partial^2 \Psi}{\partial r \partial z}$$

$$w = \frac{\partial \Phi}{\partial z} + \frac{1}{r} \frac{\partial}{\partial r} \left(r \frac{\partial \Psi}{\partial r} \right) \quad 2.1$$

where Φ and Ψ satisfy the following wave equations in all layers and the half-space

$$\frac{1}{r} \frac{\partial}{\partial r} \left(r \frac{\partial \Phi}{\partial r} \right) + \frac{\partial^2 \Phi}{\partial z^2} = \frac{1}{\alpha_i^2} \frac{\partial^2 \Phi}{\partial t^2}$$

$$\frac{1}{r} \frac{\partial}{\partial r} \left(r \frac{\partial \Psi}{\partial r} \right) + \frac{\partial^2 \Psi}{\partial z^2} = \frac{1}{\beta_i^2} \frac{\partial^2 \Psi}{\partial t^2} \quad 2.2$$

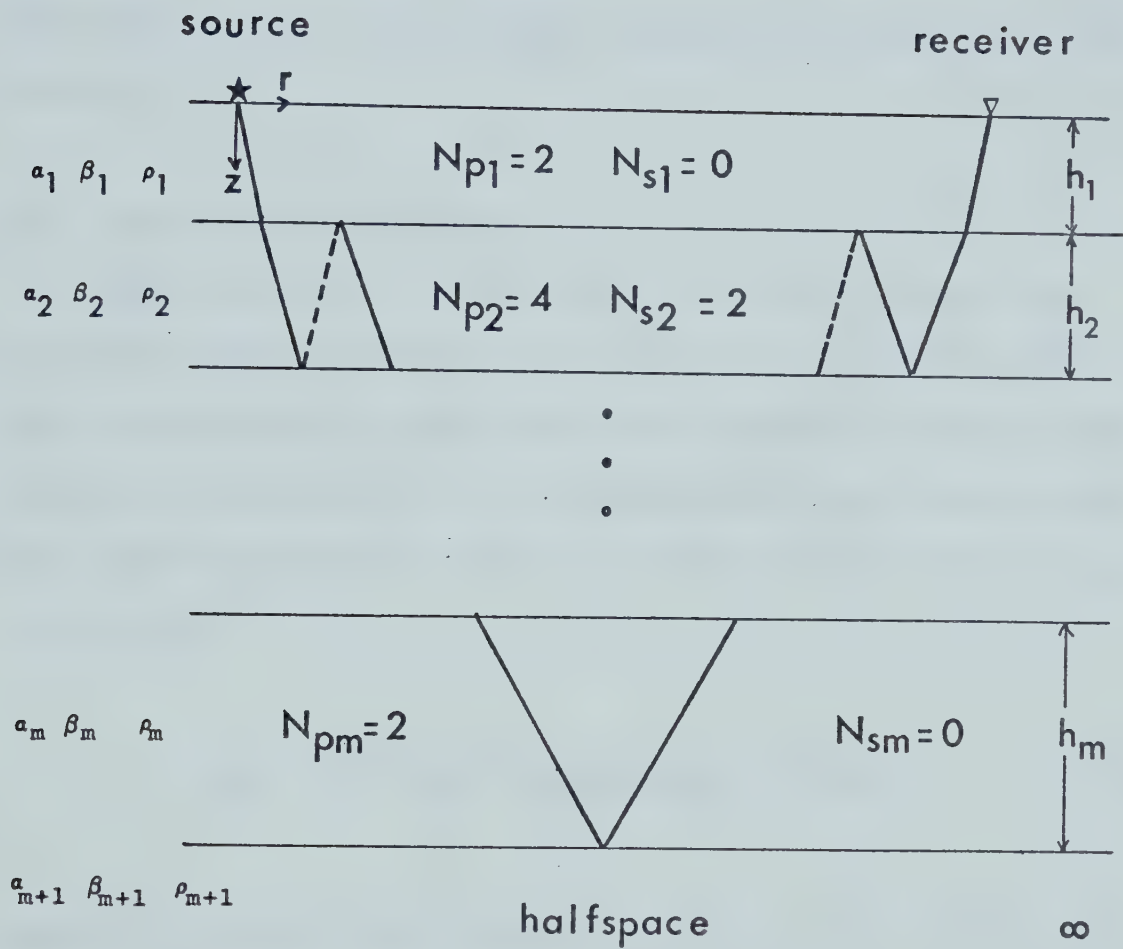


Figure 2.1. The medium description.

In this chapter we will only consider those rays which have a bottoming reflection of type PP. The PPP and PSP head waves will be discussed in reference to their interference with the reflected PP wave. The method of calculation basically follows Cervený (6,8,9). The technique has been adjusted and considerably expanded to allow an arbitrary ray.

2.2 The PP Reflected Wave

The criterion for this wave to exist is that the bottoming reflection be of type PP, i.e., an incident P wave and reflected P wave from the interface between layer m and the half-space. It is assumed that the source radiates compressional (P) waves and that their potential Φ_0 is given by

$$\Phi_0 = (i k R_0)^{-1} \exp(i k R_0 - i \omega t) \quad 2.3$$

where $R_0 = (r^2 + (h_1 - z)^2)^{1/2}$

$$\omega = 2 \pi f = 2 \pi (\text{predominant source frequency})$$

$$k = \omega / \alpha_1$$

By employing the Sommerfeld integral (see Appendix A.1) the incident wave potential can be written as.

$$\Phi_0 = \frac{e^{-i \omega t}}{2} \int_{-\infty}^{\infty} H_0^1(k r q_1) \exp(i k |z - h_1| (1 - q_1^2)^{1/2}) q_1 (1 - q_1^2)^{-1/2} dq_1 \quad 2.4$$

where H_0^1 is a Hankel function of first kind and zeroth order.

For the duration of these theoretical developments, a basic reflection will be defined as the bottoming reflection from the interface dividing the m^{th} layer from the half-space.

According to Brekhovskikh (4), the following integral expression describes the potential of the wave with a basic PP reflection as measured at the surface:

$$\Phi = \frac{e^{-i \omega t}}{2} \int_{-\infty}^{\infty} R_{11}(q) \sigma(q) H_0^1(k r q_1) \exp(i k \bar{B}(q_1)) q_1 (1 - q_1^2)^{-1/2} dq_1 \quad 2.5$$

where $R_{11}(q)$ is the reflection coefficient of plane waves at the m^{th} interface. $\sigma(q)$ is the product of all reflection and transmission coefficients suffered by the ray in its path from source to receiver, except R_{11} , q is defined by

$$q_i = \frac{q_1 \alpha_i}{\alpha_1} \quad q = q_m = \frac{q_1 \alpha_m}{\alpha_1}$$

$\overline{B}(q_1)$ is a function defined by

$$\begin{aligned}\overline{B}(q_1) = & \sum_{i=2}^m N_{P \ i} h_i \left(\frac{\alpha_1^2}{\alpha_i^2} - q_1^2 \right)^{1/2} \\ & + \sum_{i=2}^m N_{S \ i} h_i \left(\frac{\alpha_1^2}{\beta_i^2} - q_1^2 \right)^{1/2} + (z+h_1)(1-q_1^2)^{1/2}\end{aligned}$$

The reflection coefficient can be expressed as

$$\begin{aligned}R_{11}(q) = & V_0(q) + V_1(q) S(q) + V_2(q) R(q) \\ & + V_3(q) S(q) R(q)\end{aligned}\tag{2.6}$$

for

$$R = \frac{\beta_{m+1}}{\alpha_{m+1}} \left(\frac{\alpha_m^2}{\beta_{m+1}^2} - q^2 \right)^{1/2}$$

$$S = \left(\frac{\alpha_m^2}{\alpha_{m+1}^2} - q^2 \right)^{1/2}$$

For a full derivation of this consult Appendix A.2.

Because of the square roots in this coefficient, the integral in 2.5 is a multi-valued function. The Riemann surface is defined by:

$$\arg(v^2 - q_i^2)^{1/2} = \pi/2 \quad \text{for } q_i > v, \quad i=1, \dots, m$$

for an arbitrary v (say $v = 1, \alpha_i/\alpha_{i+1}, \alpha_i/\beta_{i+1}$).

Employing equations 2.1, we can determine the components of displacement of the wave

$$u = - \frac{k}{2} e^{-i \omega t} \int_{-\infty}^{\infty} R_{11}(q) \sigma(q) H_1^1(k r q_1) \exp(i k \bar{B}(q_1))$$

$$q_1^2 (1 - q_1^2)^{-1/2} dq_1$$

$$w = \frac{i k}{2} e^{-i \omega t} \int_{-\infty}^{\infty} R_{11}(q) \sigma(q) H_0^1(k r q_1)$$

$$\exp(i k \bar{B}(q_1)) q_1 dq_1$$

where H_1^1 denotes a Hankel function of first order and first kind. If we assume that we can make a change of integration contours for which $|q_1| \geq \bar{q}_1$, $\bar{q}_1 \in \text{real numbers}$, for all points along the new contour, \bar{D} , then $|k r q_1| \geq k r \bar{q}_1$. If $k r \bar{q}_1 \gg 1$, then $|k r q_1| \gg 1$ and we can employ the following asymptotic expansions for the Hankel function (see Abramowitz and Stegun (1), p. 364)

$$H_0^1(x) = \left(\frac{2}{\pi x}\right)^{1/2} \exp(i x - \frac{i \pi}{4})$$

$$H_1^1(x) = \left(\frac{2}{\pi x}\right)^{1/2} \exp\left(i x - \frac{3 i \pi}{4}\right)$$

with the source and receiver at the same distance from the first interface we have

$$u = \exp(-i \omega t + \frac{i \pi}{4}) \left(\frac{k}{2 \pi r}\right)^{1/2} \int_{\bar{D}} R_{11}(q) \sigma(q) \exp(i k B(q_1)) \\ (1-q_1^2)^{-1/2} q_1^{3/2} dq_1$$

$$w = \exp(-i \omega t + \frac{i \pi}{4}) \left(\frac{k}{2 \pi r}\right)^{1/2} \int_{\bar{D}} R_{11}(q) \sigma(q) \exp(i k B(q_1)) \\ q_1^{1/2} dq_1 \quad 2.7$$

where

$$B(q_1) = r q_1 + \sum_{i=1}^m N_{P \ i} h_i \left(\frac{\alpha_1^2}{\alpha_i^2} - q_1^2\right)^{1/2} \\ + \sum_{i=1}^m N_{S \ i} h_i \left(\frac{\alpha_1^2}{\beta_i^2} - q_1^2\right)^{1/2}$$

The choice of the contour of integration, \bar{D} , requires some discussion. The original contour $(-\infty, \infty)$ along the real axis is unsuitable for three reasons:

(1) the integrand oscillates rapidly near the singular

points;

- (2) the value of the integrals along this path yields displacements for the reflected wave in the broad sense (i.e., the sum of the contributions from simple reflected wave, head wave, Stonely wave and inhomogeneous head wave). In this investigation interest is focused on the contributions of the individual wave terms;
- (3) the asymptotic expansions of the Hankel functions are invalid along the previous contour.

The integrand contains four square roots giving it its multiplicity; these are stated below with their corresponding branch points

$$S = \left(\frac{\alpha_m^2}{\alpha_{m+1}^2} - q^2 \right)^{1/2} : \quad \pm \alpha_m / \alpha_{m+1}$$

$$R = \frac{\beta_{m+1}}{\alpha_{m+1}} \left(\frac{\alpha_m^2}{\beta_{m+1}^2} - q^2 \right)^{1/2} : \quad \pm \alpha_m / \beta_{m+1}$$

$$P = (1 - q^2)^{1/2} : \quad \pm 1$$

$$Q = \left(1 - \frac{\beta_m^2}{\alpha_m^2} q^2 \right)^{1/2} : \quad \pm \alpha_m / \beta_m$$

In this investigation only homogeneous head waves of the first kind will be considered which eliminates the need to study the effect of the last two radicals, P and Q.

The method of steepest descent is used to calculate the integrals. The saddle point is evaluated by solving

$$\left(\frac{d B(q_1)}{d q_1} \right)_{q_1=x_1} = 0$$

This point, $q_1 = x_1$, is given by numerically solving

$$r = \sum_{i=1}^m \frac{N_{P_i} h_i x_1}{\frac{\alpha_1^2}{\alpha_i^2} - x_1^2)^{1/2}} + \sum_{i=1}^m \frac{N_{S_i} h_i x_1}{\left(\frac{\alpha_1^2}{\beta_i^2} - x_1^2 \right)^{1/2}} \quad 2.8$$

By inspection of 2.8 we see that x_1 must correspond to some angle-related quantity. It is easy to see that x_1 is definable as

$$x_1 = \frac{\alpha_1 \sin \theta_1}{v_1} \quad 2.9$$

where θ_1 = angle of incidence of first ray segment upon first interface

v_1 = velocity of propagation of first ray segment.

This parameter can be transformed to an analogous quantity

in any layer by Snell's Law:

$$x_i = \frac{\alpha_i}{\alpha_1} x_1 ; \quad i=1,2,\dots,m, \quad x = x_m = \frac{\alpha_m}{\alpha_1} x_1$$

The angles θ_m^* , $\tilde{\theta}_m^*$ given by

$$\sin \theta_m^* = \frac{\alpha_m}{\alpha_{m+1}} \quad \sin \tilde{\theta}_m^* = \frac{\alpha_m}{\beta_{m+1}}$$

are called the critical angles for the formation of PPP and PSP head waves from the bottoming interface. The corresponding critical parameters in the first layer, x_1^* , \tilde{x}_1^* , can be written

$$x_1^* = \frac{\alpha_1}{\alpha_{m+1}} \quad \tilde{x}_1^* = \frac{\alpha_1}{\beta_{m+1}}$$

and in the m^{th} layer $x^* = \alpha_m/\alpha_{m+1}$, $\tilde{x}^* = \alpha_m/\beta_{m+1}$. The critical distance for this ray is the minimal distance from the source at which the head wave can appear. Using the quantities defined above, we can express these distances as

$$r_{\text{PPP}}^* = \sum_{i=1}^m \frac{\alpha_i}{\alpha_{m+1}} \frac{N_{P_i} h_i}{\left(1 - \frac{\alpha_i^2}{\alpha_{m+1}^2}\right)^{1/2}} + \sum_{i=1}^m \frac{\beta_i}{\alpha_{m+1}} \frac{N_{S_i} h_i}{\left(1 - \frac{\beta_i^2}{\alpha_{m+1}^2}\right)^{1/2}}$$

$$r_{PSP}^* = \sum_{i=1}^m \frac{\alpha_i}{\beta_{m+1}} \frac{N_P \cdot i \cdot h_i}{\left(1 - \frac{\alpha_i^2}{\beta_{m+1}^2}\right)^{1/2}} + \sum_{i=1}^m \frac{\beta_i}{\beta_{m+1}} \frac{N_S \cdot i \cdot h_i}{\left(1 - \frac{\beta_i^2}{\beta_{m+1}^2}\right)^{1/2}} \quad 2.10$$

The new integration path consists of several parts as shown in Figure 2.2. The portion D_0 is a semi-circle in the upper half-plane of the complex variable q_1 . The path D is given by the parametric equation

$$(1 - q_1^2)^{1/2} = (1 - x_1^2)^{1/2} + p \cdot \exp(-i \pi/4);$$

$$-\infty < p < \infty \quad 2.11$$

in the real parameter, p . This path passes through the saddle point $q_1 = x_1$ for $p = 0$. Depending upon the value of x_1 , and hence upon the epicentral distance, it may be necessary to introduce additional contours D_1 and D_2 , which circumvent the cuts of the radicals S and R . If these cuts had not been circumvented the change of variable of integration would have resulted in ending up on a different Riemann sheet than we had begun on, making the deformation of the path invalid. The branch cuts of the radicals S and R are given by the following parametric equations:

$$(a) \quad (1 - q_1^2)^{1/2} = (1 - x_1^{*2})^{1/2} + p \exp(-i \pi/4)$$

$$(b) \quad (1 - q_1^2)^{1/2} = (1 - \tilde{x}_1^{*2})^{1/2} + p \exp(-i \pi/4) \quad 2.12$$

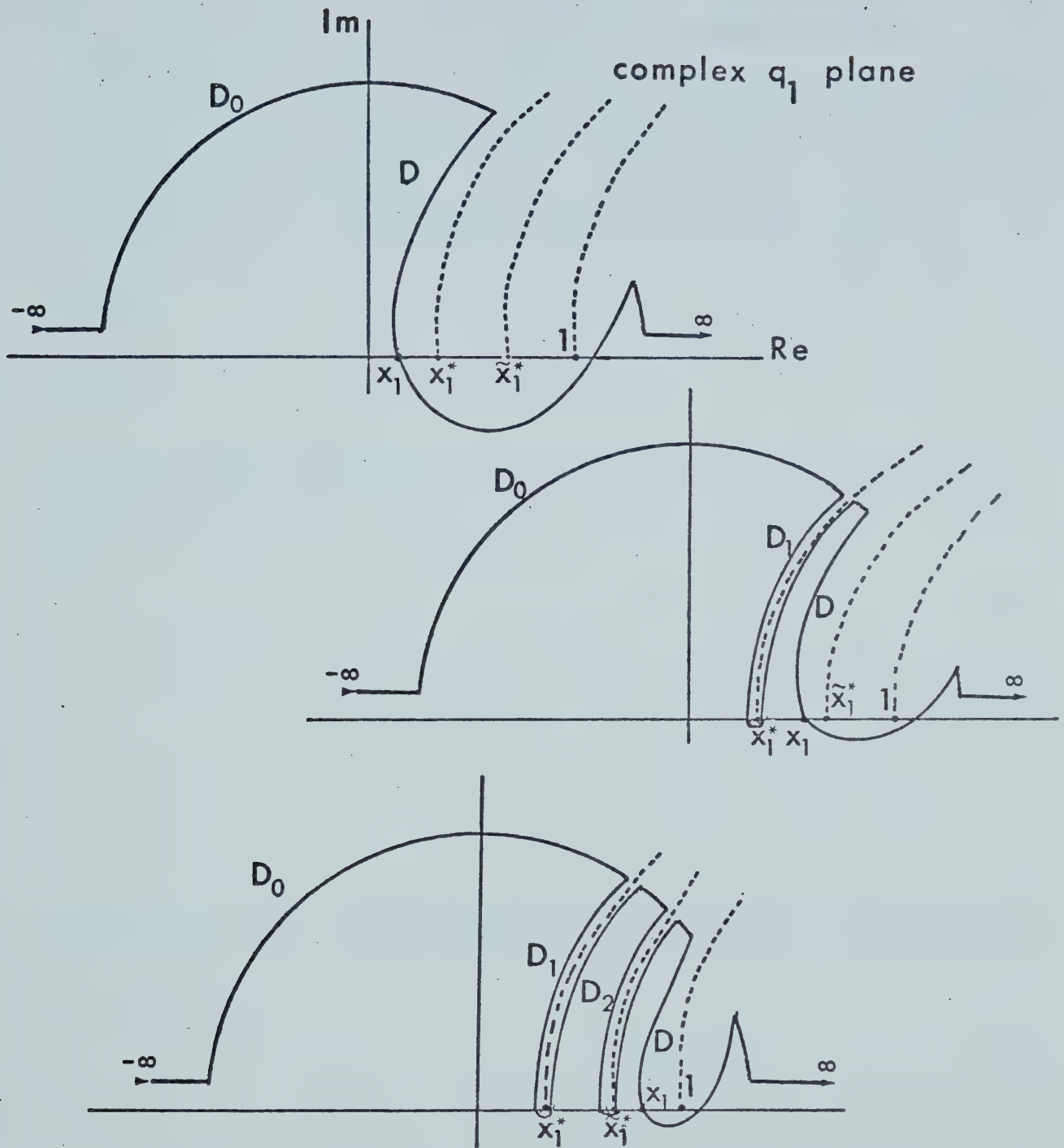


Figure 2.2. The contours of integration.

for p in the real range $(0, \infty)$.

Upon increasing the radius of the semi-circle to infinity, the contribution due to it vanishes. The original integral is then equal to the integral along D , or along D and D_1 , or along D , D_1 and D_2 depending upon the mutual position, of x_1 , x_1^* , \tilde{x}_1^* . The following three cases can occur:

$$(1) \quad x_1 < x_1^* < \tilde{x}_1^* < 1$$

In this region only the reflected wave exists, the displacements of which are denoted by $u = u^0$, $w = w^0$

$$u^0 = \exp(-i \omega t + \frac{i \pi}{4}) \left(\frac{k}{2 \pi r} \right)^{1/2} \int_D R_{11}(q) \sigma(q) \exp(i k B(q)) \\ (1-q_1^2)^{-1/2} q_1^{3/2} dq_1$$

$$w^0 = \exp(-i \omega t + \frac{i \pi}{4}) \left(\frac{k}{2 \pi r} \right)^{1/2} \int_D R_{11}(q) \sigma(q) \exp(i k B(q)) \\ q_1^{1/2} dq_1 \quad 2.13$$

All radicals are given by $\arg(S, R, P, Q) = 0$ for $p = 0$.

$$(2) \quad x_1^* < x_1 < \tilde{x}_1^* < 1$$

In this region, the epicentral distance lies beyond the first critical point and the contour D_0 intersects the

branch cut of the radical S . The displacement components of the PPP head wave will be denoted by u^* , w^* and the total displacement field by $u = u^0 + u^*$, $w = w^0 + w^*$ where

$$u^* = \exp(-i \omega t + \frac{i \pi}{4}) \left(\frac{k}{2 \pi r} \right)^{1/2} \int_D R_{11}(q) \sigma(q) \exp(i k B(q_1)) \\ (1-q_1^2)^{-1/2} q_1^{3/2} dq_1$$

$$w^* = \exp(-i \omega t + \frac{i \pi}{4}) \left(\frac{k}{2 \pi r} \right)^{1/2} \int_D R_{11}(a) \sigma(q) \exp(i k B(q_1)) \\ q_1^{1/2} dq_1 \quad 2.14$$

The branch of the square roots in the integrals for u^0 and w^0 for $p = 0$ is given by $\arg(S) = \pi/2$ and $\arg(R) = 0 = \arg(P, Q)$.

In the integrals u^* and w^* the arguments of the square roots are given by the following for $p = 0$ (i.e., for $q_1 = x_1^*$)

$$\arg(P, Q, R) = 0.$$

S has a different sign on each side of the branch cut. See the section on the PPP head wave for details.

$$(3) \quad x_1^* < \tilde{x}_1^* < x_1 < 1$$

In this region the epicentral distance lies beyond the second critical point and the contour D_0 intersects the cuts of both radicals S and R . The total displacements are given by $u = u^0 + u^* + \tilde{u}^*$, $w = w^0 + w^* + \tilde{w}^*$ where

$$\begin{aligned} \tilde{u}^* = \exp(-i \omega t + \frac{i \pi}{4}) \left(\frac{k}{2 \pi r} \right)^{1/2} \int_{D_2} R_{11}(q) \sigma(q) \exp(i k B(q_1)) \\ (1-q_1^2)^{-1/2} q_1^{3/2} dq_1 \\ \tilde{w}^* = \exp(-i \omega t + \frac{i \pi}{4}) \left(\frac{k}{2 \pi r} \right)^{1/2} \int_{D_2} R_{11}(q) \sigma(q) \exp(i k B(q_1)) \\ q_1^{1/2} dq_1 \end{aligned} \quad 2.15$$

The branch of the square roots in the integrals u^0 , w^0 for $p = 0$ is given by $\arg(R, S) = \pi/2$, $\arg(P, Q) = 0$. The same conditions hold for u^* , w^* as in the previous case. In the integrals \tilde{u}^* , \tilde{w}^* the arguments of the radicals are given by the following:

$$\arg(P, Q) = 0 \quad \arg(S) = \pi/2.$$

The radical R has a different sign on either side of the cut.

In this section, displacement components of the PP wave reflected from the m^{th} interface will be discussed.

For this purpose a saddle point method of evaluation will be employed. To do this the function B in the exponent of the integrand will be expanded in a Taylor series about the saddle point $q_1 = x_1$ for small values of P . The algebra for this is found in Appendix A.3. The expansion is

$$B(q_1) = B(x_1) + i p^2 (r - \tilde{r}) / 2 x_1^3 \quad 2.16$$

where

$$\frac{\tilde{r}}{x_1^3} = \sum_{i=1}^m \frac{N_{P \ i} h_i \left(\frac{\alpha_1^2}{\alpha_i^2} - 1 \right)}{\left(\frac{\alpha_1^2}{\alpha_i^2} - x_1^2 \right)^{3/2}} + \sum_{i=1}^m \frac{N_{S \ i} h_i \left(\frac{\alpha_1^2}{\beta_i^2} - 1 \right)}{\left(\frac{\alpha_1^2}{\beta_i^2} - x_1^2 \right)^{3/2}}$$

By using Snell's Law and carefully considering the basic geometry of the ray and the medium, it can be shown that

$$\frac{B(x_1)}{\alpha_1} = t_{pp} = \sum_{i=1}^m \frac{N_{P \ i} h_i}{\alpha_i \left(1 - \frac{\alpha_i^2 x_1^2}{\alpha_1^2} \right)^{1/2}} + \sum_{i=1}^m \frac{N_{S \ i} h_i}{\beta_i \left(1 - \frac{\beta_i^2 x_1^2}{\alpha_1^2} \right)^{1/2}}$$

which is the travel time curve of the simple reflected wave. We introduce the new variable, p , into the integrals in 2.13 to 2.15 by the parametric equation 2.11. This leads to

$$u^0 = \exp(-i \omega(t-t_{pp})) \left(\frac{k}{2 \pi r} \right)^{1/2} \int_{-\infty}^{\infty} R_{11}(q) \sigma(q)$$

$$\exp(-k \frac{(r-\tilde{r})}{2 x_1^3} p^2) q_1^{1/2} dp$$

$$w^0 = \exp(-i \omega(t-t_{pp})) \left(\frac{k}{2 \pi r} \right)^{1/2} \int_{-\infty}^{\infty} R_{11}(q) \sigma(q) \quad 2.17$$

$$\exp(-k \frac{(r-\tilde{r})}{2 x_1^3} p^2) \frac{(1-q_1^2)^{1/2}}{q_1^{1/2}} dp$$

where the variables q and q_1 are functions of the variable p in a fashion according to 2.11. The region near $p = 0$ will have the most significance due to the exponential term in the integrand. The functions in the integrand which do not vary rapidly with respect to p may be substituted by their values at $p = 0$ (i.e., $q = x$ and $q_1 = x_1$)

$$u^0 = x_1 \sigma(x) \exp(-i \omega(t-t_{pp})) \left(\frac{k}{2 \pi r x_1} \right)^{1/2} \int_{-\infty}^{\infty} R_{11}(q)$$

$$\exp(-k \frac{(r-\tilde{r})}{2 x_1^3} p^2) dp$$

$$w^0 = (1-x_1^2)^{1/2} \sigma(x) \exp(-i \omega(t-t_{pp})) \left(\frac{k}{2 \pi r x_1} \right)^{1/2} \int_{-\infty}^{\infty}$$

$$R_{11}(q) \exp(-k \frac{(r-\tilde{r})}{2 x_1^3} p^2) dp \quad 2.18$$

For brevity, let I denote the integrals in 2.18

$$I = \int_{-\infty}^{\infty} R_{11}(q) \exp\left(-k \frac{(r-\tilde{r})}{2 x_1^3} p^2\right) dp \quad 2.19$$

Expansion 2.6 is used to express the reflection coefficient in a more convenient form. Since the V_i 's are smoothly varying functions of p , we can approximate them by their values at $p = 0$ or at $q = x$.

$$V_i(q(p)) \doteq V_i(q(0)) = V_i(x) \quad i=0,1,2,3.$$

This leaves

$$\begin{aligned} I = & V_0(x) \int_{-\infty}^{\infty} \exp\left(-k \frac{(r-\tilde{r})}{2 x_1^3} p^2\right) dp \\ & + V_1(x) \int_{-\infty}^{\infty} S(p) \exp\left(-k \frac{(r-\tilde{r})}{2 x_1^3} p^2\right) dp \\ & + V_2(x) \int_{-\infty}^{\infty} R(p) \exp\left(-k \frac{(r-\tilde{r})}{2 x_1^3} p^2\right) dp \\ & + V_3(x) \int_{-\infty}^{\infty} S(p) R(p) \exp\left(-k \frac{(r-\tilde{r})}{2 x_1^3} p^2\right) dp. \end{aligned} \quad 2.20$$

The radicals S and R can be rewritten as:

$$S = \frac{\alpha_m}{\alpha_1} i((1-x_1^{*2})^{1/2} + (1-x_1^2)^{1/2} + p e^{-i \pi/4})^{1/2} ((1-x_1^{*2})^{1/2} - (1-x_1^2)^{1/2} - p e^{-i \pi/4})^{1/2}$$

$$R = \frac{\alpha_m}{\alpha_1} \frac{\beta_{m+1}}{\alpha_{m+1}} i((1-\tilde{x}_1^{*2})^{1/2} + (1-x_1^2)^{1/2} + p e^{-i \pi/4})^{1/2} ((1-\tilde{x}_1^{*2})^{1/2} - (1-x_1^2)^{1/2} - p e^{-i \pi/4})^{1/2}$$

An approximation can be made to the three integrals in equation 2.20 preceded by V_1 , V_2 and V_3 . We shall examine the approximation in detail for the integral preceded by V_1 since the other two follow the same format. Using the above substitution for $S(p)$ one arrives at an integral like

$$\int_{-\infty}^{\infty} ((1-x_1^{*2})^{1/2} + (1-x_1^2)^{1/2} + p e^{-i \pi/4})^{1/2} ((1-x_1^{*2})^{1/2} - (1-x_1^2)^{1/2} - p e^{-i \pi/4})^{1/2} \cdot \exp(-k \frac{(r-\tilde{r})}{2 x_1^3} p^2) dp$$

Let

$$\xi = (\frac{k(r-\tilde{r})}{2 x_1^3})^{1/2} ((1-x_1^{*2})^{1/2} + (1-x_1^2)^{1/2})^{1/2}$$

Then the integral becomes

$$\int_{-\infty}^{\infty} \left(\xi^2 \frac{2 x_1^3}{k(r-\tilde{r})} + p e^{-i \pi/4} \right)^{1/2} \left((1-x_1^{*2})^{1/2} - (1-x_1^2)^{1/2} \right. \\ \left. - p e^{-i \pi/4} \right)^{1/2} \cdot \exp\left(-\frac{\xi^2 p^2}{(1-x_1^{*2})^{1/2} + (1-x_1^2)^{1/2}}\right) dp$$

If $\xi \gg 1$, the main contribution to the integral will be for p near zero due to the exponential term. Since the term $(1-x_1^{*2})^{1/2} + (1-x_1^2)^{1/2}$ is always less than 2, the condition $\xi \gg 1$ is still sufficient evidence to consider contributions for p near zero. The effects of $\xi \gg 1$ will be discussed shortly. With ξ large, one can approximate the first radical as

$$\left(\xi^2 \left(\frac{2 x_1^3}{k(r-\tilde{r})} \right) + p e^{-i \pi/4} \right)^{1/2} \doteq \xi \left(\frac{2 x_1^3}{k(r-\tilde{r})} \right)^{1/2} \\ = \left((1-x_1^{*2}) + (1-x_1^2) \right)^{1/2}$$

for purposes of integration.

For ξ to be large compared to unity, $k(r-\tilde{r})$ is required to be large. Since $k = 2 \pi f/\alpha_1$, it is obvious that the condition is valid for high frequencies. From Appendix A.3 (equations A.3.3 and A.3.4) we see that $(r-\tilde{r})$ is

$$(r - \tilde{r}) = (x_1 - x_1^3) \left(\sum_{i=1}^m \frac{N_{Pi} h_i \alpha_1^2}{\alpha_i^2 \left(\frac{\alpha_1^2}{\alpha_i^2} - x_1^2 \right)^{3/2}} + \sum_{i=1}^m \frac{N_{Si} h_i \alpha_1^2}{\beta_i^2 \left(\frac{\alpha_1^2}{\beta_i^2} - x_1^2 \right)^{3/2}} \right)$$

Since $x_1 < 1$, the term $(x_1 - x_1^3)$ will always be positive, so that $(r - \tilde{r})$ is a positive quantity. For the one layer, P rays only case, it is clear that $r - \tilde{r} = r$ so that we limit ourselves to epicentral distance far from the source; far in terms of the wavelength of the source. For the case where rays with only P segment are studied, equation 2.16 shows that \tilde{r} is negative, thus $r - \tilde{r} > r$. This is for compressional velocity increasing with depth. For the general situation of mixed P and S ray segments in a multi-layered medium, the expressions become too cumbersome to examine analytically. The criterion of $k(r - \tilde{r})/2 x_1^3 = \pi(r - \tilde{r})/x_1^3 \lambda \gg 1$ is tested computationally. Finally, after employing this approximation for $S(p)$ and a similar one for $R(p)$, we arrive at the following expressions for the radicals:

$$S = \frac{i \alpha_m}{\alpha_1} \left((1 - x_1^{*2})^{1/2} + (1 - x_1^2)^{1/2} \right)^{1/2} \left((1 - x_1^{*2})^{1/2} - (1 - x_1^2)^{1/2} - p e^{-i \pi/4} \right)^{1/2}$$

$$R = \frac{i \alpha_m}{\alpha_1} \frac{\beta_{m+1}}{\alpha_{m+1}} \left((1 - \tilde{x}_1^{*2})^{1/2} + (1 - x_1^2)^{1/2} \right)^{1/2} \left((1 - \tilde{x}_1^{*2})^{1/2} - (1 - x_1^2)^{1/2} - p e^{-i \pi/4} \right)^{1/2} \quad 2.21$$

where

$$\arg((1-x_1^{*2})^{1/2} + (1-x_1^2)^{1/2})^{1/2} = 0$$

$$\arg((1-\tilde{x}_1^{*2})^{1/2} + (x-x_1^2)^{1/2})^{1/2} = 0$$

and if $p = 0$

$$\arg((1-x_1^{*2})^{1/2} - (1-x_1^2)^{1/2} - p e^{-i \pi/4})^{1/2}$$

$$= \begin{cases} -\pi/2 & \text{if } q_1 < x_1^* \\ 0 & \text{if } q_1 > x_1^* \end{cases}$$

$$\arg((1-\tilde{x}_1^{*2})^{1/2} - (1-x_1^2)^{1/2} - p e^{-i \pi/4})^{1/2}$$

$$= \begin{cases} -\pi/2 & \text{if } q_1 < \tilde{x}_1^* \\ 0 & \text{if } q_1 > \tilde{x}_1^* \end{cases}$$

Substituting 2.21 into 2.20 and setting

$$\phi = p \left(\frac{k(r-\tilde{r})}{2 x_1^3} \right)^{1/2}$$

and for brevity of notation introducing

$$b_1 = ((1 - x_1^{*2})^{1/2} - (1 - x_1^2)^{1/2}) \left(\frac{k(r-\tilde{r})}{2 x_1^3} \right)^{1/2}$$

$$b_2 = ((1 - \tilde{x}_1^{*2})^{1/2} - (1 - x_1^2)^{1/2}) \left(\frac{k(r-\tilde{r})}{2 x_1^3} \right)^{1/2}$$

we have:

$$\begin{aligned} I = & \left(\frac{2 \pi x_1^3}{k(r-\tilde{r})} \right)^{1/2} (V_0(x) + i V_1(x) \frac{\alpha_m}{\alpha_1} ((1 - x_1^{*2})^{1/2} \\ & + (1 - x_1^2)^{1/2})^{1/2} \left(\frac{2 x_1^3}{k(r-\tilde{r})} \right)^{1/4} g_1(b_1) \\ & + i V_2(x) \frac{\alpha_m}{\alpha_1} \frac{\beta_{m+1}}{\alpha_{m+1}} ((1 - \tilde{x}_1^{*2})^{1/2} \\ & + (1 - x_1^2)^{1/2})^{1/2} \left(\frac{2 x_1^3}{k(r-\tilde{r})} \right)^{1/4} g_1(b_2) \\ & - V_3(x) \frac{\alpha_m^2}{\alpha_1^2} \frac{\beta_{m+1}}{\alpha_{m+1}} ((1 - x_1^{*2})^{1/2} + (1 - x_1^2)^{1/2})^{1/2} ((1 - \tilde{x}_1^{*2})^{1/2} \\ & + (1 - x_1^2)^{1/2})^{1/2} \left(\frac{2 x_1^3}{k(r-\tilde{r})} \right)^{1/2} \cdot G_1(b_1; b_2)) \end{aligned} \quad 2.22$$

where g_1 , G_1 are defined as:

$$g_1(x) = \pi^{-1/2} \int_{-\infty}^{\infty} (x - \phi e^{-i\pi/4})^{1/2} e^{-\phi^2} d\phi$$

$$G(x; y) = \pi^{-1/2} \int_{-\infty}^{\infty} (x - \phi e^{-i\pi/4})^{1/2} (y$$

$$- \phi e^{-i\pi/4})^{1/2} e^{-\phi^2} d\phi$$

2.23

The arguments of the radicals for $\phi = 0$ are

$$\arg(x + \phi e^{-i\pi/4})^{1/2} = \begin{cases} -\pi/2 & \text{for } x < 0 \\ 0 & \text{for } x > 0 \end{cases}$$

$$\arg(y - \phi e^{-i\pi/4})^{1/2} = \begin{cases} -\pi/2 & \text{for } y < 0 \\ 0 & \text{for } y > 0 \end{cases}$$

Two cases must now be considered separately. Either the epicentral distance is near the first critical point ($x_1 = x_1^*$) or near the second critical point ($x_1 = \tilde{x}_1^*$). As was discussed in Chapter 1, it is necessary to assume that the critical points are sufficiently far apart. The term

"sufficiently" is qualified by the condition that the two interference zones do not overlap.

2.3 Receiver Near the First Critical Point

Consider b_2 near the first critical point. In general $|b_2|$ should be quite large in this region. Expressing this mathematically

$$\begin{aligned} (|b_2|)_{x_1=x_1^*} &= \left(\frac{k(r-\tilde{r})}{2 x_1^{*3}} \right)^{1/2} |((1 - \tilde{x}_1^{*2})^{1/2} \\ &\quad - (1 - x_1^{*2})^{1/2})| \gg 1. \end{aligned}$$

This condition can only be met for large k . Since $k = 2 \pi f/\alpha_1$ this implies that this result is valid only for high frequencies. The term $r - \tilde{r}$ also provides the requirement that the epicentral distances be large. If these conditions on b_2 are satisfied we can set

$$g_1(b_2) \doteq b_2^{1/2} \quad G_1(b_1; b_2) \doteq b_2^{1/2} g_1(b_1)$$

With these approximations equation 2.22 becomes

$$\begin{aligned}
I = & \left(\frac{2 \pi x_1^3}{k(r-\tilde{r})} \right)^{1/2} [V_0(x) + V_2(x) \frac{\alpha_m}{\alpha_1} \frac{\beta_{m+1}}{\alpha_{m+1}} (\tilde{x}_1^{*2} - x_1^2)^{1/2} \\
& + g_1(b_1) i \left(\frac{2 x_1^3}{k(r-\tilde{r})} \right)^{1/4} ((1 - x_1^{*2})^{1/2} + (1 - x_1^2)^{1/2})^{1/2} \\
& \cdot (V_1(x) \frac{\alpha_m}{\alpha_1} + V_3(x) \frac{\alpha_m^2}{\alpha_1^2} \frac{\beta_{m+1}}{\alpha_{m+1}} (\tilde{x}_1^{*2} - x_1^2)^{1/2})] \quad 2.24
\end{aligned}$$

The reflection coefficient R_{11} can be decomposed as follows:

$$\begin{aligned}
R_{11} &= V_0 + V_1 S + V_2 R + V_3 R S \\
&= (V_0 + V_2 R) - (-V_1 - V_3 R) S \\
&= C - D \cdot S
\end{aligned}$$

$$R_{11}(x) = C(x) - D(x) \cdot S(x)$$

With this, equation 2.24 can be written as below if we introduce

$$\mu_1(b_1) = g_1(b_1) (b_1)^{-1/2}$$

$$I = \left(\frac{2 \pi x_1^3}{k(r-\tilde{r})} \right)^{1/2} [R_{11}(x) - D(x) (x^{*2} - x^2)^{1/2} (\mu_1(b_1) - 1)] \quad 2.25$$

2.4 Receiver Near the Second Critical Point

In this region we assume

$$(|b_1|)_{x_1=\tilde{x}_1^*} \gg 1$$

$$\left(\frac{k(r-\tilde{r})}{2 x_1^{*2}} \right)^{1/2} |(1 - x_1^{*2})^{1/2} - (1 - \tilde{x}_1^{*2})^{1/2}| \gg 1$$

As in the previous case this condition requires a high frequency for fulfillment. With these conditions we can set

$$g_1(b_1) \doteq (b_1)^{1/2}$$

$$G_1(b_1; b_2) \doteq b_1^{1/2} g_1(b_2)$$

Applying these approximations to equation 2.22 yields

$$\begin{aligned}
I &= \left(\frac{2 \pi x_1^3}{k(r-\tilde{r})} \right)^{1/2} [V_0(x) + \frac{\alpha_m}{\alpha_1} V_1(x) (x_1^{*2} - x_1^2)^{1/2} \\
&+ i g_1(b_2) \frac{\alpha_m}{\alpha_1} \frac{\beta_{m+1}}{\alpha_{m+1}} ((1 - \tilde{x}_1^{*2})^{1/2} \\
&+ (1 - x_1^2)^{1/2})^{1/2} \left(\frac{2 x_1^3}{k(r-\tilde{r})} \right)^{1/4} \\
&\cdot (V_2(x) + V_3(x) \frac{\alpha_m}{\alpha_1} (x_1^{*2} - x_1^2)^{1/2})]
\end{aligned}$$

The reflection coefficient can also be decomposed as

$$\begin{aligned}
R_{11} &= V_0 + V_1 S + V_2 R + V_3 \cdot R \cdot S \\
&= (V_0 + V_1 S) - (-V_2 - V_3 S) R \\
&= C1 - D1 \cdot R
\end{aligned}$$

$$R_{11}(x) = C1(x) - D1(x) \cdot R(x)$$

We again employ μ_1 as defined above, with the result

$$I = \left(\frac{2 \pi x_1^3}{k(r-\tilde{r})} \right)^{1/2} (R_{11}(x) - D_1(x) \frac{\beta_{m+1}}{\alpha_{m+1}} (\tilde{x}^{*2} - x^2)^{1/2} (\mu_1(b_2) - 1)) \quad 2.26$$

At this point we shall summarize by stating the horizontal, u^0 , and vertical w^0 , components of displacements for the simple reflected wave. We substitute 2.25 and 2.26 into 2.18. L is the geometric spreading factor. In Appendix A.3 it is demonstrated that it is very nearly equivalent to that derived by asymptotic ray theory. In this development we define L as

$$L = \frac{(r-\tilde{r})^{1/2} r^{1/2}}{x_1}$$

Near the first critical point:

$$u^0 = \frac{x_1 \sigma(x) e^{-i \omega(t-t_{pp})}}{L} (R_{11}(x) - D(x) (x^{*2} - x^2)^{1/2} (\mu_1(b_1) - 1))$$

$$w^0 = \frac{u^0}{x_1} \cdot (1 - x_1^2)^{1/2} \quad 2.27$$

Near the second critical point:

$$\begin{aligned}
 u^0 &= \frac{x_1 \sigma(x) e^{-i \omega(t-t_{pp})}}{L} (R_{11}(x) \\
 &- D_1(x) \frac{\beta_{m+1}}{\alpha_{m+1}} (\tilde{x}^{*2} - x^2)^{1/2} (\mu_1(b_2) - 1)) \\
 w^0 &= \frac{u^0}{x_1} (1 - x_1^2)^{1/2}
 \end{aligned} \tag{2.28}$$

2.5 The PPP Head Wave

In this section the expression for displacements of a head wave, propagating along the interface between the m^{th} layer and the half-space (layer $m + 1$), as recorded at the surface, will be discussed. The expressions to be evaluated are given by 2.14. We introduce a new integration parameter, p , defined by 2.12(a), into 2.14. The values of p , on both sides of the branch cut will be in the range $(0, \infty)$. The value of $S(x)$ will have different signs on either side of the path. $(S(x))_{x=x(p)}$ can be extended using 2.12(a)

$$(S(x))_{x=x(p)} = \frac{\alpha_m}{\alpha_1} (p + 2 e^{i \pi/4} (1 - x_1^{*2})^{1/2})^{1/2} p^{1/2} e^{-i \pi/4}$$

2.29

where

$$\arg p^{1/2} = \begin{cases} 0 & \text{on left bank} \\ \pi & \text{on right bank} \end{cases}$$

$$\arg(p + 2 e^{i \pi/4} (1 - x_1^{*2})^{1/2})^{1/2} = \pi/8 \quad \text{for } p = 0$$

In the same fashion $R(x)$ is expanded

$$\begin{aligned} R(x) = & \frac{\alpha_m}{\alpha_1} \frac{\beta_{m+1}}{\alpha_{m+1}} e^{-i \pi/4} ((1 - x_1^{*2})^{1/2} \\ & + (1 - \tilde{x}_1^{*2})^{1/2}) e^{i \pi/4 + p} \end{aligned} \quad 2.30$$

$$\cdot ((1 - x_1^{*2})^{1/2} - (1 - \tilde{x}_1^{*2})^{1/2}) e^{i \pi/4 + p}$$

where both square roots have argument of $\pi/8$ for $p = 0$.

$B(q_1)$ is expanded about x_1^* . The derivation is in Appendix A.3

$$B(q_1) \doteq B(x_1^*) - p(1 - x_1^{*2})^{1/2} e^{-i \pi/4} \frac{(r - r_{ppp}^*)}{x_1^*} + \frac{i p^2 (r - \tilde{r}_{ppp}^*)}{2 x_1^{*3}}$$

where \tilde{r}_{ppp}^* is just \tilde{r} (as defined in 2.16) with x_1^* substituted for x_1 .

$$\tilde{r}_{ppp}^* = \sum_{i=1}^m \frac{N_p \ i \ h_i \left(\frac{\alpha_1^2}{\alpha_i^2} - 1 \right)}{\left(\frac{\alpha_{m+1}^2}{\alpha_i^2} - 1 \right)^{3/2}} + \sum_{i=1}^m \frac{N_p \ i \ h_i \left(\frac{\alpha_1^2}{\beta_i^2} - 1 \right)}{\left(\frac{\alpha_{m+1}^2}{\beta_i^2} - 1 \right)^{3/2}} \quad 2.32$$

By considering the geometry of the medium and the ray travelling through it, the formula for the travel-time curve of the PPP head wave can be set down as

$$t_{ppp} = \frac{r}{\alpha_{m+1}} + \sum_{i=1}^m \frac{N_p \ i \ h_i \left(1 - \frac{\alpha_i^2}{\alpha_{m+1}^2} \right)^{1/2}}{\alpha_i} + \sum_{i=1}^m \frac{N_p \ i \ h_i \left(1 - \frac{\beta_i^2}{\alpha_{m+1}^2} \right)^{1/2}}{\beta_i} \quad 2.33$$

Upon inspection of $B(x_1^*)$, it is seen that

$$t_{ppp} = B(x_1^*)/\alpha_1 = k \ B(x_1^*)/\omega \quad 2.34$$

and

$$k = \omega/\alpha_1.$$

We now introduce the concept of head wave multiplicity. Figure 2.3a depicts a ray which has M PP-type reflections from the bottoming interface. Any one (and only one) of these reflections can form a head wave which will be returned to the surface. The reason that only one reflection can form a head wave follows from wave front considerations. Head waves arise from a wave front of finite radius in the plane of incidence impinging upon a plane interface. The head wave is a conical wave in three dimensions. Hence it has an infinite radius of curvature in the plane of incidence. For this reason it cannot form another head wave. The ray depicted in Figure 2.3b is a physically impossible situation. This is often mistakenly conceived in the literature (see Hales and Nation (13), p. 532). To properly evaluate the head wave displacement we must consider $(R_{11})^M$ rather than R_{11} in the integrals 2.14.

Consider any two rays which travel the same ray path, but with one difference. The two rays form head waves from different bottoming reflections. These two rays have identical travel time curves (hence the rays are termed KINEMATIC ANALOGS). They suffer the same reflections and transmissions and their amplitude-distance curves are identi-

Figure 2.3a

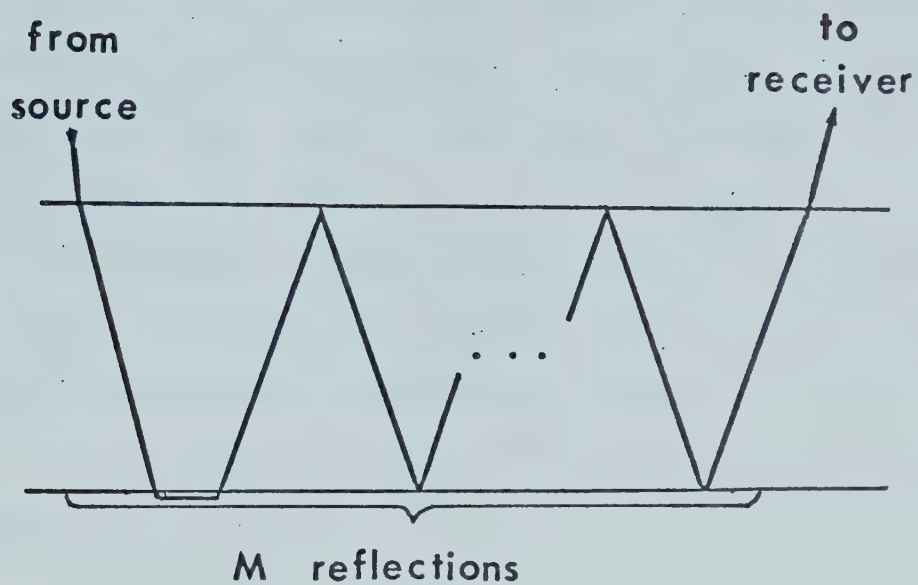


Figure 2.3b

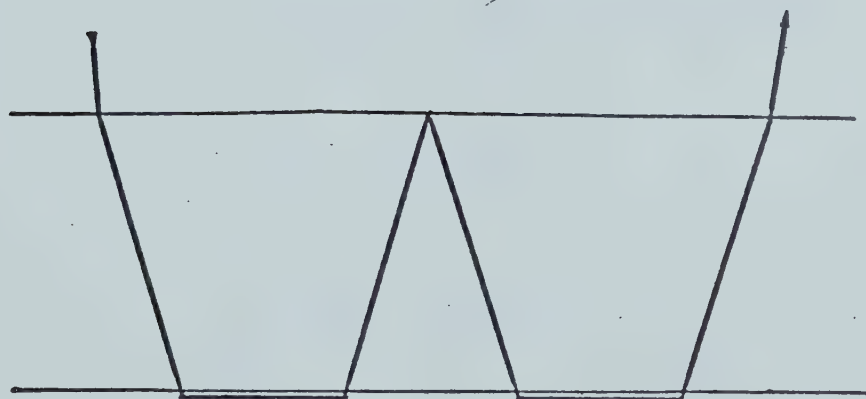


Figure 2.3. Head wave multiplicity

cal. In this case they are further termed DYNAMIC ANALOGS. For more details on kinematic and dynamic analogs refer to Hron (17). Within the critical region for the reflected wave-head wave pair each member of the group of dynamic analogs interferes equally with the reflected wave. Physical reasoning leads one to the conclusion that the total displacement of this group should be M times the displacement of an individual member. We now give a more rigorous mathematical derivation of this.

Using equation 2.6, the M^{th} power of R_{11} can be written as

$$\begin{aligned}
 [R_{11}(q)]^M &= [(V_0(q) + V_2(q) R(q)) \\
 &\quad - (-V_1(q) - V_3(q) R(q)) S(q)]^M \\
 &= [C - D \cdot S]^M \\
 &= C^M \left[1 - \frac{D}{C} S\right]^M.
 \end{aligned}$$

Near the first critical point the radical S is very nearly zero. Thus the second term in brackets is very much less than one. The expression can then be expanded in a binomial series omitting the third and higher terms:

$$[R_{11}(q)]^M = C(q)^{M-1} [R_{11}(q) - (M-1) D(q) S(q)]$$

The functions V_i do not contain the radical S or R , and hence are slowly varying functions. The saddle point approximation allows one to replace these values in the integrand by their value at $p = 0$. The same approximation is applied to $\sigma(x)$, q_1 , $(1 - q_1^2)^{1/2} q_1^{-1/2}$. Performing all these expansions and approximations to equation 2.14 yields

$$u^* = -g \int_{D_1}^{\infty} C(q)^{M-1} [R_{11}(q) - (M-1) (-V_1 - V_3 R) S(q)] e^{f(p)} dp$$

$$w^* = u^* \frac{(1 - x_1^{*2})^{1/2}}{x_1^*} \quad 2.35$$

where

$$g = e^{-i \omega(t-t_{ppp})} \sigma(x^*) x_1^* \left(\frac{k}{2 \pi r x_1^*} \right)^{1/2}$$

$$f(p) = - \frac{k p(r-r_{ppp}^*) (1 - x_1^{*2})^{1/2} e^{i \pi/4}}{x_1^*} - \frac{k p^2(r-\tilde{r}_{ppp}^*)}{2 x_1^{*3}}$$

Some further approximations can be made on equation 2.35. Since $S \rightarrow 0$ near the first critical point, it is justified to approximate the reflection coefficient as

$$R_{11} = C - D \cdot S \doteq C.$$

C does not, however, contain the radical S and therefore has a finite derivative near the critical point. C^{M-1} can then be replaced by its value at $p = 0$, namely $C^{M-1} = R_{11}^{M-1}$. This term represents all the bottoming reflections of type PP which do not form a head wave. For the duration of this discussion the term $R_{11}^{M-1}(x^*)$ will be included in the product $\sigma(x^*)$. Thus, equation 2.35 can be rewritten as

$$u^* = -g \int_{D_1}^{\infty} [V_0(q) + V_1(q) S(q) + V_2(q) R(q) + V_3(q) R(q) S(q) - (M-1) (-V_1(q) - V_3(q) R(q)) S(q)] e^{f(p)} dp$$

$$w^* = u^* \frac{(1 - x_1^{*2})^{1/2}}{x_1^*}$$

Next expand the individual terms and integrate, remembering that the arguments of the term $p^{1/2}$ in the expansion of $S(q)$ has a different sign on either bank of the cut

$$\begin{aligned}
u^* &= 2 g \left\{ \int_0^{\infty} V_1(q) S(q) e^{f(p)} dp \right. \\
&+ \int_0^{\infty} V_3(q) R(q) S(q) e^{f(p)} dp \\
&+ (M-1) \int_0^{\infty} V_1(q) S(q) e^{f(p)} dp \\
&\left. + (M-1) \int_0^{\infty} V_3(q) R(q) S(q) e^{f(p)} dp \right\}
\end{aligned}$$

$$w^* = u^* \frac{(1 - x_1^{*2})^{1/2}}{x_1^*}$$

This finally can be written as

$$\begin{aligned}
u^* &= 2 g M \left\{ \int_0^{\infty} V_1(q) S(q) e^{f(p)} dp \right. \\
&\left. + \int_0^{\infty} V_3(q) S(q) R(q) e^{f(p)} dp \right\}
\end{aligned}$$

$$w^* = u^* \frac{(1 - x_1^{*2})^{1/2}}{x_1^*}$$

In the previous expressions we have used q as a vari-

able, but it was understood that q is a function of p in a manner according to equation 2.12a. Since the V 's do not contain radicals R and S , they can be substituted by their value at $p = 0$. Using the full expansions of R and S as given by equations 2.29 and 2.30 we have

$$u^* = \exp(-i \omega(t - t_{ppp}) - \frac{i \pi}{4}) \left(\frac{2k}{\pi r}\right)^{1/2} \sigma(x^*) \frac{\alpha_m}{\alpha_1} x_1^{*1/2} M$$

$$\cdot \{V_1(x^*) \int_0^\infty (p + 2 e^{i \pi/4} (1 - x_1^{*2})^{1/2})^{1/2}$$

$$p^{1/2} \exp(- \frac{k p(r-r_{ppp}^*) (1 - x_1^{*2})^{1/2} e^{i \pi/4}}{x_1^*}$$

$$- \frac{k p^2(r-\tilde{r}_{ppp}^*)}{2 x_1^{*3}}) dp + V_3(x^*) \frac{\alpha_m}{\alpha_1} \frac{\beta_{m+1}}{\alpha_{m+1}} e^{-i \pi/4} \int_0^\infty$$

$$(p + 2 e^{i \pi/4} (1 - x_1^{*2})^{1/2})^{1/2} p^{1/2} (((1 - x_1^{*2})^{1/2}$$

$$+ (1 - \tilde{x}_1^{*2})^{1/2}) e^{i \pi/4} + p)^{1/2} \cdot (((1 - x_1^{*2})^{1/2}$$

$$- (1 - \tilde{x}_1^{*2})^{1/2}) e^{i \pi/4} + p)^{1/2}$$

$$\exp\left(-\frac{k p(r-r_{ppp}^*) (1-x_1^{*2})^{1/2} e^{i\pi/4}}{x_1^*} - \frac{k p^2(r-\tilde{r}_{ppp}^*)}{2 x_1^{*3}}\right) dp\}$$

$$w^* = u^* \frac{(1-x_1^{*2})^{1/2}}{x_1^*}$$

By considering another variable Δ defined by

$$\Delta = \left(\frac{k(r-\tilde{r}_{ppp}^*) (1-x_1^{*2})}{2 x_1^{*3}}\right)^{1/2}$$

one arrives at an exponential term in the integrand like

$$\exp\left(-\frac{p(r-r_{ppp}^*) \Delta^2}{(r-\tilde{r}_{ppp}^*)(1-x_1^{*2})^{1/2}} - \frac{p^2 \Delta^2}{(1-x_1^{*2})}\right) e^{i\pi/4}$$

The value of the integrands will be most affected by the p^2 term. If Δ is large ($(1-x_1^{*2})^{1/2}$ is always less than 1), then the largest contribution to the integral takes place for p near zero. Thus if it is assumed that

$$\Delta \gg 1$$

then approximately

$$(p + 2 e^{i \pi/4} (1 - x_1^{*2})^{1/2})^{1/2} \doteq e^{i \pi/8} 2^{1/2} (1 - x_i^{*2})^{1/2}$$

$$(((1 - x_1^{*2})^{1/2} + (1 - \tilde{x}_1^{*2})^{1/2}) e^{i \pi/4} + p)^{1/2} \doteq e^{i \pi/8}$$

$$((1 - x_1^{*2})^{1/2} + (1 - \tilde{x}_1^{*2})^{1/2})^{1/2}$$

By introducing the variable ξ we can write displacements as follows:

$$u^* = -\exp(-i \omega(t - t_{ppp}) + i 7 \pi/8)$$

$$\left(\frac{2^7 x_1^{*11} (1 - x_1^{*2})}{\pi^2 r^2 k(r - \tilde{r}_{ppp}^*)^3} \right)^{1/4} \sigma(x^*) \frac{\alpha_m}{\alpha_1} M$$

$$\cdot \{V_1(x^*) \int_0^\infty \xi^{1/2} \exp[-\xi^2 - 2^{1/2} (1+i) y^* \xi] d\xi$$

$$+ V_3(x^*) \frac{\alpha_m}{\alpha_1} \frac{\beta_{m+1}}{\alpha_{m+1}} e^{-i \pi/8} ((1 - x_1^{*2})^{1/2}$$

$$+ (1 - \tilde{x}_1^{*2})^{1/2})^{1/2} \left(\frac{2 x_1^{*3}}{k(r - \tilde{r}_{ppp}^*)} \right)^{1/4}$$

$$\cdot \int_0^{\infty} \xi^{1/2} (\delta^* e^{i\pi/4} + \xi)^{1/2}$$

$$\exp[-\xi^2 - 2^{1/2} (1+i) y^* \xi] d\xi\}$$

$$w^* = u^* \frac{(1 - x_1^{*2})^{1/2}}{x_1^*} \quad 2.36$$

where

$$\xi = \left(\frac{k(r - \tilde{r}_{ppp}^*)}{2 x_1^{*3}} \right)^{1/2} p$$

$$y^* = \left(\frac{k x_1^* (1 - x_1^{*2})}{2(r - \tilde{r}_{ppp}^*)} \right)^{1/2} (r - r_{ppp}^*)$$

$$\delta^* = \left(\frac{k(r - \tilde{r}_{ppp}^*)}{2 x_1^{*3}} \right)^{1/2} ((1 - x_1^{*2})^{1/2} - (1 - \tilde{x}_1^{*2})^{1/2})$$

By introducing two new functions g_2 and G_2 defined by

$$g_2(x) = \pi^{-1/2} 2^{10/4} e^{7i\pi/8} \int_0^{\infty} p^{1/2} \exp(-p^2 - x(1+i) 2^{1/2} p) dp$$

$$G_2(x, y) = \pi^{-1/2} 2^{10/4} e^{7i\pi/8} \int_0^{\infty} p^{1/2} \cdot (1 + \frac{p}{y} e^{-i\pi/4})^{1/2}$$

$$\cdot \exp(-p^2 - x(1+i) 2^{1/2} p) dp \quad 2.37$$

We can rewrite the displacements as follows:

$$u^* = -\exp(-i \omega(t - t_{ppp}^*)) \left(\frac{x_1^{*11} (1 - x_1^{*2})}{8 r^2 k(r - \tilde{r}_{ppp}^*)^3} \right)^{1/4} \sigma(x^*) \frac{\alpha_m}{\alpha_1} M$$

$$\cdot \{V_1(x^*) g_2(y^*) + V_3(x^*) R(x^*) G_2(y^*, \delta^*)\}$$

$$w^* = u^* \frac{(1 - x_1^{*2})^{1/2}}{x_1^*}$$

If the two critical points are sufficiently far apart, the approximation $G_2(y^*, \delta^*) \doteq g_2(y^*)$ can be made. The head wave displacements can now be written as:

$$u^* = x_1^* M \exp(-i \omega(t - t_{ppp})) \left(\frac{x_1^{*7} (1 - x_1^{*2})}{8 r^2 k(r - \tilde{r}_{ppp}^*)^3} \right)^{1/4}$$

$$\sigma(x^*) \frac{\alpha_m}{\alpha_1} g_2(y^*) \cdot D(x^*)$$

$$w^* = u^* \frac{(1 - x_1^{*2})^{1/2}}{x_1^*}$$

2.38

If the function $\mu_2(y^*) = y^{*3/2} g_2(y^*)$ is introduced, then we have

$$u^* = x_1^{*2} \frac{M \alpha_m \sigma(x^*) D(x^*)}{k \alpha_1 r^{1/2} (r-r^*)^{3/2} (1-x_1^*)^{1/2}} \mu_2(y^*)$$

$$\exp(-i \omega(t - t_{ppp}))$$

$$w^* = u^* \frac{(1 - x_1^{*2})}{x_1^*}$$

The quantity y^* is zero at the first critical point and increases as one moves away from it. For increasing y^* , $\mu_2(y^*)$ tends to i . Thus, at large distances beyond the critical point

$$u^* = \frac{x_1^{*2} \alpha_m \sigma(x^*) D(x^*) M}{k \alpha_1 r^{1/2} (r-r^*)^{3/2} (1-x_1^{*2})^{1/2}}$$

$$\exp(-i \omega(t - t_{ppp}) + \frac{i\pi}{2})$$

$$w^* = u^* \frac{(1 - x_1^{*2})^{1/2}}{x_1^*}$$

2.40

which are the values found using asymptotic ray theory (see Cerveny (9), pp. 147-148). We also note that equation 2.40 has a singularity at $r = r_{ppp}^*$ which does not exist

in the exact formula 2.38.

2.6 The PSP Head Wave

The PSP head wave exists only for epicentral distances greater than the second critical point or analogously, for $x_1 > \tilde{x}_1^*$. To calculate the displacements for this wave, we must evaluate the integrals in equation 2.15 where D_2 is the contour which circumvents the branch cut given parametrically by

$$(1 - q_1^2)^{1/2} = (1 - \tilde{x}_1^{*2})^{1/2} + p e^{-i \pi/4}; \quad \text{for } 0 < p < \infty \quad 2.41$$

The method of evaluation is very similar to that used in the previous section so that only the major highlights and final results will be discussed here.

The radicals S and R are again expanded. The results are:

$$\begin{aligned} S = & \frac{\alpha_m}{\alpha_1} e^{i \pi/2} ((1 - x_1^{*2})^{1/2} + (1 - \tilde{x}_1^{*2})^{1/2} \\ & + p e^{-i \pi/4})^{1/2} ((1 - x_1^{*2})^{1/2} \\ & - (1 - \tilde{x}_1^{*2})^{1/2} - p e^{-i \pi/4})^{1/2} \end{aligned}$$

where for $p = 0$, both radicals have argument of zero.

$$R = \frac{\alpha_m}{\alpha_1} \frac{\beta_{m+1}}{\alpha_{m+1}} p^{1/2} e^{-i\pi/4} (p + 2 e^{i\pi/4} (1 - \tilde{x}_1^{*2})^{1/2})^{1/2}$$

where

$$\arg p^{1/2} = \begin{cases} 0 & \text{on left bank} \\ \pi & \text{on right bank} \end{cases}$$

$$\arg(p + 2 e^{i\pi/4} (1 - \tilde{x}_1^{*2})^{1/2})^{1/2} = \pi/8 \quad \text{for } p = 0$$

The expansion of the exponential term in the integrals is similar to that performed in the previous section:

$$B(q_1) = B(\tilde{x}_1^*) - \frac{p(1 - \tilde{x}_1^{*2})^{1/2} e^{-i\pi/4} (r - r_{psp}^*)}{\tilde{x}_1^*} + \frac{i p^2}{2} \frac{(r - \tilde{r}_{psp}^*)}{\tilde{x}_1^{*3}}$$

where

$$\tilde{r}_{psp}^* = \sum_{i=1}^m \frac{N_{p \ i} h_i \left(\frac{\alpha_1^2}{\alpha_i^2} - 1 \right)}{\left(\frac{\beta_{m+1}^2}{\alpha_1^2} - 1 \right)^{3/2}} + \sum_{i=1}^m \frac{N_{s \ i} h_i \left(\frac{\alpha_1^2}{\beta_i^2} - 1 \right)}{\left(\frac{\beta_{m+1}^2}{\beta_i^2} - 1 \right)^{3/2}}$$

By considering medium and ray geometry and by inspecting $B(\tilde{x}_1^*)$ we see that

$$t_{psp} = B(\tilde{x}_1^*)/\alpha_1 = k B(\tilde{x}_1^*)/\omega$$

$$= \frac{r}{\beta_{m+1}} + \sum_{i=1}^m \frac{N_{p \ i} h_i \left(1 - \frac{\alpha_i^2}{\beta_{m+1}^2} \right)^{1/2}}{\alpha_i}$$

$$+ \sum_{i=1}^m \frac{N_{s \ i} h_i \left(1 - \frac{\beta_i^2}{\beta_{m+1}^2} \right)^{1/2}}{\beta_i}$$

2.42

Upon substituting these expressions into equations 2.15, and by allowing slowly varying functions of q_1 to assume their values at $q_1 = \tilde{x}_1^*$ we have

$$u^* = -\tilde{x}_1^{*1/2} e^{-i \omega(t - t_{psp})} \cdot \left(\frac{k}{2 \pi r} \right)^{1/2} \sigma(\tilde{x}^*) I$$

$$w^* = u^* \frac{(1 - \tilde{x}_1^{*2})^{1/2}}{\tilde{x}_1^*} \quad 2.43$$

where

$$I = \int_{D_2}^{\infty} (R_{11}(q))^M \exp\left(-\frac{k p (1 - \tilde{x}_1^{*2})^{1/2} e^{i\pi/4} (r - r_{psp}^*)}{x_1^*} - \frac{k p^2 (r - \tilde{r}_{psp}^*)}{2 x_1^{*3}}\right) dp.$$

The multiplicity factor, M , has the same significance here as in the case for PPP head waves. The term $((R_{11}(q))^M$ is binomially expanded and approximations similar to those for PPP head waves are made. Expansion 2.6 is employed for the reflection coefficient and the V 's are assigned their value at $p = 0$ ($q = \tilde{x}^* = \alpha_m/\beta_{m+1}$). R , which has the same modulus on either bank of the cut, has a different argument by π on either bank. For this reason V_1 drops as a result of integration and V_2 and V_3 survive integration. As in the PPP head wave section, the assumption that

$$\left(\frac{k(r - \tilde{r}_{psp}^*) (1 - \tilde{x}_1^{*2})}{2 x_1^{*3}}\right)^{1/2} \gg 1$$

is made. This again states that the bulk of the value of

the integral results from the region where p is near zero.
With this in mind, we approximate

$$(p + 2 e^{i \pi/4} (1 - \tilde{x}_1^{*2})^{1/2})^{1/2} \doteq 2^{1/2} e^{i \pi/8} (1 - \tilde{x}_1^{*2})^{1/4}$$

$$((1 - x_1^{*2})^{1/2} + (1 - \tilde{x}_1^{*2})^{1/2} + p e^{-i \pi/4})^{1/2} \doteq ((1 - x_1^{*2})^{1/2} + (1 - \tilde{x}_1^{*2})^{1/2})^{1/2}$$

Finally we will substitute ξ into the integral I where

$$\xi = \left(\frac{k(r - \tilde{r}_{psp}^*)}{2 \tilde{x}_1^{*3}} \right)^{1/2} p$$

I then has the value

$$I = \frac{\alpha_m}{\alpha_1} \frac{\beta_{m+1}}{\alpha_{m+1}} \frac{(1 - \tilde{x}_1^{*2})^{1/4} x_1^{*9/4} \pi^{1/2}}{(k(r - \tilde{r}_{psp}^*))^{3/4} 2^{1/4}} M \cdot \{V_2(\tilde{x}^*) g_2(\tilde{y}^*) + V_3(\tilde{x}^*) S(\tilde{x}^*) \cdot G_2(\tilde{y}^*, \tilde{\delta}^*)\} \quad 2.44$$

where the quantities \tilde{y}^* and $\tilde{\delta}^*$ are similar to y^* and δ^* defined in the previous section with the appropriate sub-

stitutions for the second critical point made. If the two critical points are adequately separated, or in other words

$$\left(\frac{k(r - \tilde{r}_{psp}^*)}{2 \tilde{x}_1^{*3}} \right)^{1/2} ((1 - x_1^{*2})^{1/2} - (1 - \tilde{x}_1^{*2})^{1/2})^{1/2} \gg 1$$

then we can approximate

$$G_2(\tilde{y}^*, \tilde{\delta}^*) \doteq g_2(\tilde{y}^*)$$

Then the PSP head wave displacements are given by

$$\tilde{u}^* = \tilde{x}_1^* \exp(-i \omega(t - t_{psp})) M \left(\frac{\tilde{x}_1^{*7} (1 - \tilde{x}_1^{*2})}{8 k r^2 (r - \tilde{r}_{psp}^*)^3} \right)^{1/4}$$

$$\sigma(\tilde{x}^*) \frac{\alpha_m}{\alpha_1} \frac{\beta_{m+1}}{\alpha_{m+1}} D_1(\tilde{x}^*) g_2(\tilde{y}^*)$$

$$\tilde{w}^* = \tilde{u}^* \frac{(1 - \tilde{x}_1^{*2})^{1/2}}{\tilde{x}_1^*} \quad 2.45$$

As in the previous section we can calculate the asymptotic equations for epicentral distances for beyond r_{psp}^*

$$\tilde{u}^* = \frac{\tilde{x}_1^{*2} \alpha_m \beta_{m+1} \sigma(\tilde{x}^*) D1(\tilde{x}^*)}{k \alpha_1 \alpha_{m+1} (r-r^*)^{3/2} (1 - \tilde{x}_1^{*2})^{1/2}} \frac{M}{r^{1/2}}$$

$$\exp(-i \omega(t - t_{psp}^*) + \frac{i \pi}{2})$$

$$\tilde{w}^* = \tilde{u}^* \frac{(1 - \tilde{x}_1^{*2})^{1/2}}{\tilde{x}_1^*} \quad 2.46$$

These equations again have a singularity at the critical point which is not present in 2.45.

2.7 The Interference Wave

In Chapter 1, the relationship between head waves and simple reflected waves within the interference zone was discussed. Thus, we must consider the summed total response due to the head wave interfering with the reflected wave. The previous discussions have determined that the total response of multiply-reflected head wave is M times the response due to a single head wave. With this in mind, the displacements of the interference waves can be written as follows:

$$PP - PPP \quad \bar{u} = u^0 + u^*$$

$$\bar{w} = w^0 + w^*$$

$$PP - PSP \quad \bar{u} = u^0 + \tilde{u}^*$$

$$\bar{w} = w^0 + \tilde{w}^*$$

Only the calculation for the PP-PPP case will be given in detail since the PP-PSP case follows the same procedure. The displacements referred to in the equations above are defined in equations 2.27, 2.28, 2.38 and 2.45.

$$\begin{aligned}
 \bar{u} = & \frac{x_1 \sigma(x)}{L} \exp(-i \omega(t - t_{pp})) (R_{11}(x) \\
 & - D(x) (x^{*2} - x^2)^{1/2} (\mu_1(b_1) - 1) \\
 & + M x_1^* D(x^*) \left(\frac{x_1^{*7} (1 - x_1^{*2})}{8 r^2 k(r - \tilde{r}_{ppp}^*)^3} \right)^{1/4} \sigma(x^*) \frac{\alpha_m}{\alpha_1} \\
 & g_2(y^*) \exp(-i y^2) \frac{r^{1/2} (r - \tilde{r})^{1/2}}{\sigma(x) x_1^2} \\
 \bar{w} = & \frac{(1 - x_1^2)^{1/2} \sigma(x)}{L} \exp(-i \omega(t - t_{pp})) (R_{11}(x) \\
 & - D(x) (x^{*2} - x^2)^{1/2} (\mu_1(b_1) - 1) \\
 & + M (1 - x_1^{*2})^{1/2} D(x^*) \left(\frac{x_1^{*7} (1 - x_1^{*2})}{8 r^2 k(r - \tilde{r}_{ppp}^*)^3} \right)^{1/4} \\
 & \sigma(x^*) \frac{\alpha_m}{\alpha_1} \frac{g_2(y^*) \exp(-i y^2) r^{1/2} (r - \tilde{r})^{1/2}}{(1 - x_1^2)^{1/2} x_1 \sigma(x)}
 \end{aligned}$$

where

$$y^2 = 2 \pi f \cdot (t_{pp} - t_{ppp})$$

Since the receiver lies in the vicinity of the first critical point we can make the following approximations:

$$D(x) \doteq D(\alpha_m/\alpha_{m+1}) = \Gamma_{131} = \text{PPP head wave coefficient}$$

$$x_1 \doteq x_1^* \quad \tilde{r} \doteq \tilde{r}_{ppp}^* \quad r \doteq r_{ppp}^*$$

$$\sigma(x) \doteq \sigma(\alpha_m/\alpha_{m+1})$$

$$\begin{aligned} \frac{(x_1^{*2} - x_1^2)^{\frac{1}{2}}}{b_1^{\frac{1}{2}}} &= i \frac{\frac{\alpha_m}{\alpha_1} ((1-x_1^{*2})^{\frac{1}{2}} - (1-x_1^2)^{\frac{1}{2}})^{\frac{1}{2}} ((1-x_1^{*2})^{\frac{1}{2}} + (1-x_1^2)^{\frac{1}{2}})^{\frac{1}{2}}}{\left(\frac{k(r-\tilde{r})}{2 x_1^3}\right)^{\frac{1}{4}} ((1-x_1^{*2})^{\frac{1}{2}} - (1-x_1^2)^{\frac{1}{2}})^{\frac{1}{2}}} \\ &\doteq i \frac{\alpha_m}{\alpha_1} \frac{2^{\frac{3}{4}} x_1^{*\frac{3}{4}}}{k^{\frac{1}{4}} (r-\tilde{r}_{ppp}^*)^{\frac{1}{4}}} (1-x_1^{*2})^{\frac{1}{4}} \end{aligned}$$

After these rearrangements

$$\bar{u} = \frac{x_1 \sigma(x)}{L} \exp(-i \omega(t - t_{pp})) (R_{11}(x)$$

$$- \frac{\alpha_m}{\alpha_1} \frac{\Gamma_{131} (1 - x_1^{*2})^{1/4} x_1^{*3/4}}{(k(r - \tilde{r}_{pp}^*))^{1/4}}$$

$$\cdot (M(i 2^{3/4} (g_1(b_1) - b_1^{1/2})$$

$$- 2^{-3/4} g_2(y^*) \exp(-i y^2)))$$

$$+ (M-1) D(x) (x^{*2} - x^2)^{1/2} (\mu_1(b_1) - 1))$$

$$\bar{w} = \bar{u} \frac{(1 - x_1^2)^{1/2}}{x_1} \quad 2.47$$

The function G can be defined as

$$G = i 2^{3/4} (g_1(b_1) - (b_1)^{1/2}) - 2^{-3/4} g_2(y^*) \exp(-i y^2)$$

This function depends on three parameters, y , b_1 , y^* .

These three parameters should have the following properties:

$$y, b_1, y^* < 0 \quad \text{and monotonically increasing} \\ \text{before } r = r_{pp}^*$$

$$= 0 \quad \text{at } r = r_{pp}^*$$

> 0 and monotonically increasing
beyond $r = r_{ppp}^*$.

All three quantities have these same properties and are very similar (numerically) near the critical point. They may be given a common definition as

$$y = \begin{cases} \left(\frac{k(r-\tilde{r})}{2 x_1^3} \right)^{1/2} ((1 - x_1^{*2})^{1/2} - (1 - x_1^2)^{1/2}) & \text{for } r < r_{ppp}^* \\ (2 \pi f)^{1/2} (t_{pp} - t_{ppp})^{1/2} & \text{for } r > r_{ppp}^* \end{cases} \quad 2.48$$

Thus $G(y)$ can be expressed as

$$G(y) = i 2^{3/4} (g_1(y) - y^{1/2}) - 2^{-3/4} g_2(y) \exp(-i y^2)$$

By introducing the quantity $j = \phi - y e^{i \pi/4}$ into $g_1(y)$ we get

$$G(y) = - \frac{2^{3/4} e^{7 i \pi/8 - i y^2}}{\pi^{1/2}} \int_{-\infty}^{\infty} j^{1/2} \exp(-j^2 - 2 y j e^{i \pi/4}) dj$$

$$- \frac{2^{7/4} e^{7i\pi/8 - iy^2}}{\pi^{1/2}} \int_0^{\infty} p^{1/2} \exp(-p^2 - 2py e^{i\pi/4}) dp - i 2^{3/4} y^{1/2}$$

where

$$\arg(j)^{1/2} = \pi \quad \text{for } j > 0.$$

From this we get

$$G(y) = - \frac{2^{3/4} e^{7i\pi/8 - iy^2}}{\pi^{1/2}} \int_{-\infty}^{\infty} p^{1/2} \exp(-p^2 - 2yp e^{i\pi/4}) dp - i 2^{3/4} y^{1/2} \quad 2.49$$

where

$$\arg(p)^{1/2} = 0 \quad \text{for } p > 0.$$

Properties of $G(y)$ which make it easy to evaluate numerically will be discussed in the next chapter.

The term in equation 2.47 containing $(M-1)$ can be also rearranged as

$$\frac{\alpha_m}{\alpha_1} \frac{\Gamma_{131} (1 - x_1^{*2})^{1/4} x_1^{*3/4}}{(k(r - \tilde{r}_{ppp}^*))^{1/4}} \cdot \frac{(M-1) D(x) G(b_1)}{\Gamma_{131}}$$

where

$$G(b_1) = i 2^{3/4} (g_1(b_1) - b_1^{1/2}).$$

The variable in G in this case has been left as b_1 to ensure more accuracy.

At this point a final expression for the interference head wave displacement has been derived. It can be stated as

$$\begin{aligned} \bar{u} &= \frac{x_1 \sigma(x)}{L} \exp(-i \omega(t - t_{pp})) (R_{11}(x) \\ &\quad - \frac{\Gamma_{131} \alpha_m \alpha_{m+1}^{1/4} (1 - x_1^{*2})^{1/4}}{\alpha_{m+1} (2 \pi f)^{1/2} (r - \tilde{r}_{ppp}^*)^{1/4}} \\ &\quad \cdot (M G(y) - \frac{(M-1) D(x) G(b_1)}{\Gamma_{131}})) \\ \bar{w} &= \frac{(1 - x_1^2)^{1/2} \sigma(x)}{L} \exp(-i \omega(t - t_{pp})) (R_{11}(x) \\ &\quad - \frac{\Gamma_{131} \alpha_m \alpha_{m+1}^{1/4} (1 - x_1^{*2})^{1/4}}{\alpha_{m+1} (2 \pi f)^{1/4} (r - \tilde{r}_{ppp}^*)^{1/4}} \end{aligned}$$

$$\cdot (M G(y) - \frac{(M-1) D(x) G(b_1)}{\Gamma_{131}})). \quad 2.50$$

Equation 2.50 is valid at all epicentral distances. We will note in the following chapter that the complex valued function $G(x)$ tends to zero for large values of x . Hence, the second term decreases in significance with respect to the reflection coefficient R_{11} for epicentral distances far from the critical point. Since the second term is inversely dependent on source frequency, f , it is obvious that for the high frequency case the corrective term nearly vanishes leaving

$$\bar{u} = \frac{x_1 \sigma(x)}{L} \exp(-i \omega(t - t_{pp})) R_{11}(x)$$

$$\bar{w} = \frac{(1 - x_1^2)^{1/2} \sigma(x)}{L} \exp(-i \omega(t - t_{pp})) R_{11}(x)$$

This is exactly the result that would have been obtained using asymptotic ray theory for a high frequency. For this case the head wave amplitude is negligible. The results of computations presented in the next chapter bear this out quite well.

2.8 Generalized Amplitude Formulae

The components of displacement of the interference

wave in the neighbourhood of the critical point can be described by

$$\bar{u} = A_u \cdot \exp(-i \omega(t - t_{pp}) + i Z)$$

$$\bar{w} = A_w \cdot \exp(-i \omega(t - t_{11}) + i Z)$$

where A_u and A_w are the moduli of the complex amplitudes in the horizontal and vertical direction. Z represents the argument of the complex number. To facilitate the use of one common term it proves expedient to introduce the concept of total surface incident amplitude, expressible as a complex number. For purposes of this discussion refer to Figure 2.4.

The total wave system generated by a wave incident upon the free surface is illustrated in Figure 2.4(a). What the receiver (R) records is actually the interference of the incident wave and the reflected P and S waves. To calculate the effect of the earth's surface on the recorded wave, the incident amplitude must be multiplied by an appropriate surface conversion coefficient. These are listed in detail in Hron (15). The surface conversion coefficients also resolve the recorded total wave into horizontal and vertical components.

For the remainder of this thesis only the total incident amplitude as exhibited in Figure 2.4(b) will be con-

Figure 2.4a

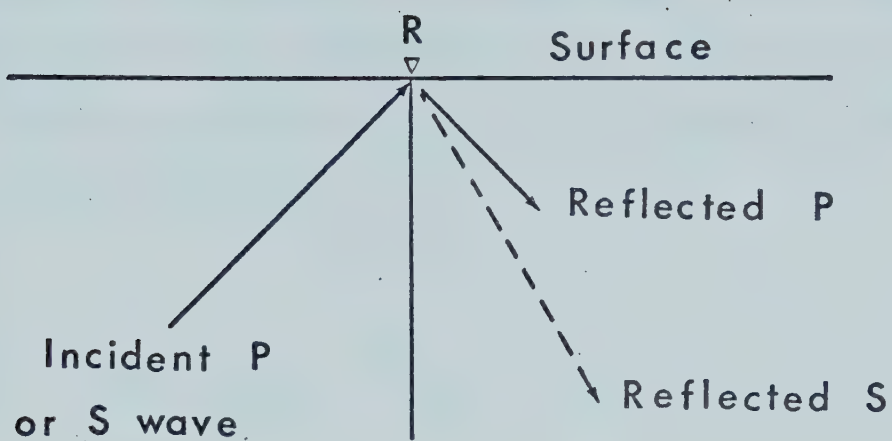


Figure 2.4b

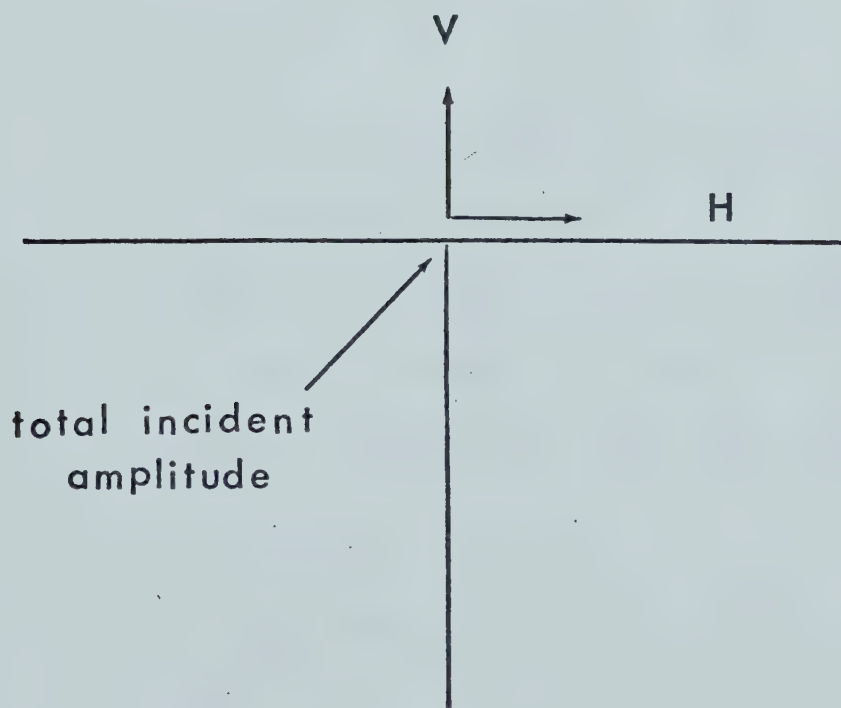


Figure 2.4. Total surface incident amplitude

sidered. For the sake of brevity, we have only discussed two of the eight head waves listed in Table 1.1. A similar evaluation was performed for the remainder. Upon completing these non-trivial computations, the complex amplitudes of all eight interference waves can be described by the complex number $A_{j \ell}^{j k \ell}$.

$$A_{j \ell}^{j k \ell} = \frac{\sigma(x)}{L} \left\{ R_{j \ell}(x) - \frac{\Gamma_{j k \ell}^n v_k^{1/4} (1 - x_1^{*2})^{1/2}}{(2 \pi f)^{1/4} (r - \tilde{r}_{j k \ell}^*)^{1/4}} \right. \\ \left. [M G(y_k) - \frac{(M-1) \Gamma_{j k \ell}^0 G(y_k^0)}{\Gamma_{j k \ell}}] \right\} \quad 2.51$$

where $j = 1$ or 2 for incident P or S waves on the bottoming interface
 $\ell = 1$ or 2 for reflected P or S waves from the bottoming interface
 $k = 3$ or 4 for P or S type head wave segments
 $n = \alpha_m / \alpha_{m+1}$

$$v_k = \begin{cases} \alpha_{m+1} & \text{for } k = 3 \\ \beta_{m+1} & \text{for } k = 4 \end{cases}$$

$$y_k^0 = \left(\frac{\pi f (r - \tilde{r})}{\alpha_1 x_1^3} \right)^{1/2} \left((1 - \alpha_1^2 / v_k^2)^{1/2} - (|1 - x_1^2|)^{1/2} \right)$$

$$y_k = \begin{cases} y_k^0 & \text{for } r < r^* \\ (2\pi f)^{1/2} (t_{j\ell} - t_{jk\ell})^{1/2} & \text{for } r \geq r^* \end{cases}$$

$t_{j\ell}, t_{jk\ell}$ = travel times of simply reflected wave (or reflected wave in the narrow sense of the word) and head wave

$\Gamma_{jk\ell}$ = head wave coefficient. They are derivable from the reflection coefficients $R_{j\ell}$ (see Cervený and Ravindra (10), p. 131f or Hron (15))

$$\Gamma_{jk\ell} = - \left(\frac{d R_{j\ell}}{d P_k} \right) \Big|_{x=\alpha_m/v_k}$$

$$P_k = \begin{cases} S(x) & \text{for } k = 3 \\ R(x) & \text{for } k = 4 \end{cases}$$

$$\Gamma'_{jk\ell} = - \left(\frac{d R_{j\ell}}{d P_k} \right) \Big|_x$$

$$x = \frac{\alpha_s \sin \theta_s}{v_B}$$

v_B = velocity of propagation of ray segment which is incident upon bottoming interface and which forms the head wave.

The parameter x as defined above is the one which was

used in all numerical evaluations. This use of a parameter will permit the same branch cuts in the complex plane for incident S waves as incident P waves.

The next chapter provides numerical evaluation of the quantities calculated here. In most instances a close resemblance between this theory and asymptotic ray theory outside the critical region can be noted.

CHAPTER 3

NUMERICAL RESULTS

3.1 The Weber Function

The function $G(y)$ as defined by equation 2.49 can be expressed in terms of an appropriate Weber function (or alternatively named a Parabolic Cylinder Function). The following integral definition is essential (see Magnus and Oberhettinger (19), p. 92)

$$\int_{-\infty}^{\infty} p^t e^{-2p^2 + 2ipz} dp = \frac{\pi^{1/2}}{2^{t+1/2}} e^{t\pi i/2} e^{-z^2/4} D_t(z)$$

$$\arg(-1)^t = t\pi \quad \text{for } p < 0; \operatorname{Re}(t) > -1$$

Using this definition, $G(y)$ may be rewritten

$$G(y) = 2^{1/2} \exp\left(\frac{i\pi}{8} - \frac{iy^2}{2}\right) D_{1/2}(y(i-1)) - i 2^{3/4} y^{1/2} \quad 3.1$$

where $G(y)$ is a complex valued function of the real parameter y , $-\infty < y < \infty$.

Kireyeva and Karpov (18) have tabulated the properties and numerical values of the Weber functions. These

functions arise when one solves the Helmholtz equation

$$\nabla^2 \Phi + k \Phi = 0$$

in parabolic coordinates by a separation of variables technique. This results in Weber's equation

$$\frac{d^2 D_t(z)}{dz^2} + \left(t + \frac{1}{2} - \frac{z^2}{4}\right) D_t(z) = 0$$

Kireyeva and Karpov have solved this equation for $z = y(1+i)$ and real t . The real and imaginary parts of $D_t(y(1+i)) = u_t(y) + i v_t(y)$ solve the following system of equations:

$$\frac{d^2 u_t(y)}{dy^2} = -y^2 u_t(y) + 2\left(t + \frac{1}{2}\right) v_t(y)$$

$$\frac{d^2 v_t(y)}{dy^2} = -2\left(t + \frac{1}{2}\right) u_t(y) - y^2 v_t(y) \quad 3.2$$

and satisfy the initial conditions

$$u_t(0) = \frac{2^{t/2} \pi^{1/2}}{\Gamma\left(\frac{1-t}{2}\right)} \quad u'_t(0) = -\frac{2^{t/2} (2\pi)^{1/2}}{\Gamma(-t/2)}$$

$$v_t(0) = 0 \quad v_t'(0) = - \frac{2^{t/2} (2\pi)^{1/2}}{\Gamma(-t/2)}$$

By using two important properties of the Weber function (Kireyeva and Karpov (18), p. x).

$$D_t(z) = D_t^*(z^*)$$

$$D_t(z) = (-1)^t D_t(-z)$$

we can find the solution for $D_{1/2}(y(i-1))$. To solve this problem numerically, one may utilize SUBROUTINE DASCUR from the International Mathematical and Statistical Library (IMSL) or any similar subroutine in standard computer libraries. This routine provides a numerical solution to a given system of first order ordinary differential equations. By introducing

$$\frac{d u_t(y)}{dy} = a_t(y) \quad \frac{d v_t(y)}{dy} = b_t(y)$$

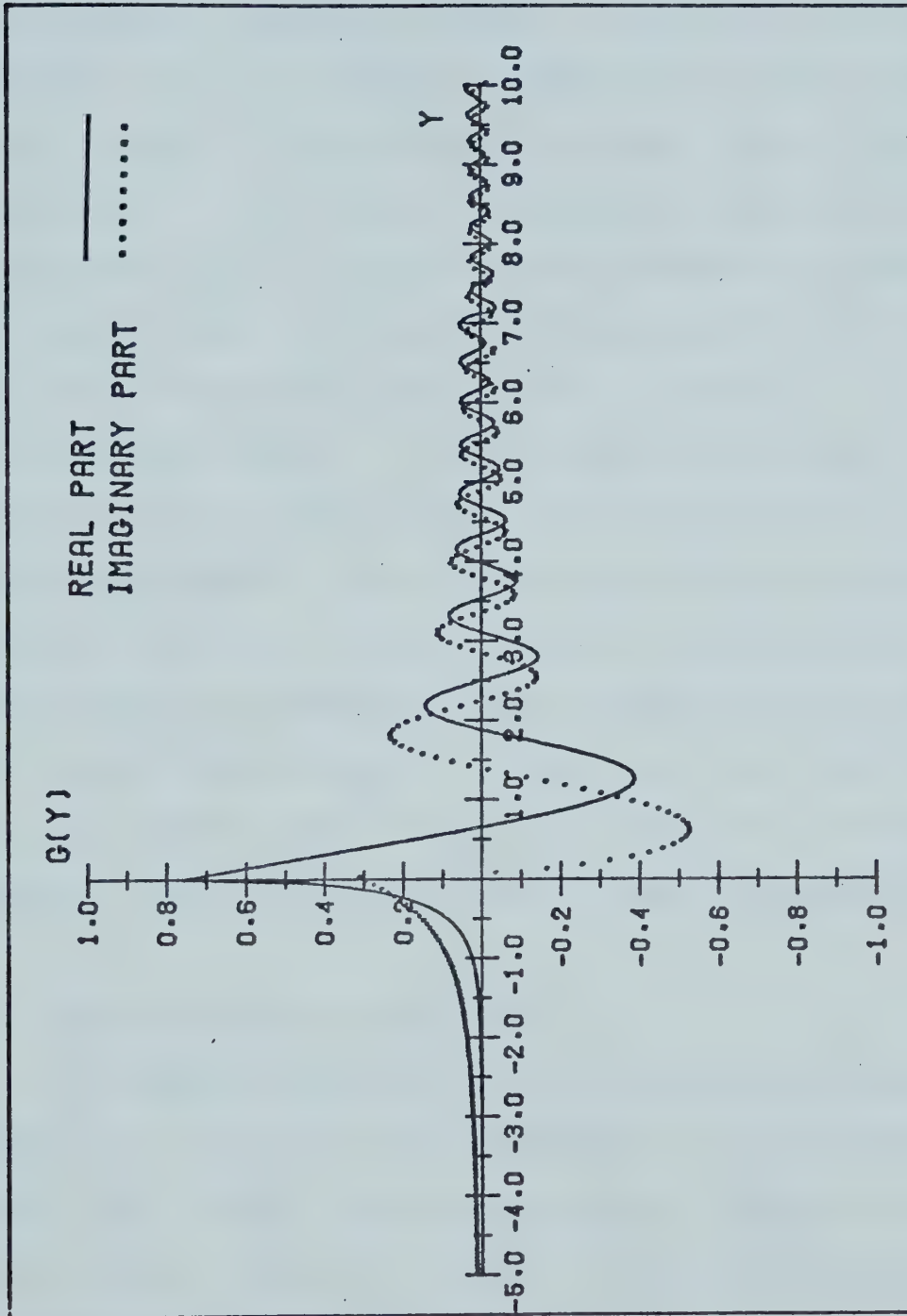
into equation 3.2, the system is transformed to first order.

By numerical tests two important results were obtained: the step size in the variable of the Weber function and the range of the variable. By checking the computed results with the results of Kireyeva and Karpov, it was determined that a step size of .005 for y would facili-

tate linear interpolation in the functional values. For most seismological situations, the parameter y , defined in equation 2.48, within the range $(-5,10)$ will sufficiently cover the interference zone and epicentral distances near it. Of course, $y = 0$ at the critical point.

A FORTRAN program has been created to compute the Weber function and write the value (unformatted) onto a disk file for future retrieval and interpolation in the construction of amplitude-distance curves. Using the unformatted write facility of the Michigan Terminal System (MTS), up to 248 bytes per line of disk file can be utilized. The program writes 30 pairs of single precision real numbers (i.e., representing real and imaginary parts of 30 complex valued numbers) onto one line. The last complex number on line j is repeated as the first complex number on line $j + 1$. This is to facilitate interpolation between any two values of a Weber function by reading only one line of the disk file. Another FORTRAN program was created to read the Weber function file and determine the functional value for any parameter. Given a certain value of the parameter, y , the program determines and reads the line of the file which contains functional values for parameters closest to y . Subsequently it selects and interpolates between the appropriate functional values. The derived Weber functional value at y is then adjusted by the proper quantities to form $G(y)$ as defined in equation 3.1.

Figure 3.1 is a computer generated plot of $G(y)$ pro-

Figure 3.1. The function $G(y)$.

duced on the CalComp plotter. Before the critical point ($y < 0$) the real and imaginary parts of $G(y)$ increase in a continuously monotonic fashion. Beyond the critical point ($y > 0$) they decrease rapidly and oscillate about zero. For $y < -3$ the real and imaginary parts of $G(y)$ become very insignificant. Consequently, the second term in equation 2.51 will become trivial compared to the reflection coefficient. The equation degenerates to the value for the reflected wave derived using asymptotic ray theory. Alternatively, for $y > 7$ the function attains very low values and again equation 2.51 tends toward the asymptotic ray theory formula. It is also advantageous to take cognizance of the fact that the function attains maximum modulus at $y = 0$ (characterizing a critical point) and that it oscillates beyond it. Thus, one can infer that the amplitude-distance curves will behave in a similar fashion. This will be displayed in the following sections.

3.2 Computed Dynamic Properties

A FORTRAN program has been written to calculate modulus and argument of the amplitude of interference waves. The results can be subsequently plotted by a Cal Comp plotter. The basic formula to be evaluated for many epicentral distances is equation 2.51.

Figures 3.2-3.4 are a series of diagrams displaying the logarithm of the modulus (base 10) and argument versus distance from the harmonic source. In all of these figures

the source frequency (F_0) is given at the top as well as the type of interference wave. The interference modulus curve is marked in a heavy solid line, whereas the head wave (which can only appear beyond the critical point R^*) has its modulus shown in the light line. This is the head wave modulus as calculated by asymptotic ray theory. The simply reflected wave modulus as computed by the ray theory is shown as a dashed line. The end of the interference zone is indicated by RI .

The argument plot, lying below the modulus plot gives the argument (expressed as a value between 0 and 2π) for the interference wave (X), the simply reflected wave (O) and the head wave (a solid dot at the critical point). Since the ray parameter for head waves and head wave coefficient are independent of epicentral distance, the argument is the same for all distances. The elastic and spatial parameters of the medium are given at the bottom of the diagram. Velocities are expressed in km./sec., densities as specific gravity and layer thickness in km.

For the remainder of this discussion the term DYNAMIC PROPERTIES will refer to the modulus and the argument of a particular type of wave.

3.3 Dynamic Properties and Frequency

Figure 3.2 shows dynamic properties for the interference of a PP reflected wave and a PPP head wave for four frequencies. The asymptotic curve for the simply reflected

Figure 3.2. Dynamic properties and frequency. A series of plots of dynamic properties is displayed for an interference PP-PPP wave system for frequencies of 2.5, 10, 15, and 30 Hertz.

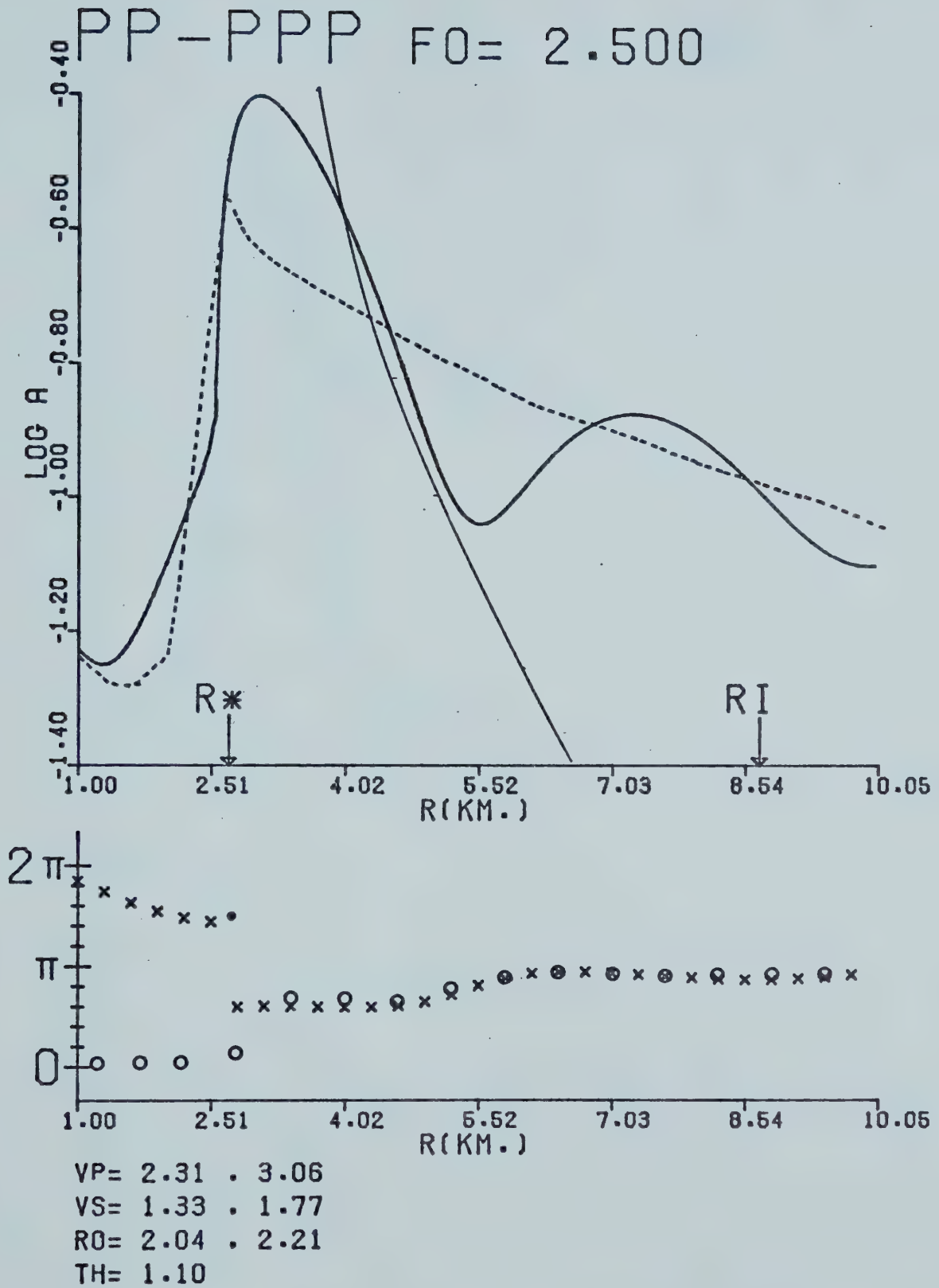


Figure 3.2a

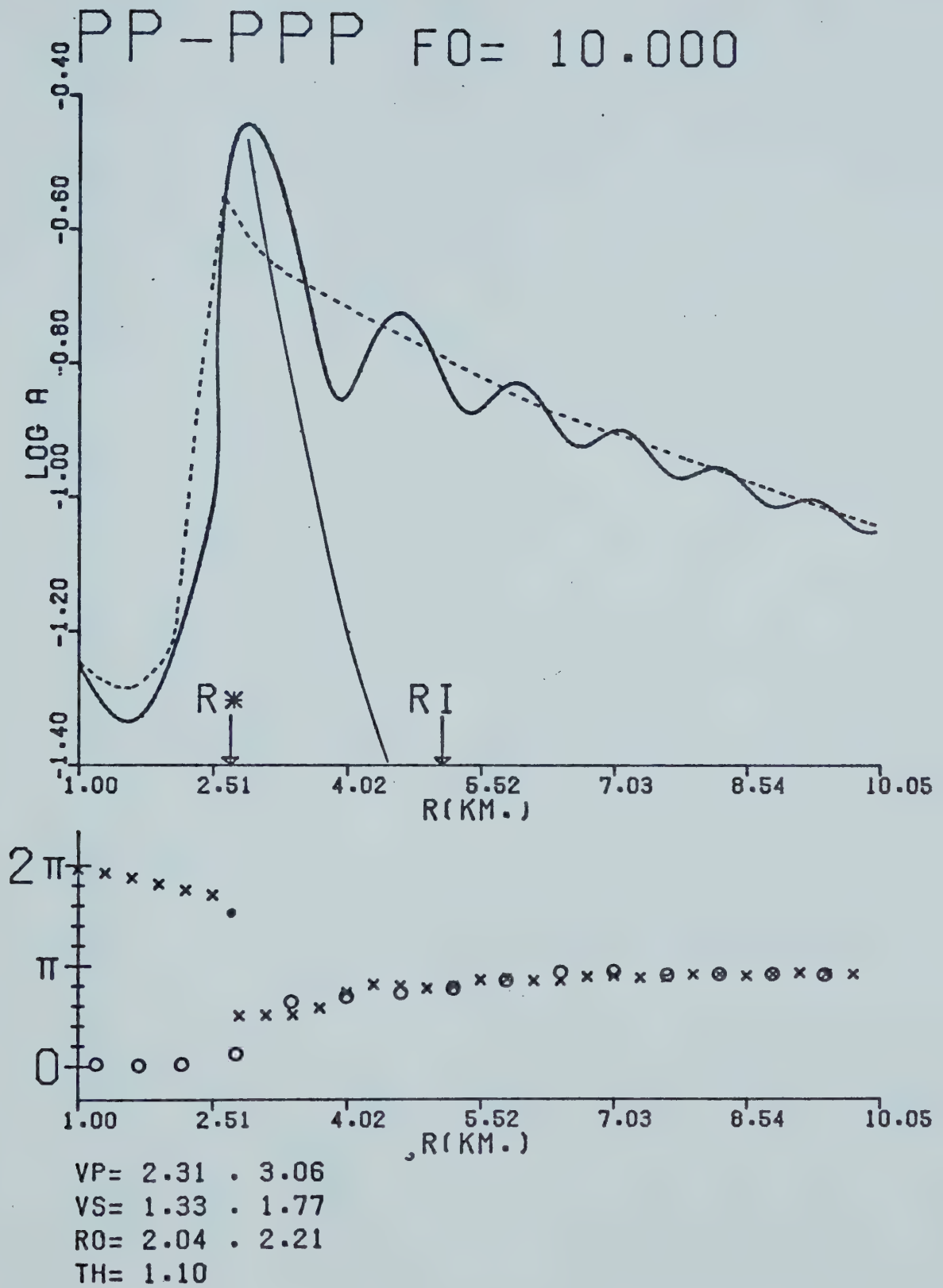


Figure 3.2b

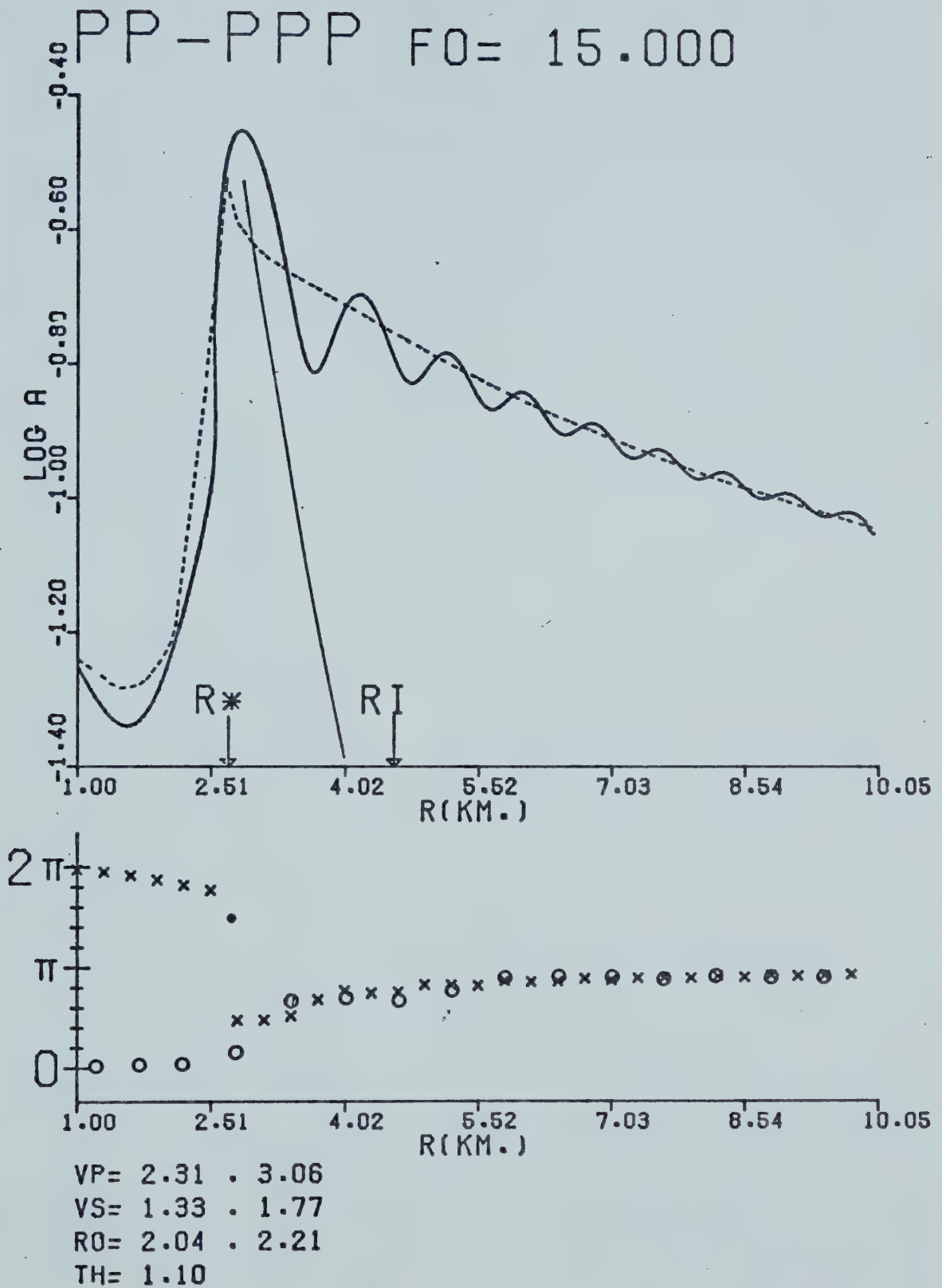
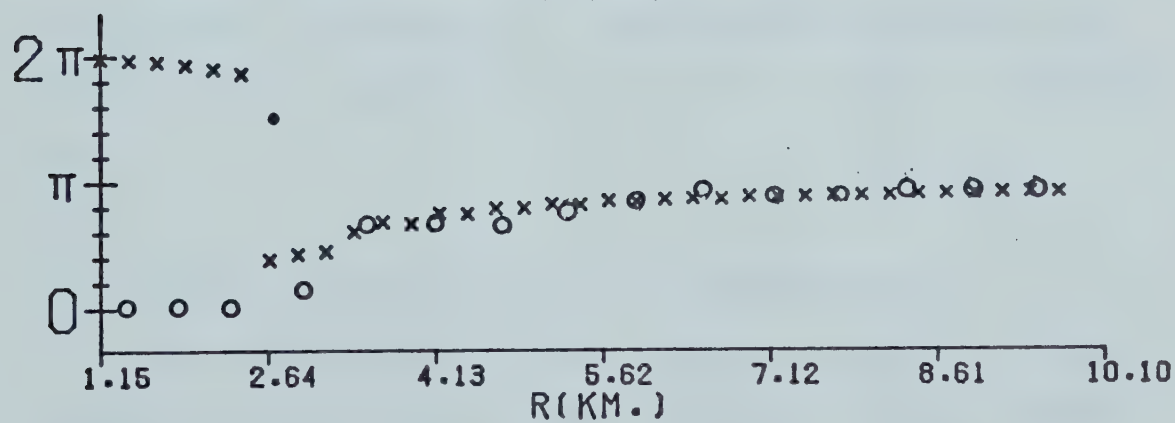
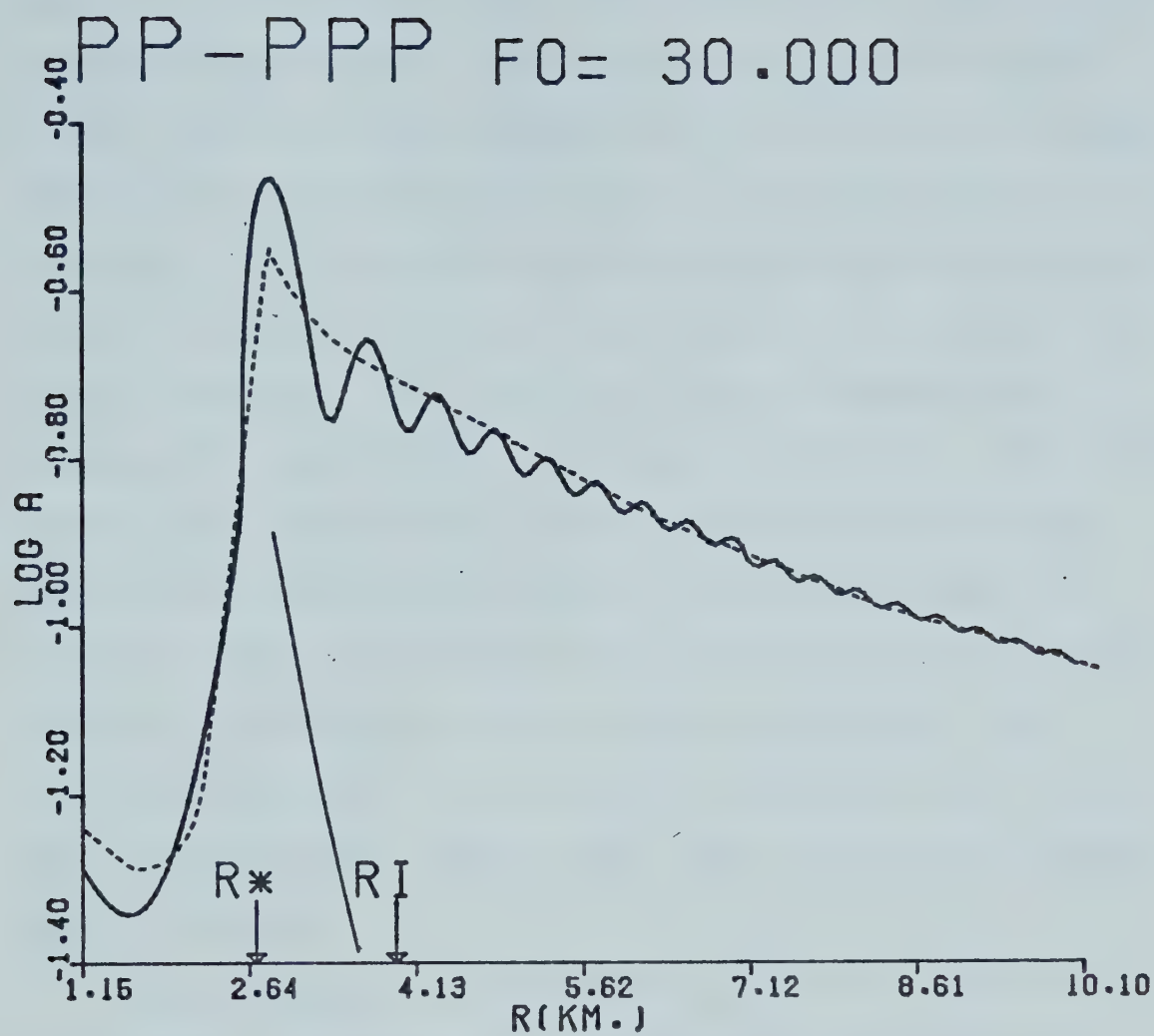


Figure 3.2c



VP= 2.31 . 3.06

VS= 1.33 . 1.77

RO= 2.04 . 2.21

TH= 1.10

Figure 3.2d

ray has a sharp peak at the critical point and continuously decreases beyond this. The interference curve is smooth in the vicinity of the critical point and attains a maximum somewhat beyond the critical point. By close examination of Figure 3.2, it can be seen that the position of the maximum shifts closer to the critical point as the source frequency increases. This result was also predicted by Cerveny (4) (pp. 215-219). At greater distances, the interference curve decreases as it oscillates about the ray theoretical curve. With higher frequency the width and height of the oscillations in the interference wave curve decrease. The argument of the interference wave also oscillates about that of the simply-reflected wave. However, for the higher frequencies these oscillations become nearly invisible.

The length of the interference zone is inversely proportional to frequency. The formulae describing the length of the interference zone are discussed in Appendix A.5.

3.4 Dynamic Properties and Multi-Layered Media

The application of this theory to a multi-layered medium is demonstrated in this section. Let us consider a model consisting of two layers over a half-space. The model chosen consists of the first two layers of the Alberta model described in Hron and Kanasewich (16). The velocity distribution at the bottoming interface is such

as to allow the formation of all eight types of head waves. In all examples shown the simply reflected ray consisted of four segments. Two of these were always P-type in the first layer. The other two were in layer two and of the type stated on each plot. The source frequency is constant at 2.5 Hertz in all cases.

It can be readily seen that the fit between interference amplitude and simple reflected amplitude grows better with increasing distance from the critical point. Upon examining the PP-PPP case it is clear that the simple reflected amplitude curve has little resemblance in general shape to that of Figure 3.2. Two reasons can be presented for this. The earth model used in constructing Figure 3.3 has a second critical point which causes a peak near this point. Secondly, when computing ray amplitude the transmission coefficients at the interface between layers 1 and 2 tend to smooth out the sharp peak which appears at the first critical point.

The PP-PSP case also requires some discussion. This head wave has the largest critical distance of all eight types. At larger epicentral distances the spreading factor, L , in equation 2.51 becomes more significant than at small ones. Thus, for the relatively large epicentral distances considered in this case the spreading factor has become large enough to damp out any oscillation present in the amplitude distance curve. A numerical experiment was performed to calculate the value of the amplitude without

Figure 3.3. Dynamic properties and multi-layered media. A series of plots of dynamic properties in a two layered medium for all eight head waves. Figure 3.3c shows the case PP-PSP with the effect of geometrical spreading removed to display the oscillatory nature of the modulus curve.

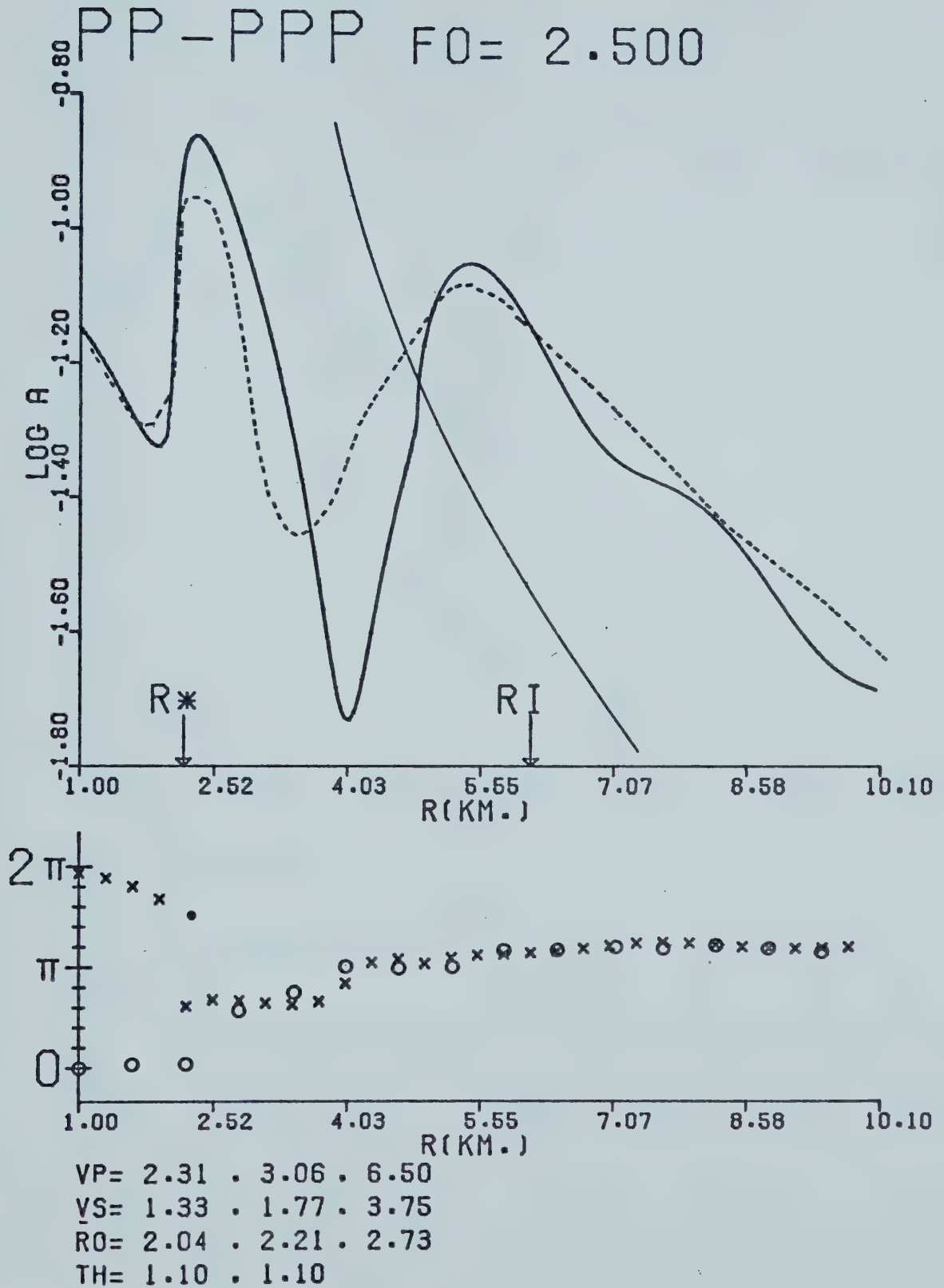


Figure 3.3a

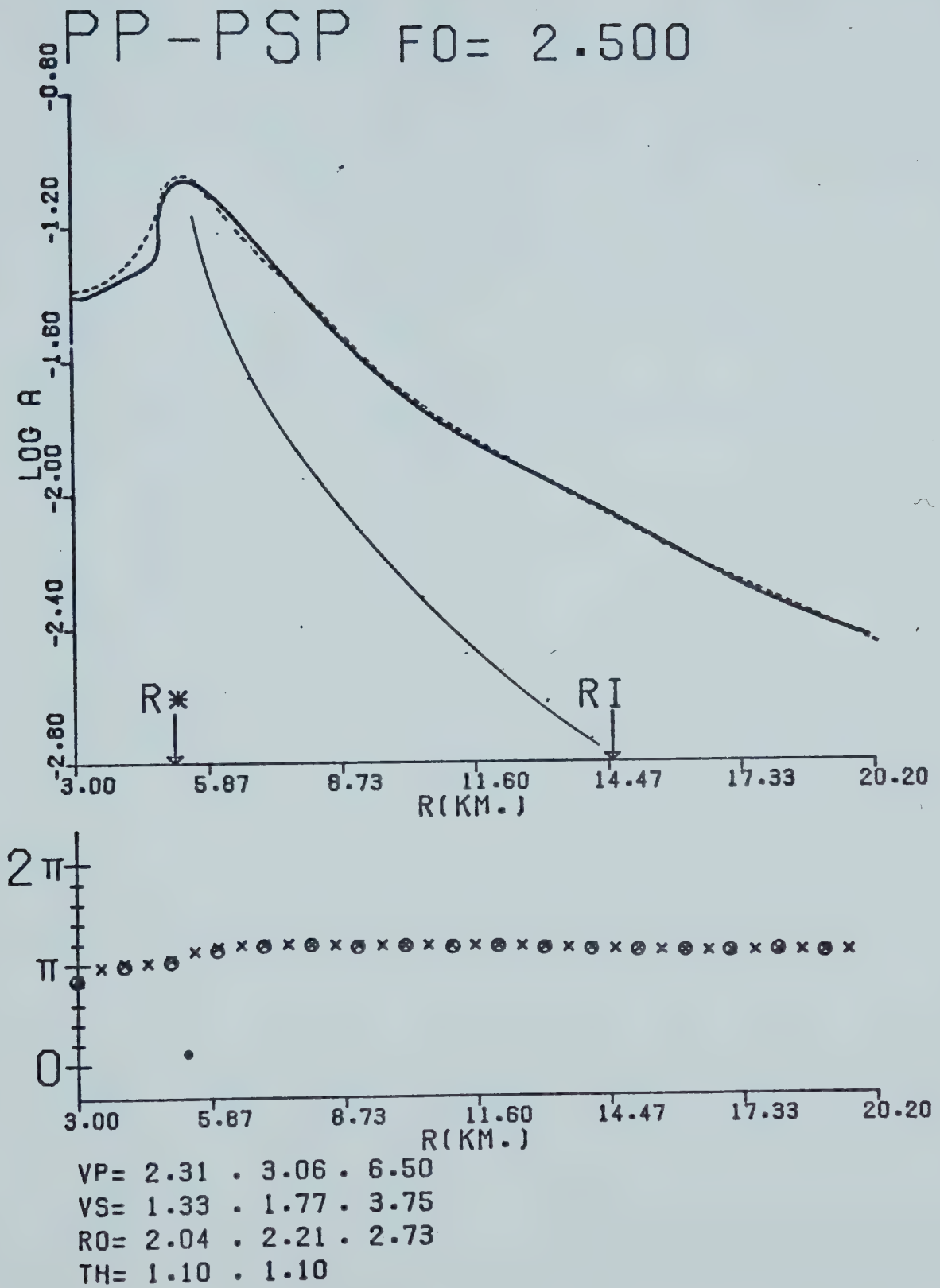


Figure 3.3b

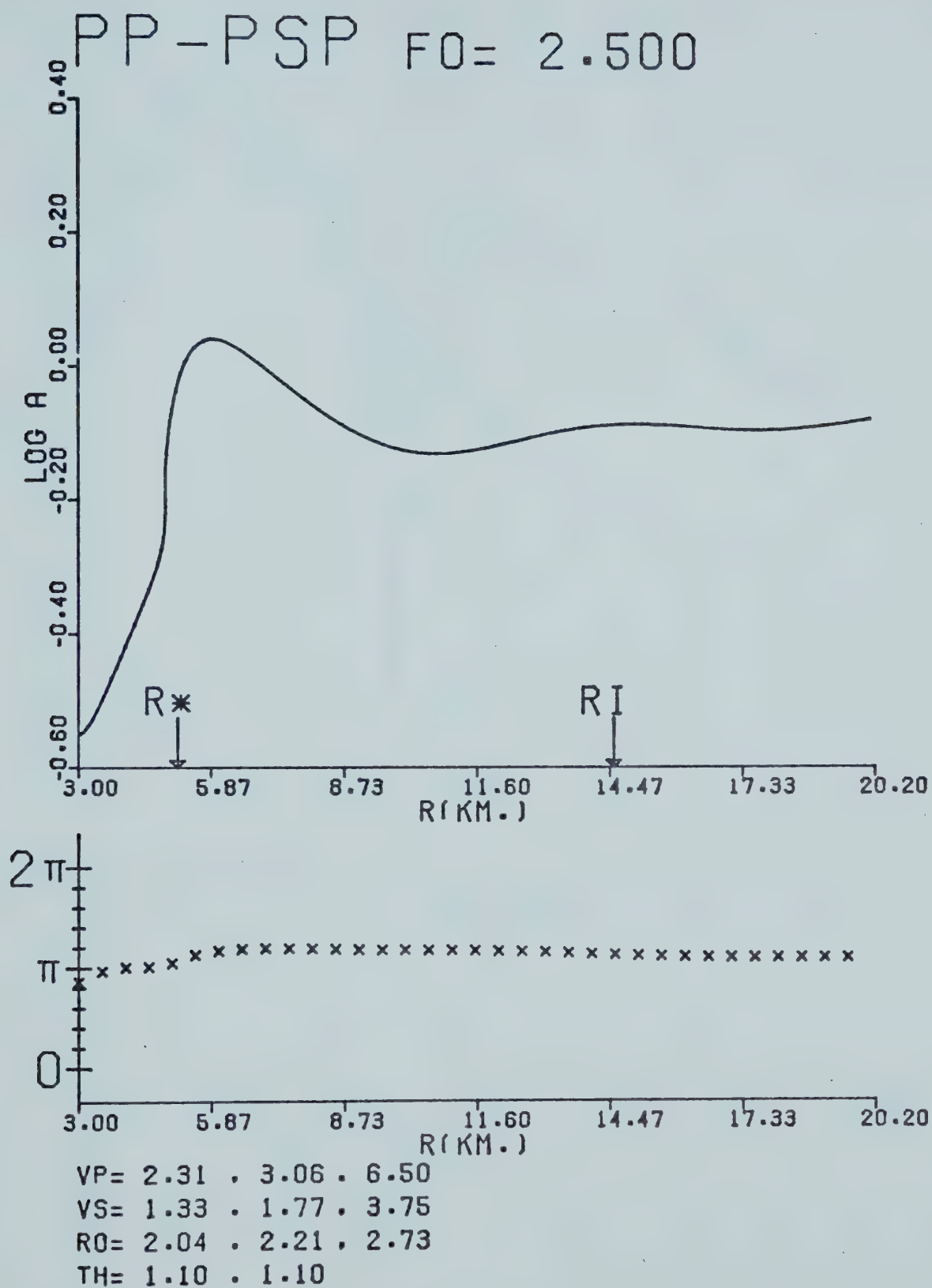
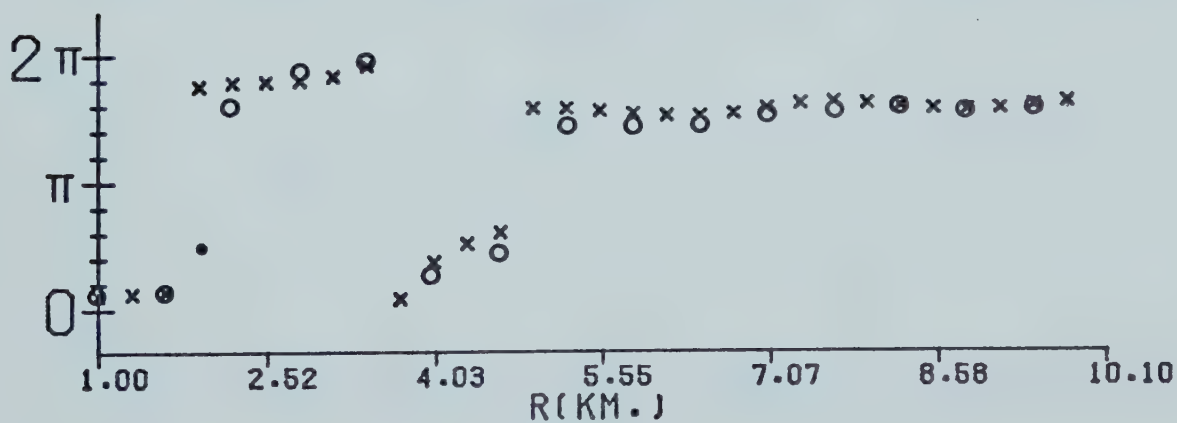
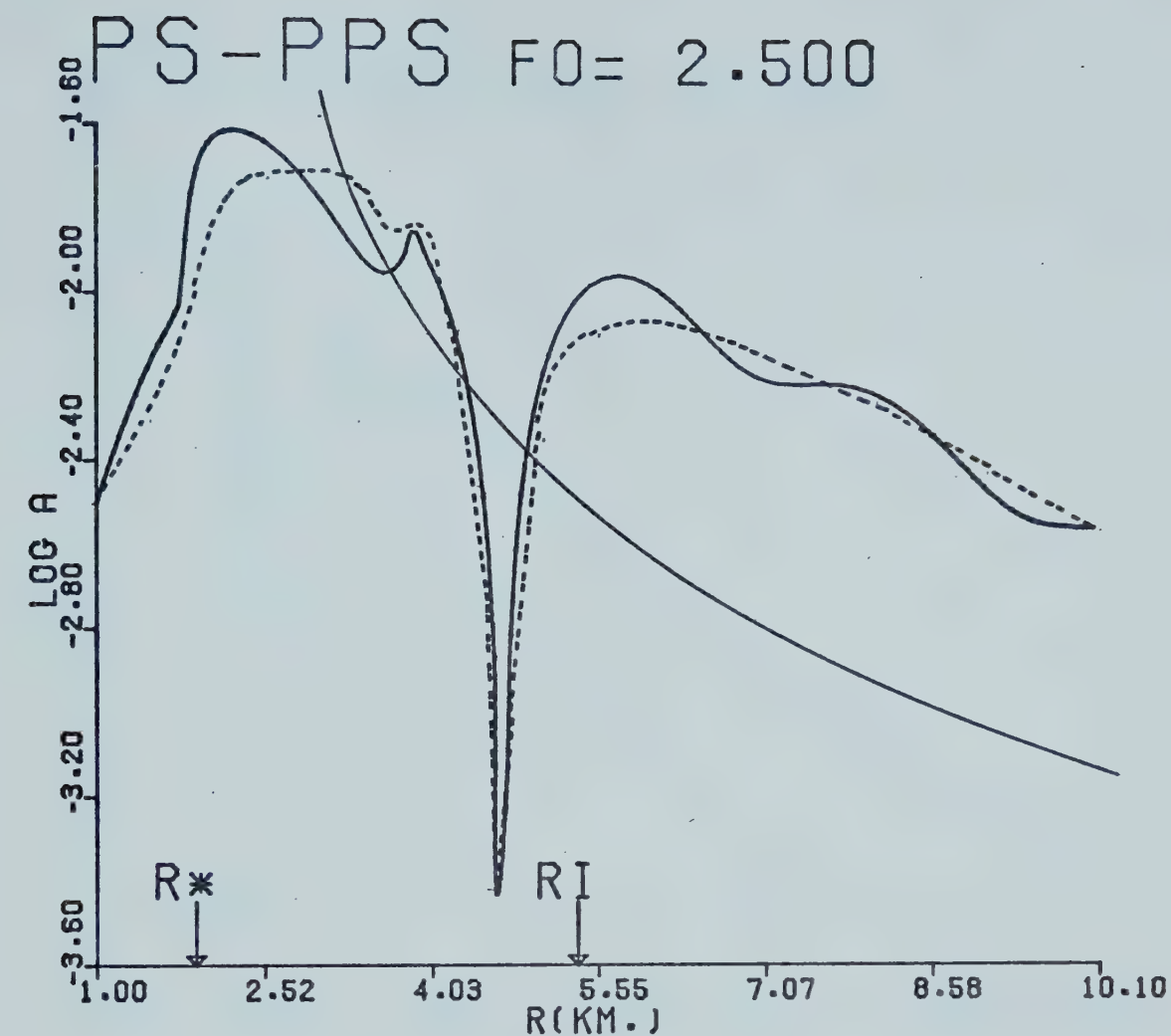


Figure 3.3c



VP= 2.31 . 3.06 . 6.50

VS= 1.33 . 1.77 . 3.75

RO= 2.04 . 2.21 . 2.73

TH= 1.10 . 1.10

Figure 3.3d

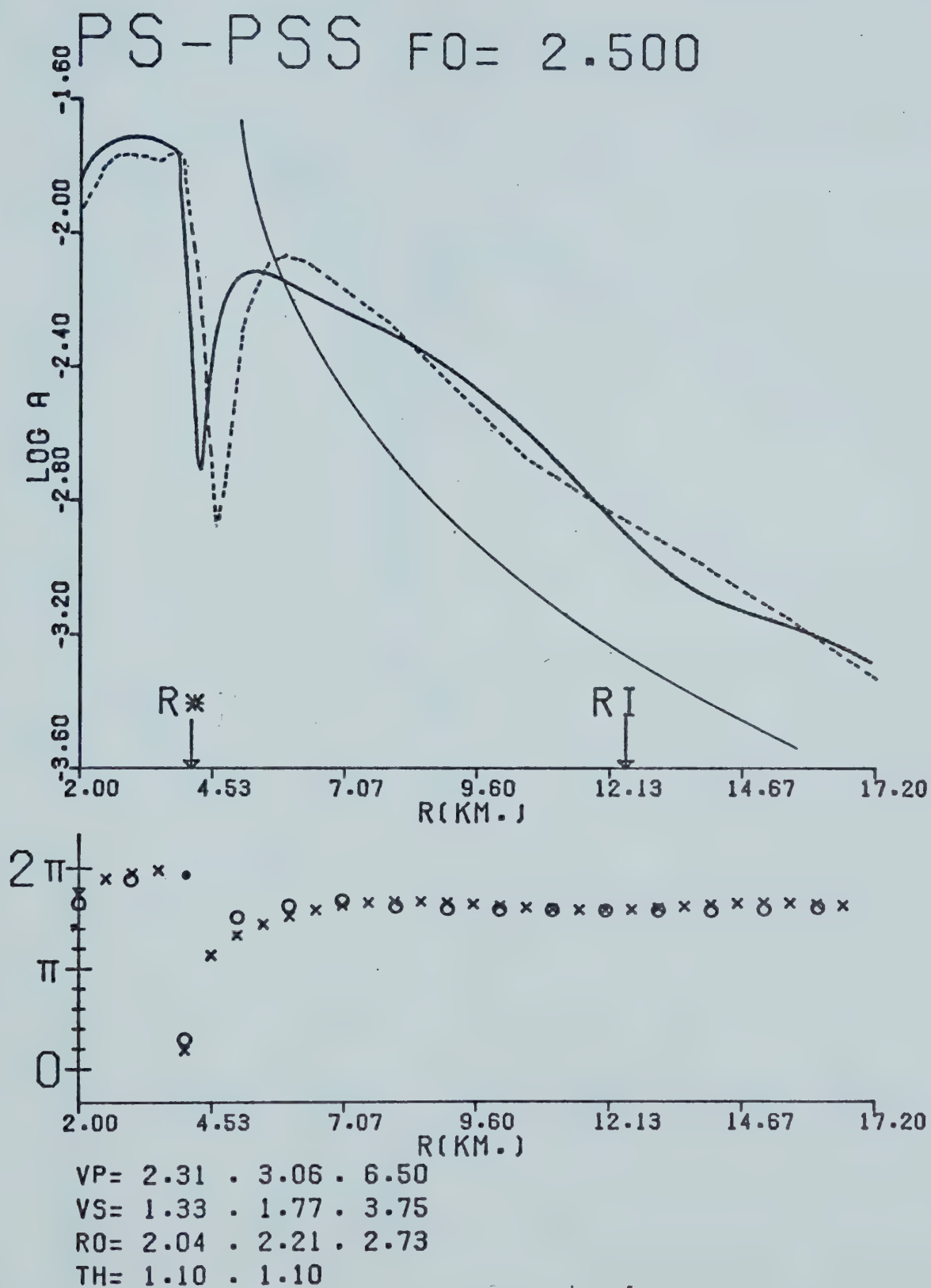


Figure 3.3e

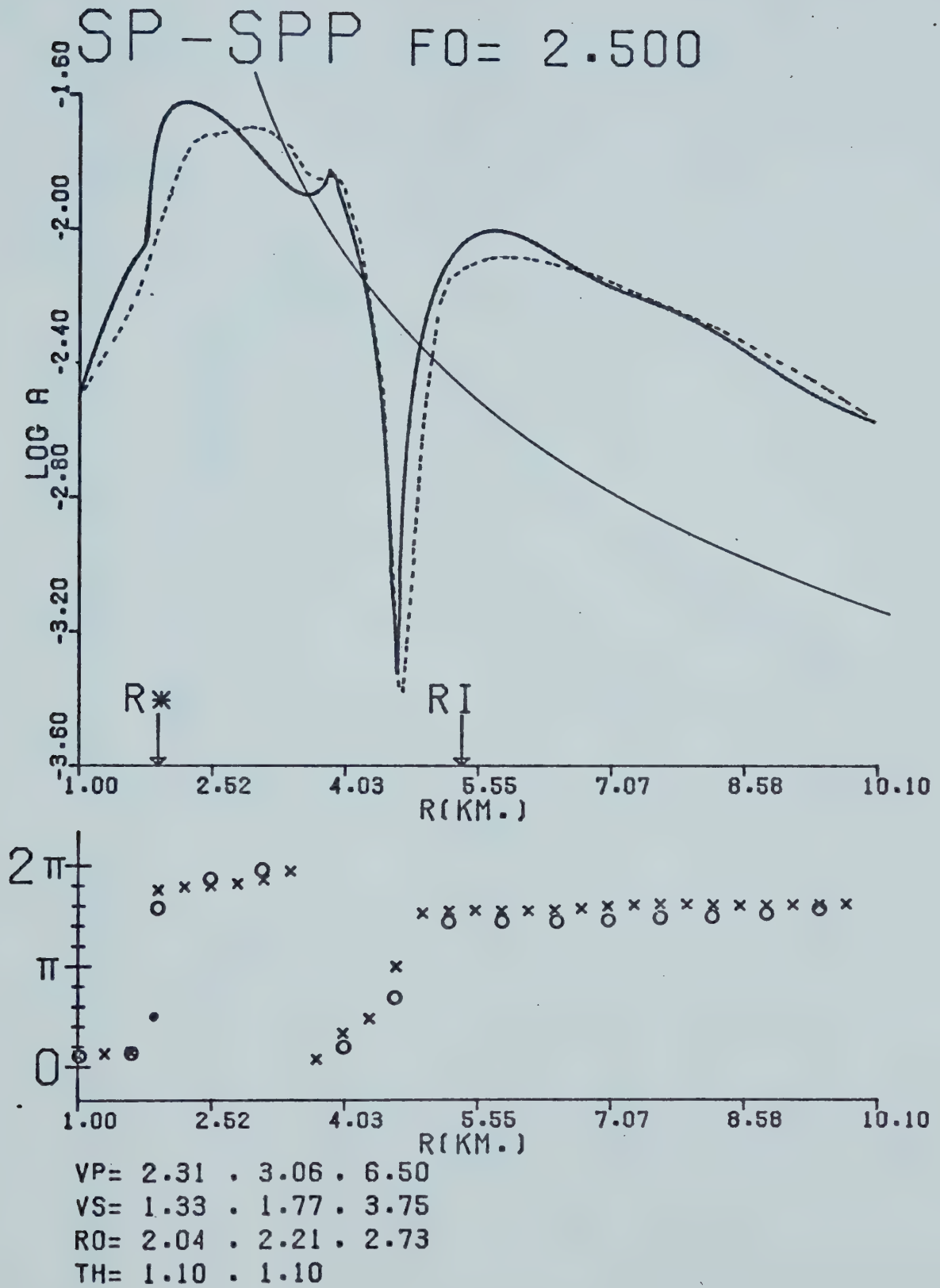


Figure 3.3f

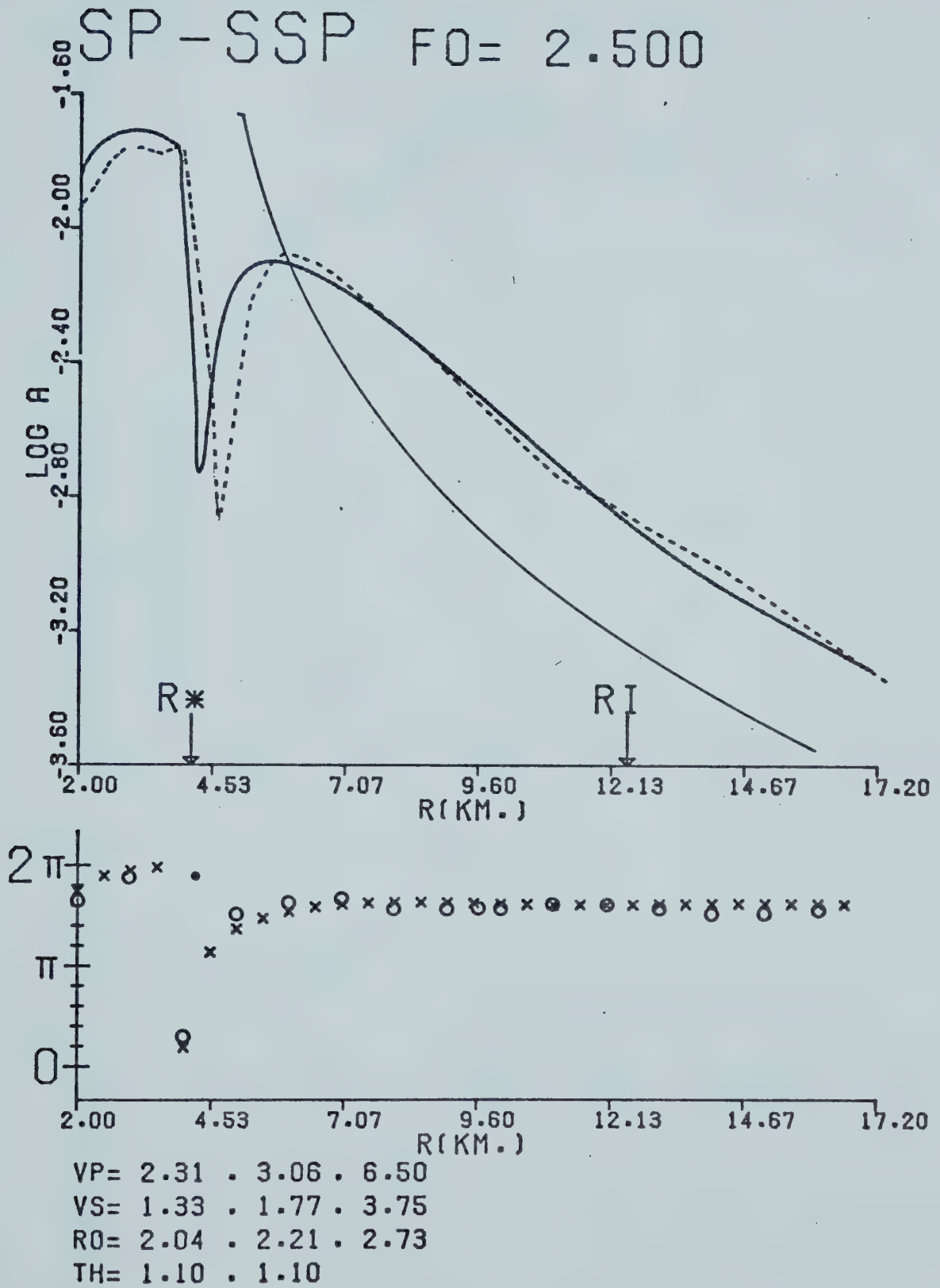


Figure 3.3g

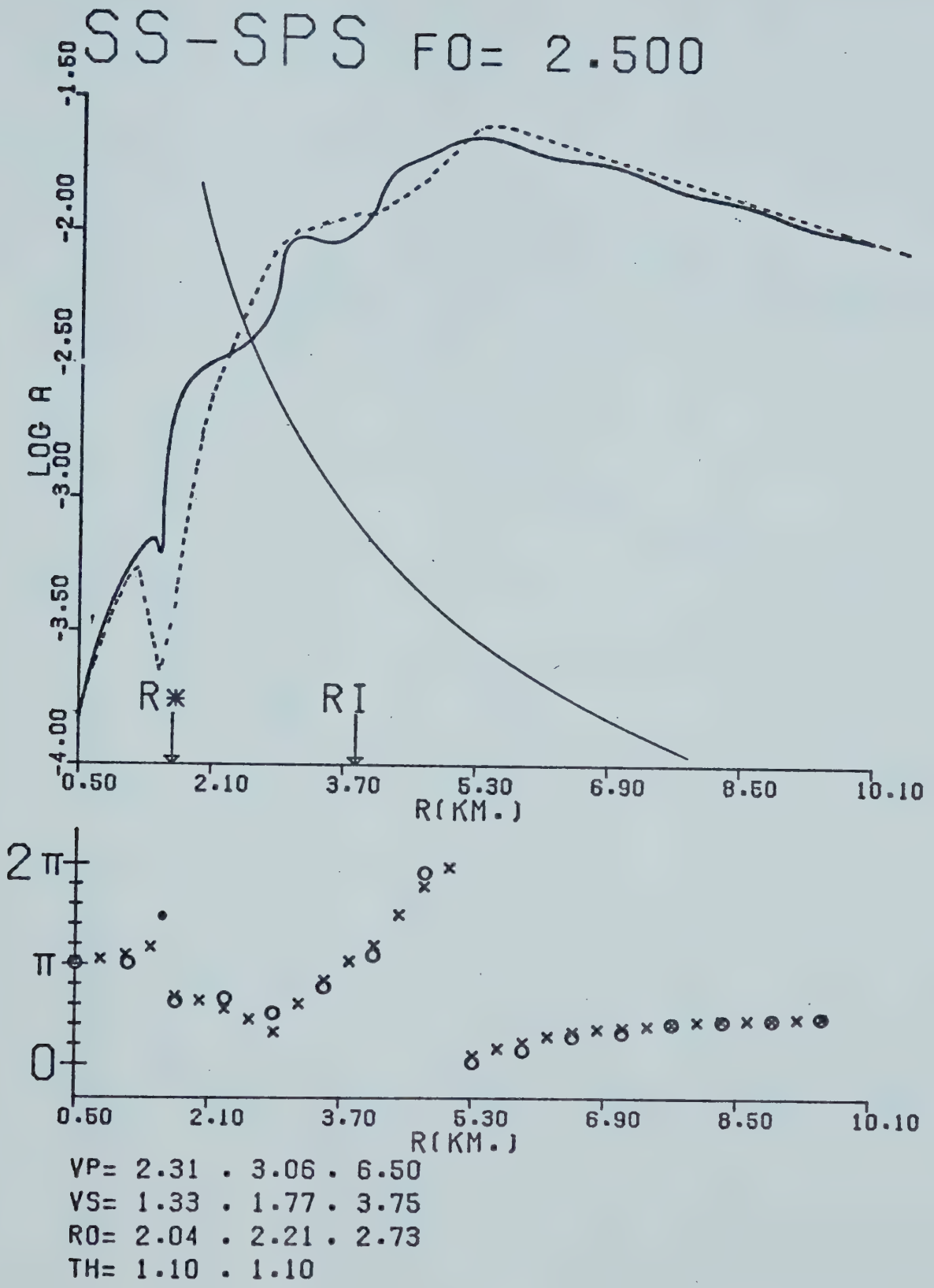


Figure 3.3h

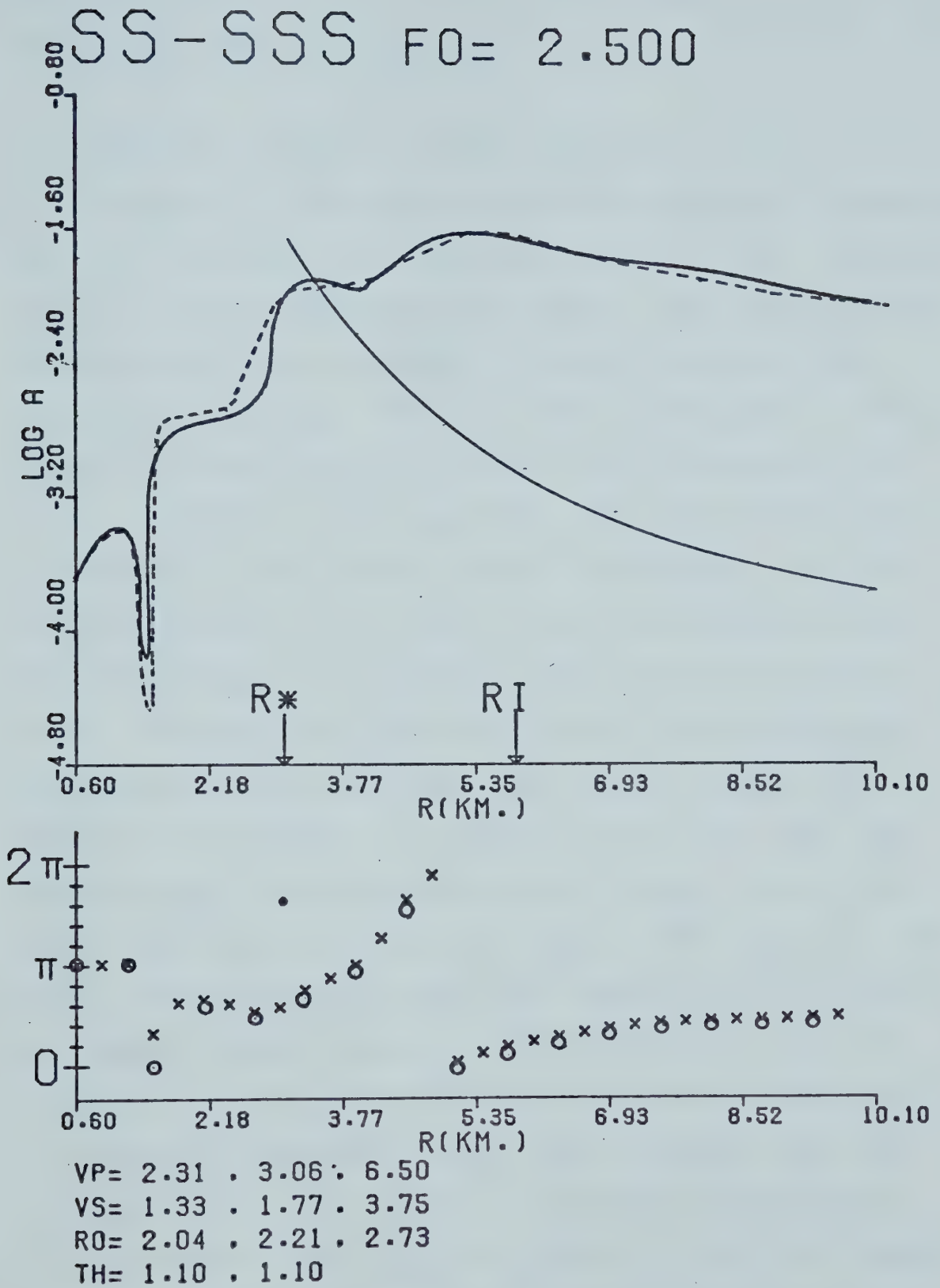


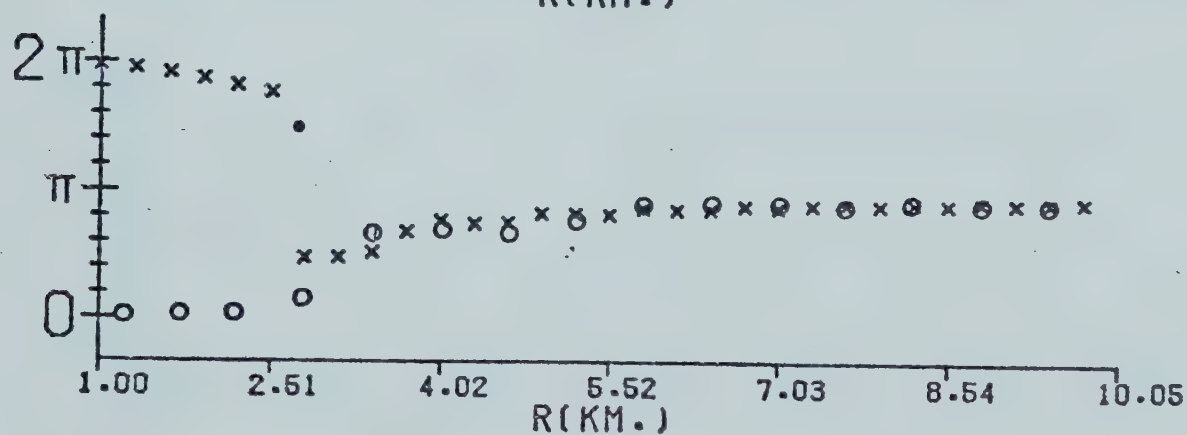
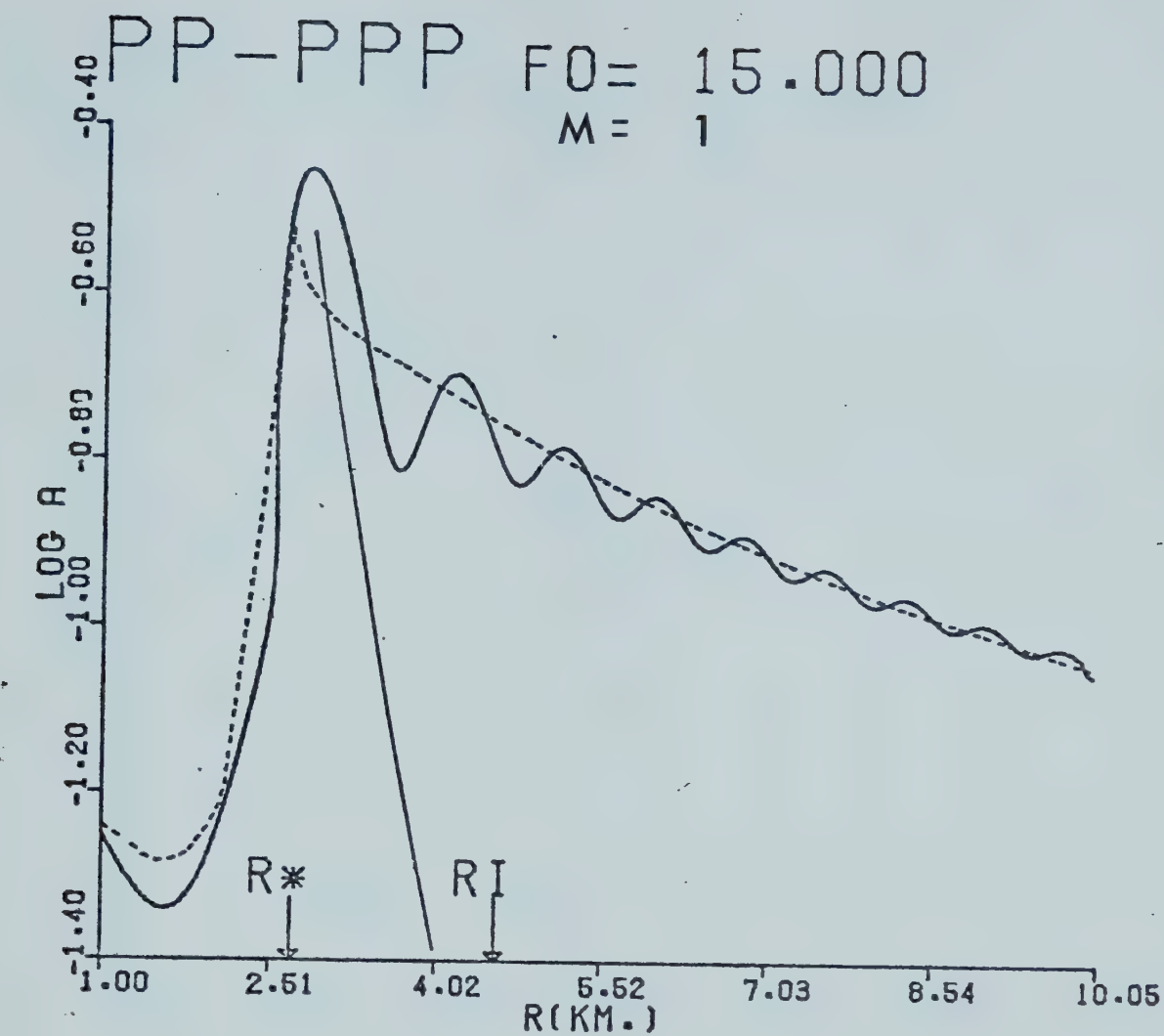
Figure 3.3i

including the effect of the spreading factor, L . The results are shown in Figure 3.3c.

3.5 Dynamic Properties and Head Wave Multiplicity

Figure 3.4 consists of four plots of dynamic properties for a PPP head wave with multiplicity $M = 1, 2, 3, 4$. For all cases the source frequency is 15 Hertz. The lines sketched on each graph have a somewhat different definition than in the previous sets. The solid line running over all epicentral distances up to the end of the interference zone is the interference wave amplitude calculated using formulae derived in this thesis. This line becomes a line of long dashes beyond this point. This is to signify a certain inaccuracy in the formulae which will be discussed later. The solid line beginning beyond the interference zone represents the head wave amplitude as derived from asymptotic ray theory. The dashed line is split into two segments each having different significance. Before the end of the interference zone the dashed line represents the simply reflected PP wave amplitude computed from asymptotic ray theory. Beyond the end of the interference zone it represents the sum of the simply reflected and head waves. To produce this sum one considers the reflected wave displacement $\exp(-i \omega(t - t_{pp})) \cdot A_R$ and the head wave displacement $\exp(-i \omega(t - t_{ppp})) A_H$ where A_R and A_H are complex numbers representing the dynamic properties of the wave. These two displacements are summed as

Figure 3.4. Dynamic properties and head wave multiplicity. A PP-PPP interference wave has its dynamic properties plotted for multiplicity, M , equal to 1, 2, 3, 4. Source frequency is constant at 15 Hertz.



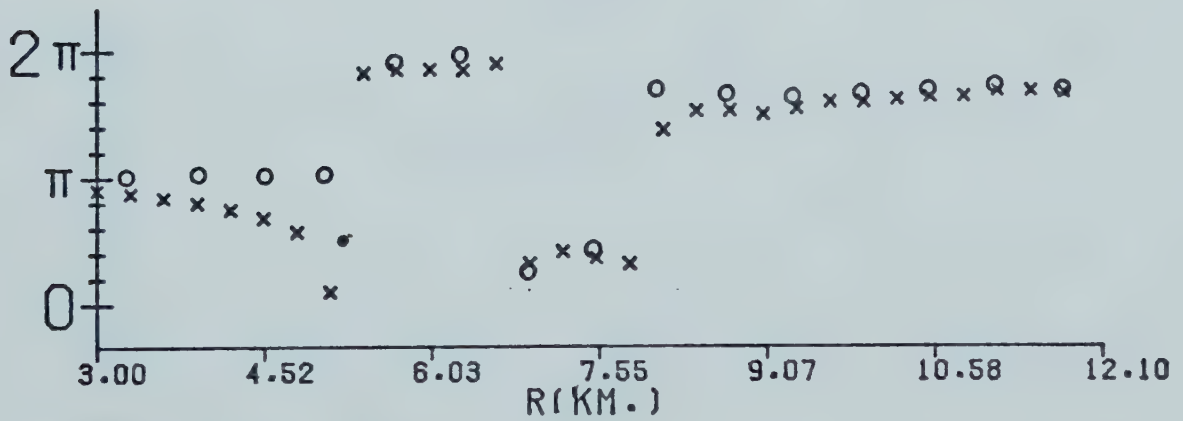
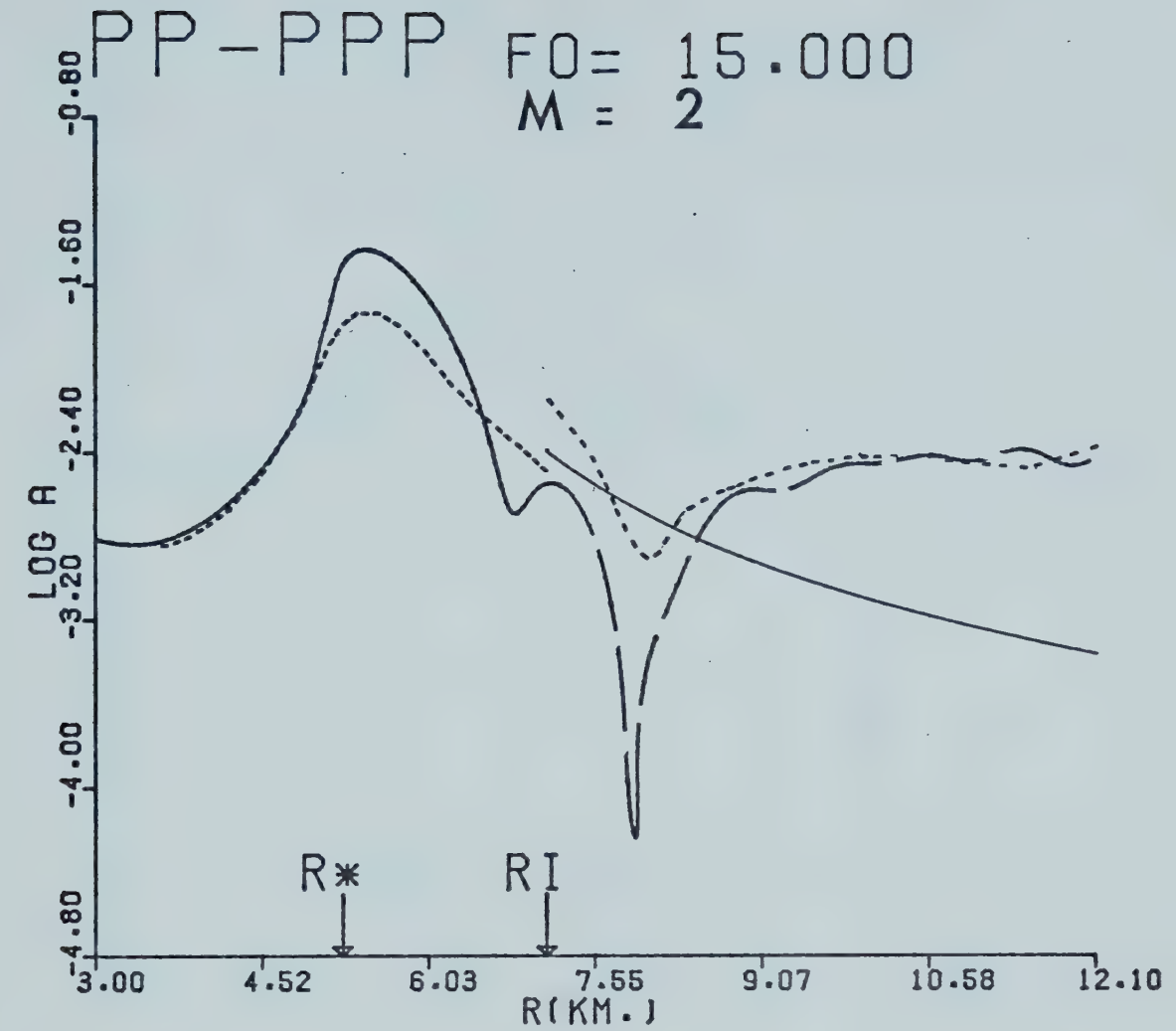
VP= 2.31 . 3.06

VS= 1.33 . 1.77

RO= 2.04 . 2.21

TH= 1.10

Figure 3.4a



VP= 2.31 . 3.06
 VS= 1.33 . 1.77
 RO= 2.04 . 2.21
 TH= 1.10

Figure 3.4b

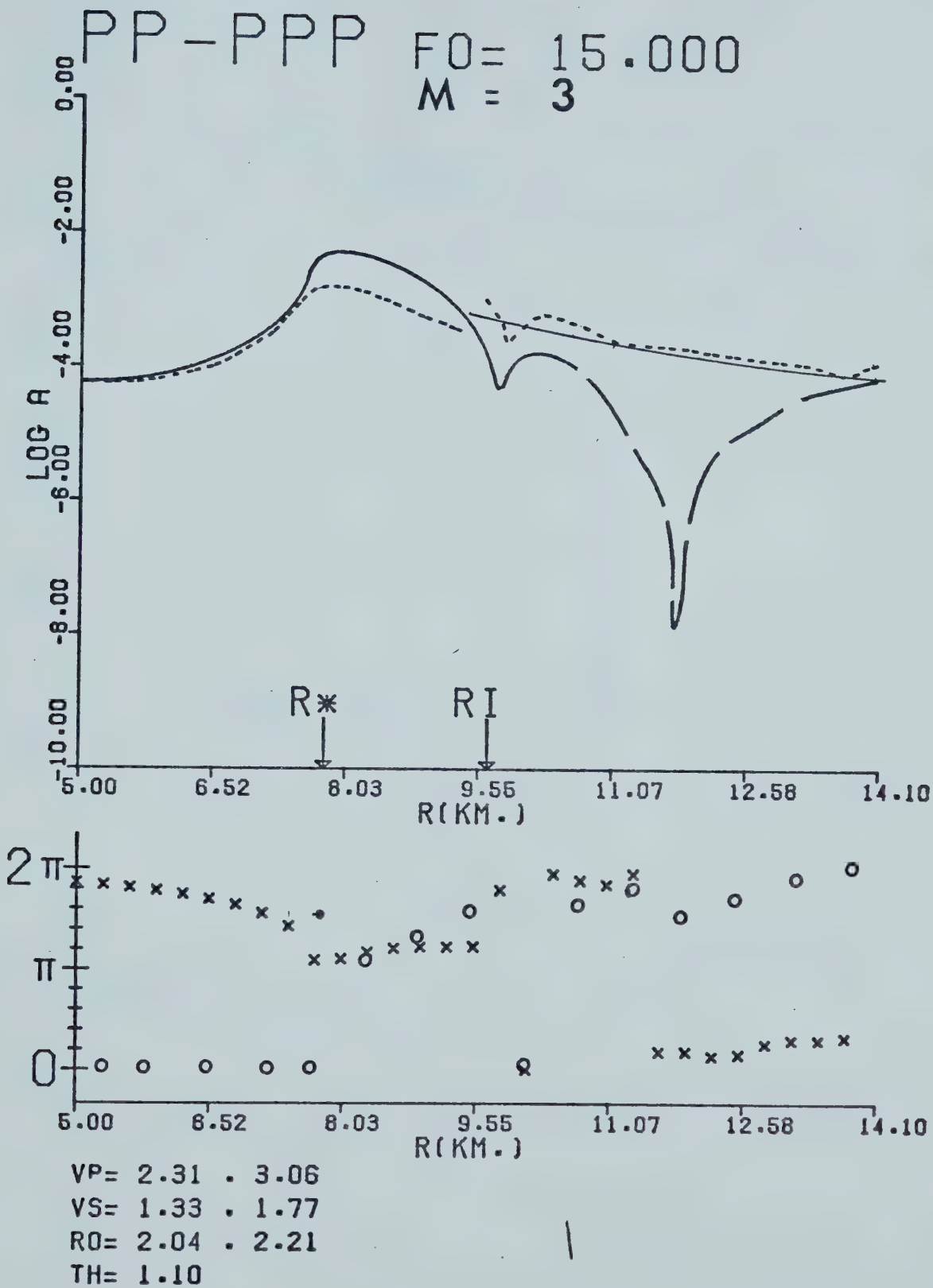
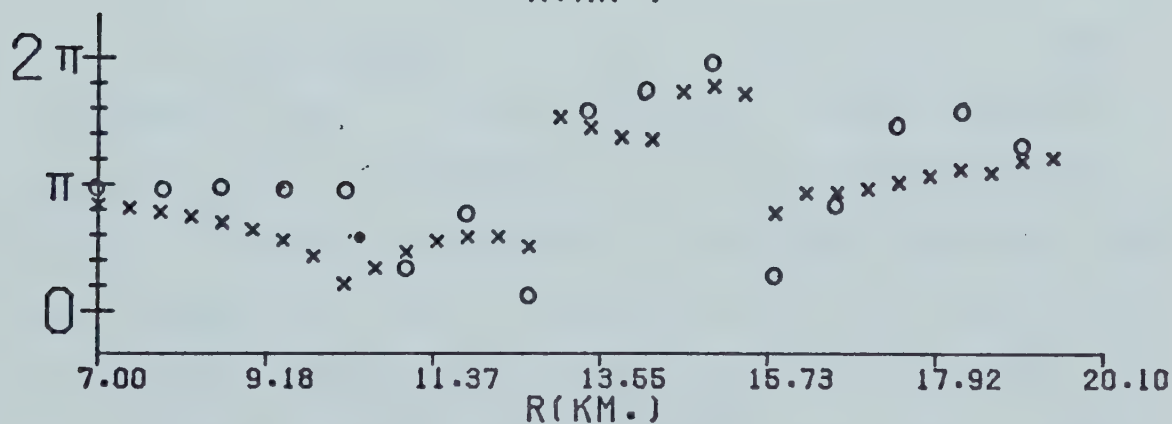
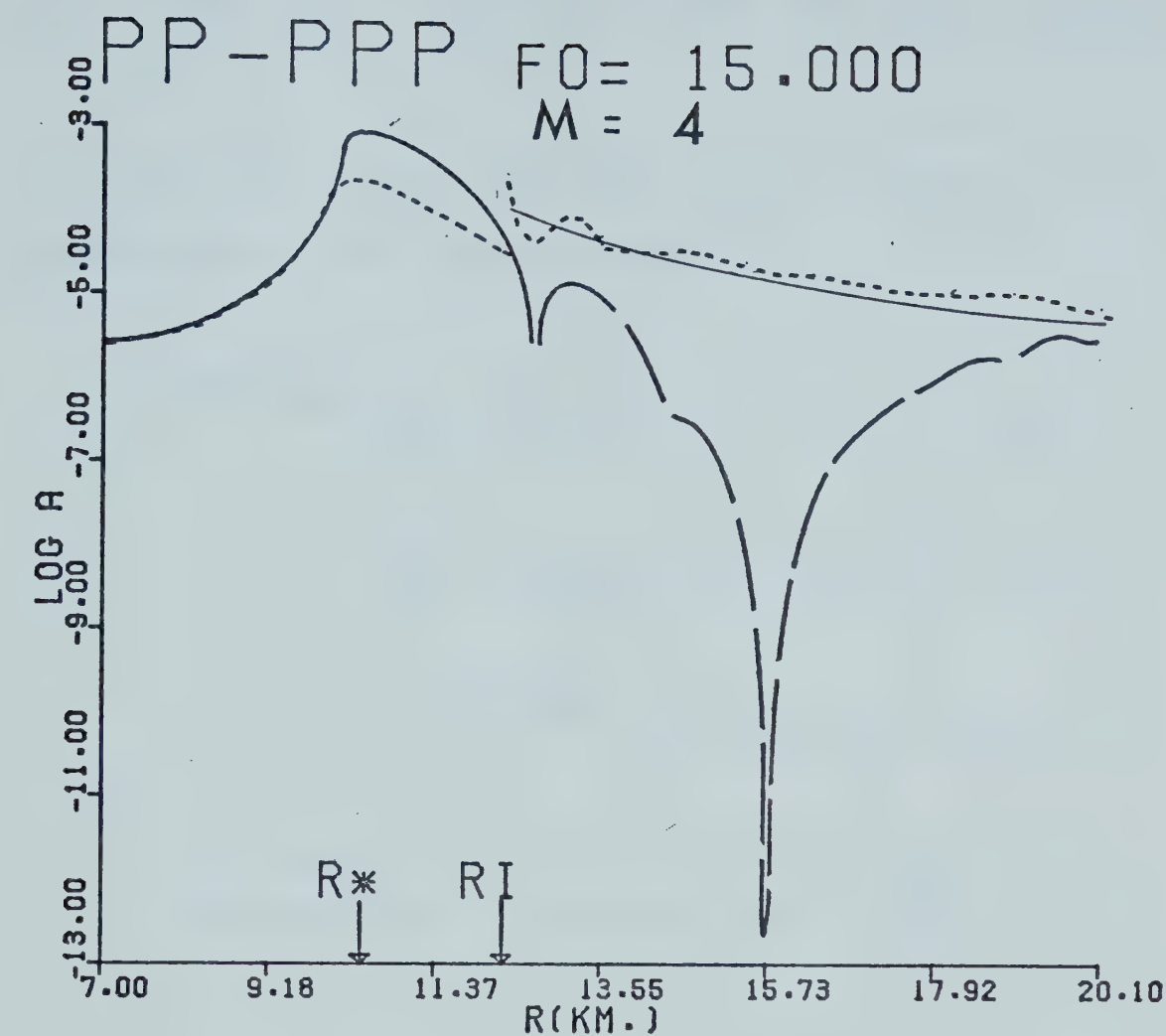


Figure 3.4c



VP= 2.31 . 3.06

VS= 1.33 . 1.77

RO= 2.04 . 2.21

TH= 1.10

Figure 3.4d

$$e^{-i \omega(t-t_{pp})} [A_{Rr} + i A_{Ri} + e^{-i \omega(t_{pp}-t_{ppp})} (A_{Hr} + i A_{Hi})]$$

The subscripts r and i refer to real and imaginary parts, respectively. This can be adjusted to

$$\begin{aligned} e^{-i \omega(t-t_{pp})} & [(A_{Rr} + A_{Hr} \cos \omega \Delta t + A_{Hi} \sin \omega \Delta t) \\ & + i(A_{Ri} + A_{Hi} \cos \omega \Delta t - A_{Hr} \sin \omega \Delta t)] \\ & = e^{-i \omega(t-t_{pp})} [A]; \quad \Delta t = t_{pp} - t_{ppp} \end{aligned}$$

$$\text{Modulus} = |A| \quad \text{Argument} = \tan^{-1} \frac{\text{Im}(A)}{\text{Re}(A)}$$

On the argument plot the x's again represent the interference wave. The open circles denote argument of the reflected wave amplitude up to the end of the interference zone and the argument of the total asymptotic amplitude beyond this point. The solid circle at the critical point gives the argument of the head wave amplitude.

Several points should be noted about these diagram:

- (1) With increasing head wave multiplicity the upward shift of the interference wave amplitude from the reflected wave amplitude increases. This is what

one would expect on the basis of physical reasoning alone. This increasing shift upwards is due to the increasing number of head waves with the same amplitude interfering with the reflected wave.

- (2) With increasing multiplicity the ray theoretical total amplitude curve tends to behave more like the head wave curve than the interference curve. This feature goes hand in hand with the fact that the head wave amplitude increases with increasing multiplicity.
- (3) With increasing multiplicity the phase shift seems to have a poorer fit between interference and asymptotic ray values. The reasons for this will be discussed in point (4).
- (4) The pronounced dip appearing in the interference wave amplitude curve can be explained by the influence of the free surface coefficient. This coefficient undergoes a phase shift where it passes through zero modulus (F. Hron, personal communication). With an increasing number of reflections from the free surface this effect becomes exaggerated. The interference curve has been drawn in long dashes beyond the interference zone due to this inaccuracy. A fuller discussion of this is necessary.

We recall from Chapter 2 that the generalized dynamic property formula was of the form

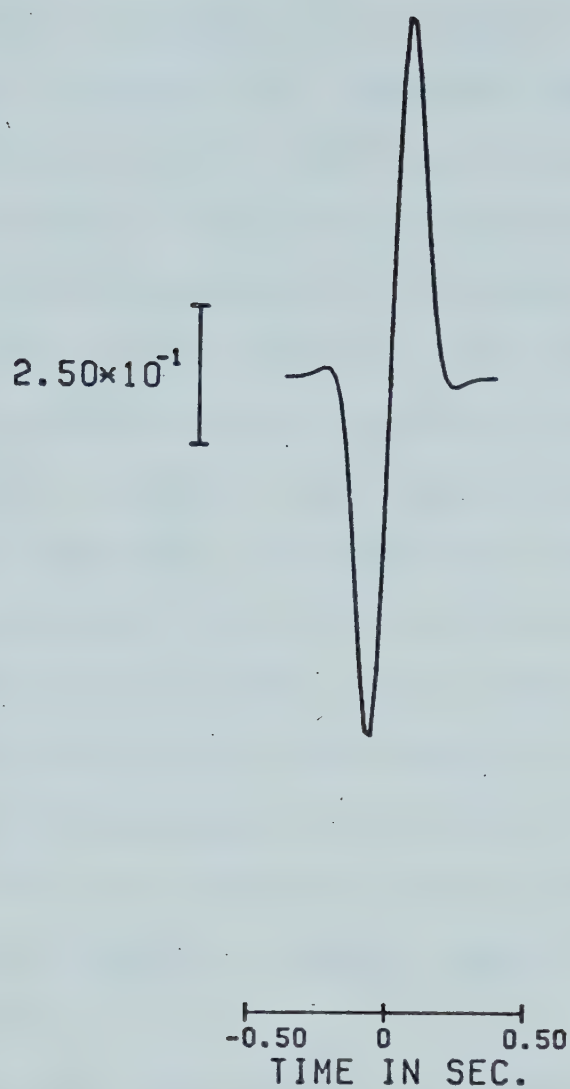
$$A = \frac{\sigma}{L} [R_{j \ell} - H_{j k \ell}]$$

where $R_{j\ell}$ represented the reflection coefficient, $H_{jk\ell}$ the correction due to the head wave in the critical region, L the geometric spreading and σ the product of all interface coefficients encountered by the ray in its path from source to receiver. We also recall that $\sigma(q_1)$ was removed from the integrand and q_1 assigned its value at the saddle point, namely x_1 . Near the saddle point this approximation is valid, but with increasing distance its validity falters. Thus when the free surface reflection coefficient passes through zero it totally suppresses the term $H_{jk\ell}$ in the above formula.

However, for the purpose for which this study was undertaken (dynamic properties in the critical region) the results are only necessary within the interference zone. Should the formulae be used for the calculation of synthetic seismograms, their use should be restricted to the critical region. Outside that region the asymptotic ray values should be taken.

3.6 Reflected Pulses Near the Critical Point

On the basis of formulae presented in this study, synthetic seismograms can be produced for interference waves near the critical point. At points far from the critical point, one may utilize the amplitude formulae from asymptotic ray theory. The model chosen for these computations has been deliberately simplified for purposes of display. Figure 3.5 shows the source pulse for this



$$s(t) = \sin(2\pi ft) \exp(-(2\pi ft/g)^2)$$

$f = 2.5$ hertz

$g = 2.0$

Figure 3.5. Source pulse for synthetic seismograms.

calculation. The synthetic seismograms for horizontal and vertical components of an interference PP-PPP wave are given in Figure 3.6. The earth model is the Manitoba model (one layer over a half-space) as given in Hron and Kanasewich (16). The critical distance (R_C) and the end of the interference zone (R_I) are marked on the plot. For continuity, the exact formulae were used from .8 times the critical distance to the end of the interference zone plus .1 times the length of the interference zone (approximately from 55 to 126 km.). Outside this range the ray theoretical expressions for amplitude were used.

Several conclusions can be drawn from Figure 3.6:

- (1) The form of the reflected pulse changes little on passing through the critical point. The pulse does suffer some distortion due to the reflection coefficient becoming a complex number beyond the critical point.
- (2) The total separation of the head wave from the reflected wave occurs only after the end of the interference zone.
- (3) The travel-time curves of the head and reflected waves are tangential at the critical point.
- (4) Beyond the interference zone the head wave amplitude is very insignificant compared to the simply reflected wave. The head wave amplitude could be enhanced (relative to the simply reflected wave amplitude) by an increase in multiplicity. With an increase in

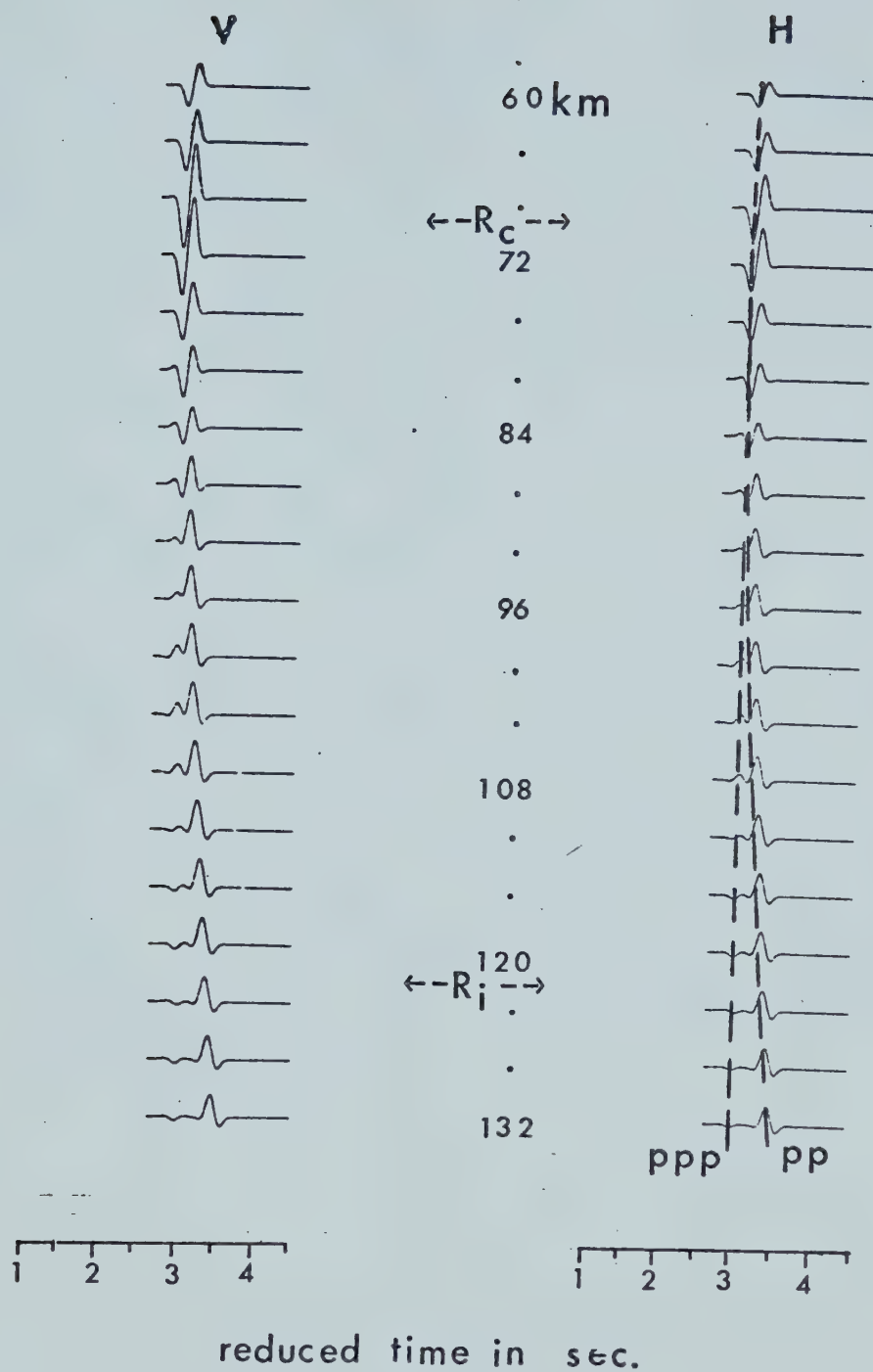


Figure 3.6. Pulse separation.

multiplicity the head wave amplitude may become non-trivial next to the simply-reflected wave.

- (5) The head wave pulse is distorted by an argument of $\pi/2$ with respect to the source pulse. Figure 3.5 displays the source pulse as a sinusoidal pulse in time, while Figure 3.6 exhibits the head wave as a negative cosine in time. In terms of asymptotic theory this is explained by the factor of $1/i$ in the head wave amplitude formula.

It was shown in previous sections that the head wave amplitude is inversely proportional to frequency. With an increasing frequency the head wave amplitude will become such a low value outside the interference zone that its contribution to the seismogram will become insignificant.

Figure 3.6 indicates that there is a very good transition between the exact formulae for dynamic properties and the asymptotic ones. This again provides us with a check upon our derivations.

CHAPTER 4

CONCLUSION

This thesis presents a theoretical study of the dynamic properties of interference head waves near the critical point. The results are valid for arbitrary velocity distributions along the vertical in the bottoming layer. All rays, including those with multiple bottoming reflections are suitable to have these calculations performed on them.

Chapter 1 gives an introduction to the study of reflected and head wave systems. An extensive, although not exhaustive, bibliography is given.

Chapter 2 states the actual theoretical solution of the problem. The integral expressions for the reflected wave in the broad sense are evaluated along special complex-valued integration paths. The contours of integration chosen are a modification of the saddle point contour, allowing certain quantities to be approximated as constants. Chapter 2 also demonstrates the similarity between this method of calculation and asymptotic ray theory. This resemblance becomes stronger for high frequencies or for distances greatly removed from the critical point.

In Chapter 3 the expressions derived in the previous

chapter are cast in a form suitable for numerical computation. In particular, attention is focused on the Weber function, $D_{1/2}$. A series of numerical results are given in which dynamic properties of interference waves are plotted against epicentral distance. The quantities varied include source frequency, number of layers in the overburden, and head wave multiplicity. Also shown in these sections are the dynamic properties as computed by asymptotic ray theory. The similarities between these results are discussed. Finally, Chapter 3 provides a set of synthetic seismograms displaying interference wave characteristics.

This thesis has presented new and original material in the following areas:

- (1) Formulae have been derived for all eight possible types of interference head waves. These formulae are valid at all epicentral distances, in particular the critical region. The formulae tend to asymptotic ray theory values for high frequency or great distance from the critical point.
- (2) The works of Cerveny have been generalized to the cases of multi-layered media, arbitrary ray paths and any of the eight possible types of interference waves. Related to arbitrary ray paths are multiple head waves, the solution of which is also presented in this study.

- (3) Numerical solution and tabulation of the Weber function $D_{1/2}$.

There are several areas of this problem that require further attention. Some of the possibilities are:

- (1) Exact numerical integration of the integral expressions for the reflected wave system could be performed. Although this is computationally expensive, it would provide an excellent check upon both the asymptotic theory and the one presented here.
- (2) A similar approach to this one should be attempted for an anisotropic medium. The major difficulty here is not so much in solution, but rather in formulation of the integral expressions.
- (3) The dynamic properties should be studied for a group of kinematic analogs rather than for a single ray. These results could then be employed in the computation of synthetic seismograms.

BIBLIOGRAPHY

1. Abramowitz, M. and I. Stegun (1970). Handbook of Mathematical Functions. Dover Publications, New York, 1064 pp.
2. Bortfeld, R. (1962). Exact Solution of the Reflection and Refraction of Arbitrary Spherical Compressional Waves at Liquid-Liquid Interfaces and at Solid-Solid Interfaces with Equal Shear Velocities and Equal Densities. Geophys. Prospect., 10, 35-67.
3. Bortfeld, R. (1962). Reflection and Refraction of Spherical Compressional Waves at Arbitrary Plane Interfaces. Geophys. Prospect., 10, 517-538.
4. Brekhovskikh, L. (1960). Waves in Layered Media. Academic Press, New York, 561 pp.
5. Cagniard, L. (1962). Reflection and Refraction of Progressive Seismic Waves. McGraw-Hill, New York, 282 pp.
6. Cerveny, V. (1962). On Reflected and Head Waves Around the First and Second Critical Point. Geofysikalni Sbornik, 165, 43-94.
7. Cerveny, V. (1962). On the Length of the Interference Zone of a Reflected and Head Wave Beyond the Critical Point and on the Amplitudes of Head Waves. Studia Geophys. et Geod., 6, 49-64.
8. Cerveny, V. (1965). The Dynamic Properties of Reflected and Head Waves Around the Critical Point. Geofysikalni Sbornik, 221, 135-245.
9. Cerveny, V. (1967). The Theory of Reflected and Head Waves in the case of a Layered Overburden. Geofysikalni Sbornik, 269, 133-180.
10. Cerveny, V. and R. Ravindra (1971). Theory of Seismic Head Waves. University of Toronto Press, Toronto, 312 pp.
11. Dix, C. (1963). Cagniard's Method and Associated Numerical Techniques. J. Geophys. Res., 68, 1184-1185.

12. Ewing, W., W. Jardetzky and F. Press (1957). Elastic Waves in Layered Media. McGraw-Hill, New York, 380 pp.
13. Hales, A. and J. Nation (1966). Reflections at the M Discontinuity and the Origin of Microseisms, in The Earth Beneath the Continents. J. Steinhardt and T. Smith, editors. American Geophysical Union, Washington, D.C., 529-537.
14. Heelan, P. (1953). On the Theory of Head Waves. Geophysics, 18, 871-893.
15. Hron, F. (1968). Koeficienty Odrezu a Loma Rovinnych Vln a Koeficienty Celných Vln (Program H1), in Vyzkum Seismických Vln, Vol. 9, Charles University, Prague (in Czechoslovakian).
16. Hron, F. and E. Kanasevich (1971). Synthetic Seismograms for Deep Seismic Sounding Studies Using Asymptotic Ray Theory. Bull. Seism. Soc. Am., 61, 1169-1200.
17. Hron, F. (1972). Numerical Methods of Ray Generation in Multilayered Media. Methods in Computational Physics, 12, 1-34.
18. Kireyeva, I. and K. Karpov (1961). Tables of Weber Functions. Pergamon Press, London, 340 pp.
19. Magnus, W. and F. Oberhettinger (1949). Formulas and Theorems for the Special Functions of Mathematical Physics. Chelsea Publishing, New York, 172 pp.
20. Muller, G. (1968). Theoretical Seismograms for Some Types of Point Sources in Layered Media I, II. Zeitschr. Geophys., 34, 15-35, 147-162.
21. Musgrave, A. (ed.) (1967). Seismic Refraction Prospecting. The Society of Exploration Geophysicists, Tulsa, 604 pp.
22. Muskat, M. (1933). The Theory of Refraction Shooting. Physics, 4, 14-28.

APPENDIX A.1

THE SOMMERFELD INTEGRAL

The Sommerfeld integral is defined in Ewing et al. (12) as:

$$\frac{e^{i k R_0}}{R_0} = \int_0^\infty J_0(pr) e^{-(p^2 - k^2)^{1/2} |z-h|} \frac{p dp}{(p^2 - k^2)^{1/2}}$$

where for $p < k$, we have

$$(p^2 - k^2)^{1/2} = -i(k^2 - p^2)^{1/2}$$

The wave potential Φ_0 is given as

$$\Phi_0 = (i k R_0)^{-1} \exp(-i \omega t + i k R_0)$$

In terms of the Sommerfeld integral we have

$$\Phi_0 = \frac{e^{-i \omega t}}{i k} \int_0^\infty J_0(pr) e^{-(p^2 - k^2)^{1/2} |z-h|} \frac{p dp}{(p^2 - k^2)^{1/2}} dp.$$

Let $J_0(pr) = 1/2[H_0^{(1)}(pr) + H_0^{(2)}(pr)]$ where $H_0^{(1)}$ and $H_0^{(2)}$ are Hankel functions of the first and second kind. Refer to Abramowitz and Stegun (1). Doing this we obtain the sum of two integrals:

$$\Phi_0 = \frac{e^{-i \omega t}}{i k} \left[\frac{1}{2} \int_0^{\infty} H_0^{(1)}(pr) e^{-(p^2 - k^2)^{1/2}} |z-h| \frac{p dp}{(p^2 - k^2)^{1/2}} \right. \\ \left. + \frac{1}{2} \int_0^{\infty} H_0^{(2)}(pr) e^{-(p^2 - k^2)^{1/2}} |z-h| \frac{p dp}{(p^2 - k^2)^{1/2}} \right].$$

In the second integral replace p by $-p$ and utilize the fact that

$$H_0^{(2)}(e^{-i \pi} pr) = -H_0^{(1)}(pr)$$

Two integrals are obtained with identical integrands but with limits $(0, \infty)$ and $(-\infty, 0)$. Combining these yields

$$\Phi_0 = \frac{e^{-i \omega t}}{2 i k} \int_{-\infty}^{\infty} H_0^{(1)}(pr) e^{-(p^2 - k^2)^{1/2}} |z-h| \frac{p dp}{(p^2 - k^2)^{1/2}}$$

Substitute $p = q_1 k$ and we arrive at

$$\Phi_0 = \frac{e^{-i \omega t}}{2} \int_{-\infty}^{\infty} H_0^{(1)}(k r q_1) \exp(i k(1-q_1^2)^{1/2} |z-h|) \frac{q_1 dq_1}{(1-q_1^2)^{1/2}}$$

This is the expression for the incident wave potential.

APPENDIX A.2

TRANSMISSION AND REFLECTION COEFFICIENTS

All reflection and transmission coefficients which were used in these derivations and in numerical evaluations are obtained from the work of Hron (15). An in-depth account of how the V_i 's are derived from the PP reflection coefficient will be given. The other three coefficients follow a similar routine.

Hron (15) makes the following preliminary definitions:

$$K1 = \beta_m / \alpha_m$$

$$K2 = \beta_{m+1} / \alpha_{m+1}$$

$$N = \alpha_m / \alpha_{m+1}$$

$$T = \rho_m / \rho_{m+1}$$

$$M = 2(K2^2 / N^2 - K1^2 \cdot T)$$

$$P = (1 - x^2)^{1/2}$$

$$Q = (1 - K1^2 x^2)^{1/2}$$

$$R = \frac{\beta_{m+1}}{\alpha_{m+1}} (\alpha_m^2 / \beta_{m+1}^2 - x^2)^{1/2}$$

$$S = (\alpha_m^2 / \alpha_{m+1}^2 - x^2)$$

$$a_1 = K1 \cdot K2 \cdot x^2 \cdot (1 - T - M x^2)^2 + K2 \cdot P \cdot Q \cdot (1 - M x^2)^2$$

$$a_2 = -K1 \cdot K2 \cdot x^2 \cdot (1 - T - M x^2)^2 + K2 \cdot P \cdot Q \cdot (1 - M x^2)^2$$

$$b = K1 \cdot T \cdot P$$

$$c = K2 \cdot T \cdot Q$$

$$d_1 = M^2 \cdot x^2 \cdot P \cdot Q + K1 \cdot (M x^2 + T)^2$$

$$d_2 = M^2 \cdot x^2 \cdot P \cdot Q - K1 \cdot (M x^2 + T)^2$$

Then the PP reflection coefficient (R_{11}) is given as

$$R_{11} = \frac{a_2 + b \cdot R - c \cdot S + d_2 \cdot R \cdot S}{a_1 + b \cdot R + c \cdot S + d_1 \cdot R \cdot S}$$

We wish to express this as

$$R_{11} = V_0 + V_1 \cdot S + V_2 \cdot R + V_3 \cdot R \cdot S$$

where the V's do not depend on R or S, but only on even powers of them. This is performed by the following multiplications.

$$R_{11} = \frac{a_2 + b R - c S + d_2 R S}{(a_1 + b R) + S(c + d_1 R)} \\ \times \frac{(a_1 + b R) - S(c + d_1 R)}{(a_1 + b R) - S(c + d_1 R)}$$

$$\times \frac{P_1 - R P_2}{P_1 - R P_2}$$

where $P_1 = a_1^2 + b^2 R^2 - S^2 c^2 - d_1^2 R^2 S^2$

$$P_2 = 2 a_1 b - 2 c d_1 S^2$$

After considerable algebra we find that

$$V_0 = \frac{P_1 P_5 - P_2 P_6 R^2}{P_1^2 - R^2 P_2^2}$$

$$V_1 = \frac{P_1 P_3 - P_2 P_4 R^2}{P_1^2 - R^2 P_2^2}$$

$$V_2 = \frac{P_1 P_6 - P_2 P_5}{P_1^2 - R^2 P_2^2}$$

$$V_3 = \frac{P_1 P_4 - P_2 P_3}{P_1^2 - R^2 P_2^2}$$

where $P_3 = -c(a_1 + a_2) + b R^2(d_2 - d_1)$

$$P_4 = a_1 d_2 - a_2 d_1 - 2 b c$$

$$P_5 = a_1 a_2 + b^2 R^2 + c^2 S^2 - d_1 d_2 R^2 S^2$$

$$P_6 = c S^2 (d_1 - d_2) + b(a_1 + a_2)$$

Head wave coefficients can be derived from these coefficients by using a simple relationship involving the reflection coefficient. Head wave coefficients yield the relationship between the amplitude of an incident wave and the resultant amplitude of the head wave arising from its critical refraction. In general any of the four basic reflection coefficients can be written as

$$R_{j\ell} = \frac{L + M \cdot H}{\tilde{L} + \tilde{M} \cdot H}$$

where H is either S (when considering a P type head wave) or R (when considering an S type head wave). The terms $L, M, \tilde{L}, \tilde{M}$ are in general complex and do not contain the radical H .

Head wave coefficients can be obtained from reflection coefficients in the following fashion (Cerveny and Ravindra (10))

$$\Gamma_{j k \ell} = - \left(\frac{d R_{j\ell}}{d H} \right)_{H=0}$$

Thus

$$\Gamma_{j k \ell} = \frac{\tilde{M} L - \tilde{L} M}{(\tilde{L})^2}$$

where $L, M, \tilde{L}, \tilde{M}$ are evaluated at the critical x value for

the particular type of head wave under consideration.

The numbering system used to identify the various reflection and head wave coefficients requires some explanation. It is necessary to label the four velocities at the basic reflecting interface. These are labelled as $\alpha_m:1$, $\beta_m:2$, $\alpha_{m+1}:3$, $\beta_{m+1}:4$. To determine the number of the reflection or head wave coefficient one considers the velocity at which each ray segment propagates. Thus a PP reflection requires the coefficient labelled 11 (R_{11}). As well a PPP (PSP) head wave has a head wave coefficient labelled 131 (141). The PPP (PSP) head wave coefficient is r_{131} (r_{141}).

APPENDIX A.3

THE EXPANSION OF $B(q_1)$

$B(q_1)$ is defined in Section 2.2 as

$$\begin{aligned}
 B(q_1) = & r q_1 + \sum_{i=1}^m N_{p_i} h_i (\alpha_1^2 / \alpha_i^2 - q_1^2)^{1/2} \\
 & + \sum_{i=1}^m N_{s_i} h_i (\alpha_1^2 / \beta_i^2 - q_1^2)^{1/2}
 \end{aligned}
 \tag{A.3.1}$$

A new contour of integration and a new variable of integration, p , are introduced via

$$(1 - q_1^2)^{1/2} = (1 - x_1^2)^{1/2} + p e^{-i \pi/4}$$

The function $B(q_1)$ can be expanded in a Taylor series at the point

$$x_1 = \sin \theta_1 \cdot \frac{\alpha_1}{v_1}$$

where x_1 is the root of equation 2.8. The series can be written as

$$\begin{aligned}
 B(q_1) \doteq & B(x_1) + \left. \frac{d B}{d q_1} \right|_{q_1=x_1} (q_1 - x_1) \\
 & + \frac{1}{2!} \left. \left(\frac{d^2 B}{d q_1^2} \right) \right|_{q_1=x_1} (q_1 - x_1)^2
 \end{aligned}
 \tag{A.3.2}$$

Both derivatives in the expansion are to be evaluated at the saddle point, $q_1 = x_1$. The first derivative when evaluated at this point gives zero results since this is the definition of the saddle point. We are then left with

$$B(q_1) \doteq B(x_1) + \frac{1}{2!} \cdot \left. \frac{d^2 B}{d q_1^2} \right|_{q_1=x_1} \cdot \left. \left(\frac{d q_1}{d p} \right) \right|_{p=p_0}^2 \cdot (p - p_0)^2$$

Considering individual terms

$$\left. \frac{d^2 B}{d q_1^2} \right|_{q_1=x_1} = - \sum_{i=1}^m \frac{N_{p_i} h_i \alpha_1^2}{\alpha_i^2 \left(\frac{\alpha_1^2}{\alpha_i^2} - x_1^2 \right)^{3/2}} - \sum_{i=1}^m \frac{N_{s_i} h_i \alpha_1^2}{\beta_i^2 \left(\frac{\alpha_1^2}{\beta_i^2} - x_1^2 \right)^{3/2}}$$

and

$$\left. \left(\frac{d q_1}{d p} \right) \right|_{p=p_0}^2 = - i \frac{(1 - x_1^2)}{x_1^2}$$

where p_0 is the value of p at the saddle point. Obviously, $p_0 = 0$. Substituting these back into the expansion one obtains

$$\begin{aligned}
 B(q_1) \doteq B(x_1) + \frac{i p^2}{2 x_1^3} (x_1 - x_1^3) \cdot \sum_{i=1}^m \left[\frac{N_p i h_i \alpha_1^2}{\alpha_i^2 \left(\frac{\alpha_1^2}{2} - x_1^2 \right)^{3/2}} \right. \\
 \left. + \frac{N_s i h_i \alpha_1^2}{\beta_i^2 \left(\frac{\alpha_1^2}{2} - x_1^2 \right)^{3/2}} \right]
 \end{aligned}
 \tag{A.3.3}$$

One then multiplies the term $(x_1 - x_1^3)$ into the brackets. After doing this it proves expedient to add and subtract the term $N_p i h_i x_1^3$ to the first term in brackets and to do the same with $N_s i h_i x_1^3$ to the second term in brackets. After some rearrangements the following result is obtained.

$$\begin{aligned}
 B(q_1) \doteq B(x_1) + \frac{i p^2}{2 x_1^3} \left\{ \sum_{i=1}^m \left[\frac{N_p i h_i x_1}{\alpha_i^2 \left(\frac{\alpha_1^2}{2} - x_1^2 \right)^{1/2}} \right. \right. \\
 \left. \left. - \frac{N_p i h_i x_1^3 \left(\frac{\alpha_1^2}{2} - 1 \right)}{\alpha_i^2 \left(\frac{\alpha_1^2}{2} - x_1^2 \right)^{3/2}} \right] + \sum_{i=1}^m \left[\frac{N_s i h_i x_1}{\beta_i^2 \left(\frac{\alpha_1^2}{2} - x_1^2 \right)^{1/2}} \right. \right. \\
 \left. \left. - \frac{N_s i h_i x_1^3 \left(\frac{\alpha_1^2}{2} - 1 \right)}{\beta_i^2 \left(\frac{\alpha_1^2}{2} - x_1^2 \right)^{3/2}} \right] \right\}
 \end{aligned}$$

Equation 2.8 is then employed. This equation gives the relationship between x_1 and epicentral distance r . As well, the quantity \tilde{r} is introduced as

$$\tilde{r} = x_1^3 \cdot \sum_{i=1}^m h_i \left[\frac{N_{p_i} \left(\frac{\alpha_1^2}{\alpha_i^2} - 1 \right)}{\left(\frac{\alpha_1^2}{\alpha_i^2} - x_1^2 \right)^{3/2}} + \frac{N_{s_i} \left(\frac{\alpha_1^2}{\beta_i^2} - 1 \right)}{\left(\frac{\alpha_1^2}{\beta_i^2} - x_1^2 \right)^{3/2}} \right]$$

Then

$$B(q_1) \doteq B(x_1) + \frac{i p^2}{2 x_1^3} (r - \tilde{r}) \quad \text{A.3.4}$$

The expansion of $B(q_1)$ along the contour used to evaluate head wave terms will have some vital differences. Let us only consider the P-type head wave term. The S-type head wave term is similar. The contour in this case circumvents the cut given by

$$(1 - q_1^2)^{1/2} = (1 - x_1^{*2})^{1/2} + p e^{-i \pi/4}$$

where

$$x_1^* = \alpha_1 / \alpha_{m+1}$$

Thus, the first term in A.3.4 should read $B(x_1^*)$ rather than $B(x_1)$. As well, the second term should read $i p^2 (r - \tilde{r}_{ppp}^*) / 2 x_1^{*3}$ where \tilde{r}_{ppp}^* is just \tilde{r} with x_1^* substituted for x_1 . Going back to equation A.3.2 we shall show that the second term does not vanish for this case. Evaluating,

$$\left(\frac{d B}{d q_1} \right) (q_1 - x_1^*) = \left(\frac{d B}{d q_1} \right) \Big|_{q_1=x_1^*} \cdot \left(\frac{d q_1}{d p} \right) \Big|_{p=p_0} (p - p_0)$$

Considering the terms individually

$$\left(\frac{d B}{d q_1} \right) \Big|_{q_1=x_1^*} = r - \sum_{i=1}^m \frac{N_{p_i} h_i x_1^*}{\left(\frac{\alpha_i^2}{2} - x_1^{*2} \right)^{1/2}} - \sum_{i=1}^m \frac{N_{s_i} h_i x_1^*}{\left(\frac{\alpha_i^2}{\beta_i^2} - x_1^{*2} \right)^{1/2}}$$

According to equation 2.10 these last two summations yield the critical distance r_{ppp}^* . As before $p_0 = 0$ at the saddle point and

$$\left(\frac{d q_1}{d p} \right) \Big|_{p=p_0} = - e^{-i \pi/4} \frac{(1 - x_1^{*2})^{1/2}}{x_1^*}$$

Therefore the term can be written

$$\left(\frac{dB}{dq_1}\right) (q_1 - x_1^*) = -p \frac{(1 - x_1^{*2})^{1/2}}{x_1^*} e^{-i\pi/4} (r - r_{ppp}^*)$$

and

$$B(q_1) \doteq B(x_1^*) - p \frac{(1 - x_1^{*2})^{1/2}}{x_1^*} e^{-i\pi/4} (r - r_{ppp}^*)$$

$$+ \frac{i p^2 (r - \tilde{r}_{ppp}^*)}{2 x_1^{*3}}$$

We now demonstrate the close resemblance between the geometrical spreading factor derived in this thesis, L , with that from asymptotic ray theory, L_R . The formula presented early in Chapter 1 showed the geometrical spreading from ray theory to be

$$L_R = \frac{\cos \theta_1}{v_1} \left(\sum_{i=1}^k \frac{h_i v_i}{\cos \theta_i} \cdot \sum_{i=1}^k \frac{h_i v_i}{\cos^3 \theta_i} \right)^{1/2}$$

Some adjustments should be made to this formula to make it consistent with the notation used in this work. First, the summation should take place over m layers rather than k ray segments. The number of P and S ray segments per layer, N_{p_i} and N_{s_i} are introduced. Second, the ray parameters, x , are used rather than $\cos \theta_i$. These changes enable one

to express asymptotic ray theoretical spreading as

$$\begin{aligned}
 L_R = & \frac{1}{\alpha_1} \left(\frac{\alpha_1^2}{v_1^2} - x_1^2 \right)^{1/2} \left(\sum_{i=1}^m \frac{N_{p_i} \alpha_1 h_i}{\left(\frac{\alpha_1^2}{\alpha_i^2} - x_1^2 \right)^{1/2}} \right. \\
 & + \sum_{i=1}^m \frac{N_{s_i} \alpha_1 h_i}{\left(\frac{\alpha_1^2}{\beta_i^2} - x_1^2 \right)^{1/2}} \left. \right)^{1/2} \cdot \left(\sum_{i=1}^m \frac{N_{p_i} \alpha_1^3 h_i}{\left(\frac{\alpha_1^2}{\alpha_i^2} - x_1^2 \right)^{3/2}} \right. \\
 & + \sum_{i=1}^m \frac{N_{s_i} \alpha_1^3 h_i}{\left(\frac{\alpha_1^2}{\beta_i^2} - x_1^2 \right)^{3/2}} \left. \right)^{1/2}
 \end{aligned}$$

where v_1 represents the velocity of propagation of the first ray segment. The geometrical spreading factor derived here is expressed as

$$L = \frac{r^{1/2} (r - \tilde{r})^{1/2}}{x_1}.$$

Employing A.3.3 for $(r - \tilde{r})^{1/2}$ and equation 2.8 for r we arrive at

$$\begin{aligned}
 L = & \frac{(x_1 - x_1^3)^{1/2}}{\alpha_1 x_1^{1/2}} \left(\sum_{i=1}^m \frac{N_{p \ i} \alpha_1 h_i}{\left(\frac{\alpha_1^2}{\alpha_i^2} - x_1^2\right)^{1/2}} \right. \\
 & + \sum_{i=1}^m \frac{N_{s \ i} \alpha_1 h_i}{\left(\frac{\alpha_1^2}{\beta_i^2} - x_1^2\right)^{1/2}} \left. \right)^{1/2} \cdot \left(\sum_{i=1}^m \frac{N_{p \ i} \alpha_1^3 h_i}{\left(\frac{\alpha_1^2}{\alpha_i^2} - x_1^2\right)^{3/2}} \right. \\
 & + \sum_{i=1}^m \frac{N_{s \ i} \alpha_1^3 h_i}{\left(\frac{\alpha_1^2}{\beta_i^2} - x_1^2\right)^{3/2}} \left. \right)^{1/2} .
 \end{aligned}$$

L and L_R are identical for rays whose first segment is of type P. However, for first segment of type S, they differ by a factor of $(\alpha_1^2/\beta_1^2 - x_1^2)^{1/2}/(1 - x_1^2)^{1/2}$.

APPENDIX A.4

LENGTH OF THE INTERFERENCE ZONE

It is known that at the critical point a head wave forms in addition to the reflected wave in the narrow sense of the word. Up to a certain distance the waves interfere. The length of this interference zone or critical region has been ably discussed by Cerveny (7,9) and Cerveny and Ravindra (10). The formulae presented in this appendix are derived in these works and are presented here for completeness.

The end of the interference zone is defined as the distance beyond the critical point at which the difference in arrival times of simply reflected and head waves equals the duration of the source pulse. This can be stated as

$$t_{j\ell} - t_{jk\ell} = \Delta t = 1/f.$$

For a multi-layered medium each layer is treated separately for each type of head wave that can possibly exist at the base of that layer. Two types of head waves must be considered; symmetric and non-symmetric. A symmetric head wave is one in which the incident ray segment is of the same type (P or S) as the reflected ray segment. These are the head waves PPP, PSP, SPS, SSS. Conversely, the non-symmetric head waves are PPS, PSS, SPP, SSP. For symmetric head waves, an analytic expression can be found for the length of the interference zone. According to Cerveny and Ravindra (10) this length can be expressed as

$$\Delta R_{j \ k \ j} = \frac{V_j}{f(1 - V_j^2/V_k^2)^{1/2}} \left\{ \frac{V_j}{V_k} + \left(\frac{4 h f}{V_j} \right)^{1/2} \left(1 - \frac{V_j^2}{V_k^2} \right)^{1/4} \right\}.$$

V_j represents the velocity of propagation of both incident and reflected ray segments of the head wave. V_k is the head wave velocity along the bottoming interface. The frequency and layer thickness are given by f and h respectively.

This formula shows that for increasing frequency f the length of the interference zone decreases.

For non-symmetric head waves we consider the travel-times of the reflected and head waves through the layer as

$$t_{j \ \ell} = \frac{r}{V_j} \sin \theta_j + h \left(\frac{\cos \theta_j}{V_j} + \frac{\cos \theta_\ell}{V_\ell} \right)$$

$$t_{j \ k \ \ell} = \frac{r}{V_k} + h \left(\frac{1}{V_j} \left(1 - \frac{V_j^2}{V_k^2} \right)^{1/2} + \frac{1}{V_\ell} \left(1 - \frac{V_\ell^2}{V_k^2} \right)^{1/2} \right)$$

The dependence of r on θ_j , θ_ℓ is $r = h(\tan \theta_j + \tan \theta_\ell)$ where $\sin \theta_\ell = (V_\ell/V_j)\sin \theta_j$. The equation for the difference in travel-times may now be solved numerically for the parameter $\sin \theta_j$ and thus for the distance, r , from where the ray entered the layer. Subtracting this distance from the critical distance, $r_{j \ k \ \ell}^*$, one arrives at the length

of the interference zone. $r_{j k \ell}^*$ is expressible as

$$r_{j k \ell}^* = h \left(\frac{v_j}{v_k \left(1 - \frac{v_j^2}{v_k^2} \right)^{1/2}} + \frac{v_\ell}{v_k \left(1 - \frac{v_\ell^2}{v_k^2} \right)^{1/2}} \right).$$

For all interference zone calculations in this thesis the equations for the zone length of non-symmetric waves were solved using a computer library subroutine. The actual solution was performed by interval halving. The subroutine produces accuracy greater than 10^{-5} .

APPENDIX A.5

FORMULAE FOR INTERFERENCE WAVE AMPLITUDE

In this Appendix, we give the explicit formulae for calculating the total incident amplitude of any of the eight interference waves. The numbering system of the waves is explained in Appendix A.1.

$$A_{11}^{131} = \frac{\sigma(x)}{L} \{R_{11}(x) - \frac{\Gamma_{131} n \alpha_{m+1}^{1/4} (1 - \alpha_1^2 / \alpha_{m+1}^2)^{1/4}}{(2 \pi f)^{1/4} (r - \tilde{r}_{131}^*)^{1/4}} [M G(y_3) - \frac{(M-1) \Gamma_{131}' G(y_3^0)}{\Gamma_{131}}]\}$$

$$A_{11}^{141} = \frac{\sigma(x)}{L} \{R_{11}(x) - \frac{\Gamma_{141} n \beta_{m+1}^{1/4} (1 - \alpha_1^2 / \beta_{m+1}^2)^{1/4}}{(2 \pi f)^{1/4} (r - \tilde{r}_{141}^*)^{1/4}} [M G(y_4) - \frac{(M-1) \Gamma_{141}' G(y_4^0)}{\Gamma_{141}}]\}$$

$$A_{12}^{132} = \frac{\sigma(x)}{L} \{R_{12}(x) - \frac{\Gamma_{132} n \alpha_{m+1}^{1/4} (1 - \alpha_1^2 / \alpha_{m+1}^2)^{1/4}}{(2 \pi f)^{1/4} (r - \tilde{r}_{132}^*)^{1/4}} [M G(y_3) - \frac{(M-1) \Gamma_{132}' G(y_3^0)}{\Gamma_{132}}]\}$$

$$A_{12}^{142} = \frac{\sigma(x)}{L} \{R_{12}(x) - \frac{\Gamma_{142} n \beta_{m+1}^{1/4} (1 - \alpha_1^2 / \beta_{m+1}^2)^{1/4}}{(2 \pi f)^{1/4} (r - \tilde{r}_{142}^*)^{1/4}} [M G(y_4) - \frac{(M-1) \Gamma_{142}' G(y_4^0)}{\Gamma_{142}}]\}$$

$$[M G(y_4) - \frac{(M-1) \Gamma'_{142} G(y_4^0)}{\Gamma_{142}}]]$$

$$A_{21}^{231} = \frac{\sigma(x)}{L} \{R_{21}(x) - \frac{\Gamma_{231} n \alpha_{m+1}^{1/4} (1 - \alpha_1^2 / \alpha_{m+1}^2)^{1/4}}{(2 \pi f)^{1/4} (r - \tilde{r}_{231}^*)^{1/4}}\}$$

$$[M G(y_3) - \frac{(M-1) \Gamma'_{231} G(y_3^0)}{\Gamma_{231}}]]$$

$$A_{21}^{241} = \frac{\sigma(x)}{L} \{R_{21}(x) - \frac{\Gamma_{241} n \beta_{m+1}^{1/4} (1 - \alpha_1^2 / \beta_{m+1}^2)^{1/4}}{(2 \pi f)^{1/4} (r - \tilde{r}_{241}^*)^{1/4}}\}$$

$$[M G(y_4) - \frac{(M-1) \Gamma'_{241} G(y_4^0)}{\Gamma_{241}}]]$$

$$A_{22}^{232} = \frac{\sigma(x)}{L} \{R_{22}(x) - \frac{\Gamma_{232} n \alpha_{m+1}^{1/4} (1 - \alpha_1^2 / \alpha_{m+1}^2)^{1/4}}{(2 \pi f)^{1/4} (r - \tilde{r}_{232}^*)^{1/4}}\}$$

$$[M G(y_3) - \frac{(M-1) \Gamma'_{232} G(y_4^0)}{\Gamma_{232}}]]$$

$$A_{22}^{242} = \frac{\sigma(x)}{L} \{R_{22}(x) - \frac{\Gamma_{242} n \beta_{m+1}^{1/4} (1 - \alpha_1^2 / \beta_{m+1}^2)^{1/4}}{(2 \pi f)^{1/4} (r - \tilde{r}_{242}^*)^{1/4}}\}$$

$$[M G(y_4) - \frac{(M-1) \Gamma'_{242} G(y_4^0)}{\Gamma_{242}}] \}$$

All quantities have been defined in equation 2.51.

B30156